Stock-driven scenarios on global material demand: the story of a lifetime

Deetman, S.P.

Acknowledgements

The story of a lifetime is shaped through the lessons of our teachers. They manifest as constructive karma, which reminds us that we are standing on the shoulders of giants. I'm thankful for all the teachers I've had. In particular my promotors. I would like to thank Ester van der Voet, who has been exceptionally patient and supportive and who showed me how modesty can, sometimes, be an obstacle to overcome. I thank Detlef van Vuuren, whose optimism, scientific curiosity and sense of humor have been inspirational for many years. And I thank Arnold Tukker, who continuously encourages the professional growth of a vibrant research community at the Institute of Environmental Sciences (CML). I would also like to thank Matthijs Schouten for sharing the teachings of the Buddha so vividly.

Encouragement and inspiration go a long way. I am thankful for the encouragements to continue this research from Thomas Graedel and for the help in improving it, to set higher scientific standards, by Reinout Heijungs and by Stefan Pauliuk, who have been indispensable in shaping the methods underlying this research. Others have been influential through many memorable and inspirational conversations, such as with Ruben Huele, Rene Kleijn, Jeroen Guinee, Arjan de Koning, Rianne de Bree, Bernhard Steubing, Sylvia Marinova, Paul Behrens, Krijn Trimbos, José Mogollón, Ellen Cieraad, Kiki Boomgaard, Maarten van den Berg, Vassilis Daioglou and Oreane Edelenbosch.

Sometimes, we learn most through teaching. I have had the privilege to supervise several students throughout their thesis research. Their work has contributed to this research in many ways and I have always learned something new from each of them. So, I would like to thank Merve, Niels, Janze, Luja, Martijn, Rombout, Emmi and Boris for this opportunity to work and learn with them.

The upside of taking some more time to complete this work, is that I have gotten to know several generations of fellow PhDs, partners in crime. A big thanks to 'the old gang', Patrik, Laura, Jeroen, David, Benjamin, Coen, Stefano and especially Angelica, best roommate and a great friend, for a wonderful start of this adventure. I'm also lucky to know the friendly bunch of PhDs that accompanied me during the later years, such as Di, Xiaoyang, Carlos Pablo, Janneke, Teun and especially Bertram, Franco and Glenn whom I admire for their exceptional brightness as well as their kindness.

Unconditional support is hard to find, yet so important for personal growth, and indispensable even when recovering from illness. I'm glad that I've been able to find such support, both professionally with wonderful people at the CML like Susanna, Sammy and Paul. And also, with friends and family. I'd like to thank my parents, Barend and Jeannet for their support and their confidence in me. I also thank my sister, Iris, whose dedication to

the wellbeing of others, big or small, I admire a lot. I could not have completed this research without them, or without the support of dear friends like Bram, Jan, Marleen, Ian and Ingrid.

Last but not least, I'm grateful for meeting the love of my life, Willemijn, who has stood by my side all these years. Your joyful attitude to life is disarming, contagious even, and has simply made things brighter. We both endured the hardships of Lyme disease, but thanks to you I have never felt alone. I admire your creativity, your perseverance and your talent to bring people together. I love that we share a passion for cats, nature, a sustainable future and, surprisingly, Star Trek. You are everything I could hope for.

Curriculum Vitae

Sebastiaan Deetman was born on the 7th of August 1985 in Voorburg, the Netherlands. After finishing secondary school (VWO) in Groningen in 2003, he studied *Sustainable Molecular Science and Technology*, a combined Bachelor education programme at the Universities of Delft, Leiden and Rotterdam. He completed the Camino de Santiago pilgrimage by bike in 2007 and continued to study *Industrial Ecology* at Leiden University, where he graduated in 2010 with a master thesis on the co-benefits of climate change policy for air pollution. Continuing a career in research, he worked on Integrated Assessment modelling, climate policy and energy demand scenarios at the Netherlands Environmental Assessment agency for two years, where he contributed to various international research projects, such as the OECD Environmental Outlook to 2050, the Energy Modelling Forum (EMF), and the development of the Representative Concentration Pathways (RCPs). In 2013 he started work at the Institute of Environmental Sciences (CML) at Leiden University, initially with a focus on resource efficiency and the use of critical raw materials in several European research projects like DESIRE and SCRREEN. Later, he expanded this scope to include global use of bulk materials in an effort to make his work more relevant to climate policy scenarios, through connecting the research fields of Industrial Ecology and Integrated Assessment Modelling. Ultimately, this led to the combined work presented in a PhD thesis in 2021. Since 2018 up to the present, he has also been working at the Copernicus Institute of Sustainable Development at Utrecht University.

List of peer-reviewed publications

S. Deetman, H.S. de Boer, M. Van Engelenburg, E. van der Voet, D.P. van Vuuren, Projected material requirements for the global electricity infrastructure – generation, transmission and storage, Resour. Conserv. Recycl. 164 (2021). doi:10.1016/j.resconrec.2020.105200.

S. Deetman, S. Marinova, E. van der Voet, D.P.D.P. van Vuuren, O. Edelenbosch, R. Heijungs, Modelling global material stocks and flows for residential and service sector buildings towards 2050, J. Clean. Prod. 245 (2020) 118658. doi:10.1016/j.jclepro.2019.118658.

S. Deetman, S. Pauliuk, D.P. Van Vuuren, E. Van Der Voet, A. Tukker, Scenarios for Demand Growth of Metals in Electricity Generation Technologies, Cars, and Electronic Appliances, Environ. Sci. Technol. 52 (2018) null. doi:10.1021/acs.est.7b05549.

S. Deetman, L. van Oers, E. van der Voet, A. Tukker, Deriving European Tantalum Flows Using Trade and Production Statistics, J. Ind. Ecol. 22 (2018). doi:10.1111/jiec.12533.

S. Deetman, A.F. Hof, B. Girod, D.P. van Vuuren, Regional differences in mitigation strategies: an example for passenger transport, Reg. Environ. Chang. (2014) 987–995. doi:10.1007/s10113-014-0649-1.

S. Deetman, A.F. Hof, D.P. Van Vuuren, Deep CO2 emission reductions in a global bottom-up model approach, Clim. Policy. 15 (2015) 253–271. doi:10.1080/14693062.2014.912980.

S. Deetman, A.F. Hof, B. Pfluger, D.P. van Vuuren, B. Girod, B.J. van Ruijven, Deep greenhouse gas emission reductions in Europe: Exploring different options, Energy Policy. 55 (2013) 152–164. doi:10.1016/j.enpol.2012.11.047.

X. Zhong, M. Hu, **S. Deetman**, B. Steubing, H.X. Lin, G.A. Hernandez, C. Harpprecht, C. Zhang, A. Tukker, P. Behrens, Global greenhouse gas emissions from residential and commercial building materials and mitigation strategies to 2060, Nat. Commun. 12 (2021) 6126. doi:10.1038/s41467-021-26212-z.

G.A. Aguilar-Hernandez, **S. Deetman**, S. Merciai, J.F.D. Rodrigues, A. Tukker, Global distribution of material inflows to in-use stocks in 2011 and its implications for a circularity transition, J. Ind. Ecol. (2021) jiec.13179. doi:10.1111/jiec.13179.

X. Zhong, M. Hu, **S. Deetman**, J.F.D. Rodrigues, H.-X. Lin, A. Tukker, P. Behrens, The evolution and future perspectives of energy intensity in the global building sector 1971–2060, J. Clean. Prod. 305 (2021) 127098. doi:10.1016/j.jclepro.2021.127098.

S. Marinova, **S. Deetman**, E. van der Voet, V. Daioglou, Global construction materials database and stock analysis of residential buildings between 1970-2050, J. Clean. Prod. 247 (2020) 119146. doi:10.1016/j.jclepro.2019.119146.

A. Mendoza Beltran, B. Cox, C. Mutel, D.P. van Vuuren, D. Font Vivanco, **S. Deetman**, O.Y. Edelenbosch, J. Guinée, A. Tukker, When the Background Matters: Using Scenarios from Integrated

Assessment Models in Prospective Life Cycle Assessment, J. Ind. Ecol. 24 (2020). doi:10.1111/jiec.12825.

D. Font Vivanco, R. Wang, **S. Deetman**, E. Hertwich, Unraveling the Nexus: Exploring the Pathways to Combined Resource Use, J. Ind. Ecol. 23 (2019). doi:10.1111/jiec.12733.

N.A. Mancheri, B. Sprecher, **S. Deetman**, S.B.S.B. Young, R. Bleischwitz, L. Dong, R. Kleijn, A. Tukker, Resilience in the tantalum supply chain, Resour. Conserv. Recycl. 129 (2018) 56–69. doi:10.1016/j.resconrec.2017.10.018.

G. Huppes, **S. Deetman**, R. Huele, R. Kleijn, A. De Koning, E. van der Voet, Strategic design of long-term climate policy instrumentations, with exemplary EU focus, Clim. Policy. 17 (2017). doi:10.1080/14693062.2016.1242059.

O. Braspenning Radu, M. van den Berg, Z. Klimont, **S. Deetman**, G. Janssens-Maenhout, M. Muntean, C. Heyes, F. Dentener, D.P. van Vuuren, Exploring synergies between climate and air quality policies using long-term global and regional emission scenarios, Atmos. Environ. 140 (2016) 577–591.

A. de Koning, G. Huppes, **S. Deetman**, A. Tukker, Scenarios for a 2 °C world: a trade-linked input–output model with high sector detail, Clim. Policy. 16 (2015) 1–17. http://www.tandfonline.com/doi/abs/10.1080/14693062.2014.999224.

A.F. Hof, A. Kumar, **S. Deetman**, S. Ghosh, D.P. van Vuuren, Disentangling the ranges: climate policy scenarios for China and India, Reg. Environ. Chang. (2014) 1025–1033. doi:10.1007/s10113-014-0721-x.

J. van Vliet, A.F. Hof, A. Mendoza Beltran, M. van den Berg, **S. Deetman**, M.G.J. den Elzen, P.L. Lucas, D.P. van Vuuren, The impact of technology availability on the timing and costs of emission reductions for achieving long-term climate targets, Clim. Change. 123 (2014) 559–569. doi:10.1007/s10584-013-0961-7.

C. Chuwah, T. van Noije, D.P. van Vuuren, W. Hazeleger, A. Strunk, **S. Deetman**, A.M. Beltran, J. van Vliet, Implications of alternative assumptions regarding future air pollution control in scenarios similar to the Representative Concentration Pathways, Atmos. Environ. 79 (2013) 787–801.

D.P. van Vuuren, **S. Deetman**, J. van Vliet, M. van den Berg, B.J. van Ruijven, B. Koelbl, The role of negative CO2 emissions for reaching 2 °C—insights from integrated assessment modelling, Clim. Change. 118 (2013) 15–27. doi:10.1007/s10584-012-0680-5.

B.J. van Ruijven, D.P. van Vuuren, J. van Vliet, A. Mendoza Beltran, **S. Deetman**, M.G.J. den Elzen, Implications of greenhouse gas emission mitigation scenarios for the main Asian regions, Energy Econ. 34 (2012) S459–S469. doi:10.1016/j.eneco.2012.03.013.

B. Girod, D.P. van Vuuren, **S. Deetman**, Global travel within the 2°C climate target, Energy Policy. 45 (2012) 152–166. doi:10.1016/j.enpol.2012.02.008.

D. van Vuuren, E. Stehfest, M. den Elzen, T. Kram, J. van Vliet, **S. Deetman**, M. Isaac, K. Klein Goldewijk, A. Hof, A. Mendoza Beltran, R. Oostenrijk, B. van Ruijven, RCP 2.6: exploring the possibility to keep global mean temperature increase below 2°C, Clim. Change. 109 (2011) 95–116. doi:10.1007/s10584-011-0152-3.

Appendix 1

1.1 Scenario narratives of the SSPs

The narratives underlying the three selected SSP scenarios discussed throughout the chapters are given below. The text is copied from Riahi et al.[1] and a more elaborate background to these narratives is given by O'Neill et al.[2].

SSP1: Sustainability – Taking the Green Road (Low challenges to mitigation and adaptation) The world shifts gradually, but pervasively, toward a more sustainable path, emphasizing more inclusive development that respects perceived environmental boundaries. Management of the global commons slowly improves, educational and health investments accelerate the demographic transition, and the emphasis on economic growth shifts toward a broader emphasis on human well-being. Driven by an increasing commitment to achieving development goals, inequality is reduced both across and within countries. Consumption is oriented toward low material growth and lower resource and energy intensity.

SSP2: Middle of the Road (Medium challenges to mitigation and adaptation) The world follows a path in which social, economic, and technological trends do not shift markedly from historical patterns. Development and income growth proceeds unevenly, with some countries making relatively good progress while others fall short of expectations. Global and national institutions work toward but make slow progress in achieving sustainable development goals. Environmental systems experience degradation, although there are some improvements and overall the intensity of resource and energy use declines. Global population growth is moderate and levels off in the second half of the century. Income inequality persists or improves only slowly and challenges to reducing vulnerability to societal and environmental changes remain.

SSP3: Regional Rivalry – A Rocky Road (High challenges to mitigation and adaptation) A resurgent nationalism, concerns about competitiveness and security, and regional conflicts push countries to increasingly focus on domestic or, at most, regional issues. Policies shift over time to become increasingly oriented toward national and regional security issues. Countries focus on achieving energy and food security goals within their own regions at the expense of broader-based development. Investments in education and technological development decline. Economic development is slow, consumption is material-intensive, and inequalities persist or worsen over time. Population growth is low in industrialized and

high in developing countries. A low international priority for addressing environmental concerns leads to strong environmental degradation in some regions.

1.2 IMAGE Region definitions

The regional classification used throughout the chapters and in the underlying model distinguishes 26 global regions, which can be seen in in Figure A1.1.

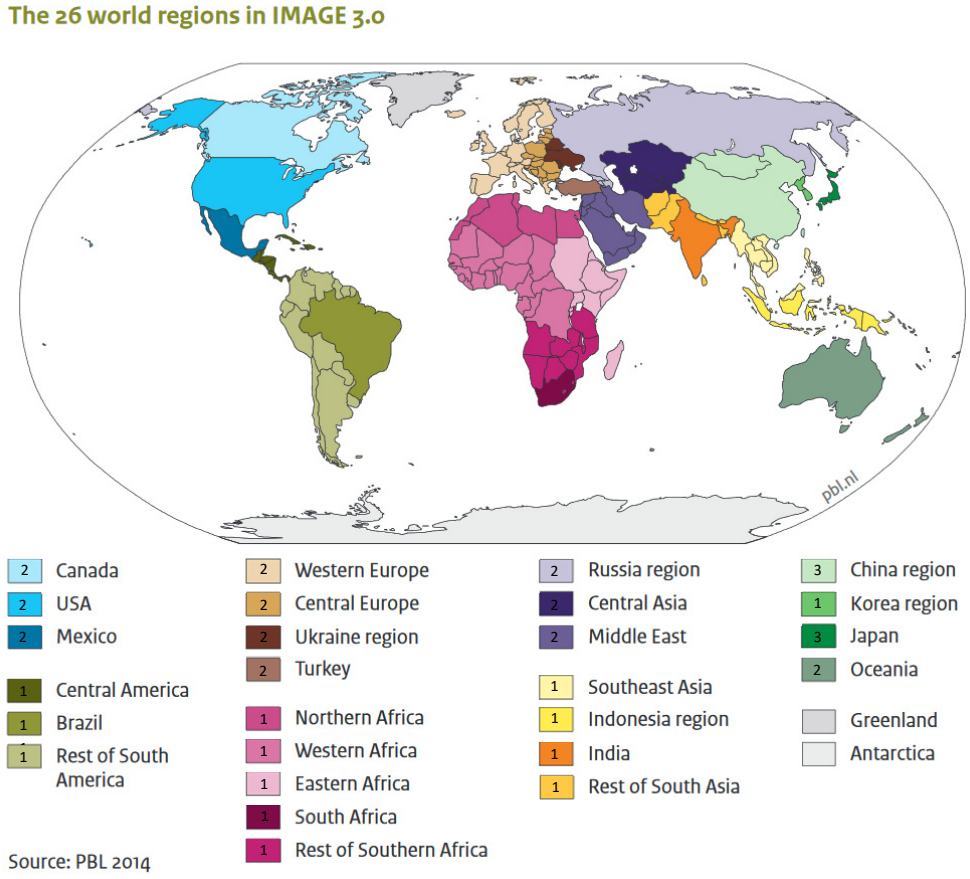

Figure A1.1. *The 26 world regions in IMAGE 3.0. Source: Stehfest et al.*[3]*, reproduced with permission of the editor. Regions tagged with a 1 are part of the group classified as fast-developing regions in the main text. Regions with a 2 represent the steady developed regions and group 3 indicates China & Japan.*

Regions are grouped under Fast developing regions are indicated with a 1, and Steady developed regions with a 2, according to the identified regional typologies used in various chapters. Greenland & Antarctica are not taken into account in any of the chapters.

References to Appendix 1

1. Riahi, K. *et al.* The Shared Socioeconomic Pathways and their energy, land use, and greenhouse gas emissions implications: An overview. *Glob. Environ. Chang.* 42, 153–168 (2017).
2. O'Neill, B. C. *et al.* The roads ahead: Narratives for shared socioeconomic pathways describing world futures in the 21st century. *Glob. Environ. Chang.* 42, 169–180 (2017).
3. Stehfest, E., van Vuuren, D., Bouwman, L. & Kram, T. *Integrated assessment of global environmental change with IMAGE 3.0: Model description and policy applications*. (Netherlands Environmental Assessment Agency (PBL), 2014).

Appendix 2

Based on supplementary information provided with:
Deetman et al. (2017) - *Deriving European tantalum flows using trade and production statistics* - Journal of Industrial Ecology – Vol. 22, Issue 1, p. 166-179
https://doi.org/10.1111/jiec.12533

A2.1 Linking of relevant product categories in Europroms

Table A2.1, below, presents the linking between Europroms commodities and the tantalum containing product categories used in the main document[1]. Mind that the given quantities of imports, exports and production (in kilograms or pieces) are already completed for missing data, so the table presents the numbers used after step 3 as referred to in Chapter 2. Notice that the three types of vehicles (passenger cars, public transport vehicles and freight vehicles) are lumped into one category called 'automotive' in the main text and figures.

Commodity	Prodcom code	Export quantity	Import quantity	Production quantity	Unit	Link to product category
Non-ferrous metal ores and concentrates (including of cobalt, chromium, molybdenum, titanium, tantalum, vanadium, zirconium, antimony, beryllium, bismuth, germanium, mercury)	13201690	70671200	2.95E+09	96997489	kg	concentrates
Carbides whether or not chemically defined	24135450	44035100	1.65E+08	5.34E+08	kg	carbides
Non-agglomerated metal carbides mixed together or with metallic binders	24664740	2266100	5645800	9527520	kg	carbides
Tantalum, articles thereof, powders, waste and scrap (excluding carbide)	27453023	345200	492800	253782	kg	articles
Drilling tools with working part of sintered metal carbide, for working metal excluding unmounted sintered metal carbide plates, sticks, tips and the like for tools	28624027	268300	198200	5200000	kg	carbide tools
Turning tools with working part of sintered metal carbide, for working metal excluding unmounted sintered metal carbide plates, sticks, tips and the like for tools	28624071	115100	188800	6224332	kg	carbide tools
Interchangeable hand tools with working part of sintered metal carbide excluding unmounted sintered metal carbide plates, sticks, tips and the like for tools	28624087	536900	465400	16000000	kg	carbide tools
Indexable inserts for tools, unmounted, of sintered metal carbides and cermets	28625067	0	0	0	kg	carbide tools
Furnace burners for liquid fuel	29211130	441206	238140	1278878	p/st	furnaces
Furnace burners for solid fuel or gas (including combination burners)	29211150	761017.6	46651.96	1600000	p/st	furnaces
Non-electric furnaces and ovens for the roasting, melting or other heat-treatment of ores, pyrites or of metals	29211230	2053.327	183.3014	7420	p/st	furnaces
Non-electric furnaces and ovens for the incineration of rubbish	29211250	4576100	431600	8395159	kg	furnaces
Other furnaces and ovens	29211290	36380500	4064600	85789303	kg	furnaces
Parts for furnace burners for liquid fuel, for pulverized solid fuel or for gas, for mechanical stokers, mechanical grates, mechanical ash discharges and similar appliances	29211430	0	0	0	:	furnaces
Laptop PCs and palm-top organisers	30021200	4582293	32747581	13385580	p/st	Laptop PCs
Desktop PCs	30021300	4462230	1908385	2291445	p/st	Desktop PCs
Digital data processing machines: presented in the form of systems(1996-2500)	30021400	7057494	3065011	20221969	p/st	Desktop PCs
Other digital automatic data processing machines whether or not containing in the same housing 1 or 2 of the following units: storage units, input/output units	30021500	2926015	7097226	647512	p/st	Desktop PCs
Central storage units	30021730	1327225	3472262	592547	p/st	Central storage
Hard and floppy disk drives	30021757	18082030	1.12E+08	858232	p/st	HDD
Fixed tantalum capacitors	32101230	3.68E+09	2.01E+09	8E+09	p/st	capacitors
Television cameras (including closed circuit TV cameras) (excluding camcorders)	32201290	2353607	33670162	606664	p/st	Cameras

Flat panel colour TV receivers, lcd/plasma, etc. excluding television projection equipment, apparatus with video recorder/player, video monitors, television receivers with integral tube	32302060	3157357	7175559	24609985	p/st	TVs
Electronic still cameras and video camcorders	32303335	6502389	60063259	2400000	p/st	Cameras
Video recorders or player/recorders (including laser or digital video disc players/recorders) (excluding those combined with a television, for magnetic tape)	32303370	2834678	51123937	6539524	p/st	DVD players
Artificial joints	33101735	1717467	1996521	6000000	p/st	Artificial joints
Appliances for overcoming deafness (excluding parts and accessories)	33101833	2069371	3794268	4045341	p/st	hearing aid
Parts and accessories of hearing aids (excluding for headphones, amplifiers and the like)	33101839	0	0	0	:	hearing aid
Pacemakers for stimulating heart muscles (excluding parts and accessories)	33101850	454941	714604	1144302	p/st	pacemakers
Instruments and appliances for aeronautical or space navigation (excluding compasses)	33201155	5052900	7241794	30000000	p/st	GPS
Instruments and appliances for navigation (including for marine or river navigation) (excluding for aeronautical or space navigation, compasses)	33201159	440479.6	243604.8	1564245	p/st	GPS
Parts and accessories for direction finding compasses and other navigational instruments and appliances	33208110	0	0	0	:	GPS
Unmounted spectacle lenses other than for the correction of vision	33401153	14854048	64397108	73170687	p/st	other lenses
Unmounted single focal spectacle lenses for the correction of vision, with both sides finished	33401155	8341712	85726775	72403009	p/st	vision correction lenses
Unmounted spectacle lenses for the correction of vision, with both sides finished other than single focal lenses	33401159	3235392	18422793	54123237	p/st	vision correction lenses
Unmounted spectacle lenses for the correction of vision, other than those with both sides finished	33401170	15983042	88218437	40261663	p/st	vision correction lenses
Mounted objective lenses of any material (excluding for cameras, projectors or photographic enlargers /reducers)	33402170	2384864	2252059	232529	p/st	other lenses
Mounted objective lenses, of any material, for cameras, projectors or photographic enlargers or reducers	33403100	596036	4298792	463393	p/st	camera lenses
Telephones for cellular networks or for other wireless networks	32202025	1.17E+08	2.05E+08	2.07E+08	p/st	Mobile phones
Motor vehicles with a petrol engine <= 1000 cm³ (excluding vehicles for transporting >= 10 persons, snowmobiles, golf cars and similar vehicles)	34102133	36288	517505	417162	p/st	passenger cars
Other motor vehicles (including motor caravans) with spark-ignition engine of a cylinder capacity > 1.000 cm³ but <= 1.500 cm³	34102136	405192	585992	3612995	p/st	passenger cars
Motor vehicles with a petrol engine greater than 1000cc but =< 1500cc excl. motor caravans - snowmobiles,golf cars and similar vehicles ,those for carrying =>10 people	34102135	0	0	0	:	passenger cars
Other vehicles with spark-ignition engine of cylinder capacity > 1500 mü, <= 2000 cmü	34102233	0	0	0	:	passenger cars
Other vehicles with spark-ignition engine of cylinder capacity > 2000 mü, <= 2500 cmü	34102235	0	0	0	:	passenger cars
Other vehicles with spark-ignition engine of cylinder capacity > 2500 cmü	34102237	0	0	0	:	passenger cars
Motor vehicles with a petrol engine > 1500 cm³ (including motor caravans of a capacity > 3000 cm³) (excluding vehicles for transporting >= 10 persons, snowmobiles, golf cars and similar vehicles)	34102230	0	0	0	:	passenger cars
Motor caravans with a spark-ignition internal combustion reciprocating piston engine of a cylinder capacity > 1500 cm³ but <= 3000 cm³	34102250	557	5472	8000	p/st	passenger cars
Motor vehicles with a diesel or semi-diesel engine <= 1500 cm³ (excluding vehicles for transporting >= 10 persons, snowmobiles, golf cars and similar vehicles)	34102310	100589	157206	1697146	p/st	passenger cars
Motor vehicles with a diesel or semi-diesel engine > 1500 cm³ but <= 2500 cm³ (excluding vehicles for transporting >= 10 persons, motor caravans, snowmobiles, golf cars and similar vehicles)	34102330	383870	735501	6165900	p/st	passenger cars
Motor vehicles with a diesel or semi-diesel engine > 2500 cm³ (excluding vehicles for transporting >= 10 persons, motor caravans, snowmobiles, golf cars and similar vehicles)	34102340	83611	217292	342214	p/st	passenger cars
Motor vehicles for the transport of >= 10 persons with a compression-ignition internal combustion piston engine (diesel or semi-diesel) of a cylinder capacity <= 2500 cm³	34103033	1259	831	3341	p/st	passenger cars
Public transport type vehicles for >= 10 persons, with a compression-ignition internal combustion piston engine (diesel or semi-diesel) of a cylinder capacity > 2500 cm³	34103035	18904	5124	23681	p/st	public transport vehicles
Public transport type vehicles for >= 10 persons, with a spark-ignition internal combustion piston engine of a cylinder capacity <= 2800 cm³	34103053	61	5	0	p/st	public transport vehicles
Public transport type vehicles for >= 10 persons, with a spark-ignition internal combustion piston engine of a cylinder capacity > 2800 cm³	34103055	659	26	1400	p/st	public transport vehicles
Public transport type vehicles for >= 10 persons (excluding with a compression-ignition or spark-ignition internal combustion piston engine)	34103059	31303	5822	3910	p/st	public transport vehicles
Goods vehicles with a diesel or semi-diesel engine, of a gross vehicle weight <= 5 tonnes (excluding dumpers for off-highway use)	34104110	170890	321846	1808255	p/st	freight vehicles
Goods vehicles with a diesel or semi-diesel engine, of a gross vehicle weight > 5 tonnes but <= 20 tonnes (including vans) (excluding dumpers for off-highway use, tractors)	34104130	35727	973	210207	p/st	freight vehicles

Goods vehicles with compression-ignition internal combustion piston engine (diesel or semi-diesel), of a gross vehicle weight > 20 tonnes (excluding dumpers designed for off-highway use)	34104140	27817	2123	151490	p/st	freight vehicles
Goods vehicles with a spark-ignition internal combustion piston engine, of a gross vehicle weight <= 5 tonnes (excluding dumpers designed for off-highway use)	34104230	23677	38287	62986	p/st	freight vehicles
Goods vehicles with a spark-ignition internal combustion piston engine, of a gross vehicle weight > 5 tonnes (excluding dumpers designed for off-highway use)	34104250	100	57	0	p/st	freight vehicles
Goods vehicles (excluding vehicles with a compression-ignition or spark-ignition internal combustion piston engine, dumpers designed for off-highway use)	34104290	4389	13036	25092	p/st	freight vehicles
Tools for tapping, with working parts of sintered met. carb.	28624011	0	0	0	:	carbide tools
Tools for threading, wiht working part of sintered met. car.	28624015	0	0	0	:	carbide tools
Tools for boring, for work metal, with work park of sintered metal carbide	28624041	0	0	0	:	carbide tools
Tools for broaching, for work metal, with work part, of sintered met. carbide	28624047	0	0	0	:	carbide tools
Tools for milling, for working metal, with working part of sintered metal carbide	28624053	0	0	0	:	carbide tools
Hobs for milling, for working metal, with working part of sintered metal carbide	28624055	0	0	0	:	carbide tools
Rock drilling or earth boring tools with working part of cermets	28625013	3587700	1524200	40266914	kg	carbide tools
Indexable inserts for tools, unmounted, of sintered metal carbides and cermets	28625067	0	0	0	kg	carbide tools
Plates for tools, unmounted, of metal carbides or cermet, tool-tip	28625070	0	0	0	:	carbide tools
Unmounted sintered metal carbides or cermet plates, sticks, tips and the like for tools (excl. indexable inserts)	28625090	2166400	1807800	7005005	kg	carbide tools
Mounted piezo-electric crystals (including quartz, oscillator and resonators)	32105270	1.4E+08	2.37E+08	1.24E+08	p/st	wave filters
Semiconductor diodes	32105120	0	0	0	:	semiconductors
Semiconductor diodes	32105125	9.86E+09	1.32E+10	9.72E+09	p/st	semiconductors
Semiconductor small signal transistors with a dissipation rate < 1 W	32105155	3.31E+10	2.38E+10	1.4E+10	p/st	semiconductors
Semiconductor power transistors with a dissipation rate >= 1 W	32105157	4.04E+09	4.98E+09	7.07E+09	p/st	semiconductors
Semiconductor thyristors, diacs and triacs	32105170	8.25E+08	5.08E+08	1.8E+09	p/st	semiconductors
Semiconductor devices (excluding photosensitive semiconductor devices, photovoltaic cells, thyristors, diacs and triacs, transistors, diodes, and light-emitting diodes)	32105250	3.87E+09	8.95E+08	3.59E+09	p/st	semiconductors
Milling tools with working part of sintered metal carbide, for working metal excluding unmounted sintered metal carbide plates, sticks, tips and the like for tools	28624050	252700	281600	19292183	kg	carbide tools
Turbojets or turbofans of a dry thrust <= 25 kN	35301210	6099	36245	0	p/st	Aerospace
Turbo-jets of a thrust <= 25 kN, for aircraft for civil and parapublic use	35301213	0	0	0	:	Aerospace
Turbo-jets of a thrust <= 25 kN, for aircraft for military use	35301215	0	0	0	:	Aerospace
Turbojets or turbofans of a dry thrust > 25 kN	35301230	2032	1857	2000	p/st	Aerospace
Turbo-jets of a thrust > 25 kN, for aircraft for civil and parapublic use	35301233	0	0	0	:	Aerospace
Turbo-jets of a thrust > 25 kN, for aircraft for military use	35301235	0	0	0	:	Aerospace
Turboprops of a power <= 1100 kW	35301250	2762	2075	1378	p/st	Aerospace
Turboprops of a power > 1100 kW	35301270	1344	4581	200	p/st	Aerospace
Parts of turbo-jets or turbo-propellers	35301600	0	0	0	:	Aerospace

Table A2.1. *Data extracts and linkage table between Europroms*[1] *and product categories used.*

A2.2. Elaboration on the data availability in Eurostat Europroms

The study only presented a detailed substance flow analysis for the year 2007. The reason behind this is the availability of data at the highest level of detail in the Europroms database. Out of the 88 Europroms commodities relevant to tantalum, data on 55 commodities was actually available in the year 2007. The database contained significantly less information on more recent years as can be seen in Figure A2.1, so it was decided to prefer completeness over recency and do the analysis for the year 2007.

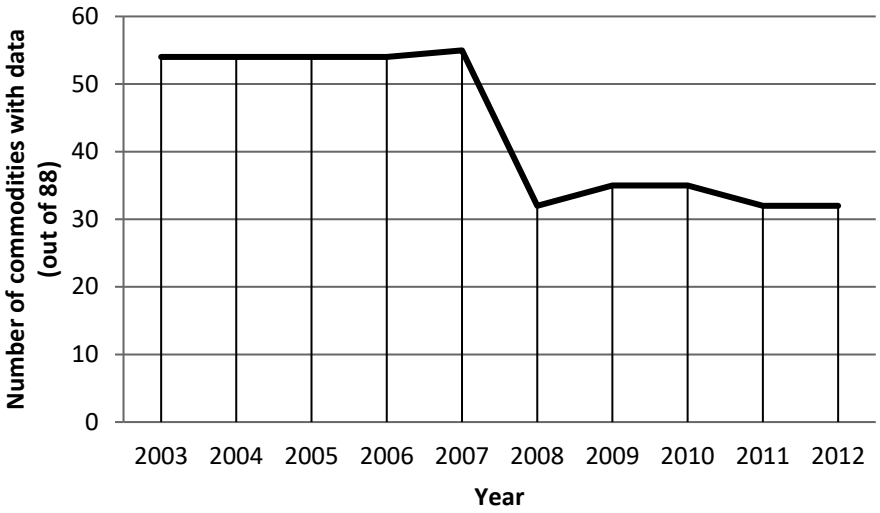

Figure A2.1. *Coverage of data on tantalum relevant products in the Europroms*[1] *statistics.*

A2.3. Elaboration on market shares & product weights

Table A2.2. *Weight conversion used, in case no weight conversion was available.*

Production commodity	Weight (kg/unit)	Source	Comments
Furnaces	3000	[2] & [3]	Supplier specification of large walk-in type ovens.
Capacitors (fixed Ta)	0.00014	[4] & [5]	Average of tantalum capacitor weight found in two sources
Artificial joints	0.175	[6]	Rough estimate ('one or two pounds')
GPS	0.0195	[7]	Average of 10 GPS products, based on commercial specs
Surface Acoustic Wave filters	3.7E-05	[8]	Company data sheet
Semiconductors	0.00031	[4]	Average of "diode, glass-, SMD type, for surface mounting, at plant" (32 mg) & "transistor, SMD type, for surface mounting, at plant" (0.593 g)

Table A2.3. *List of representative fractions applied to link product weights and tantalum concentrations.*

Prodcom Product name	Prodcom code	Applied	Assumption
Central storage units	30021730	0.112	assuming 5 disks in a single central storage unit of the given weight of 5,65 kg
Hard and floppy disk drives	30021757	0.268	Given the estimates of Coughlin (2006)[9], this represents the market-share of hard disks using perpendicular recording by 2007.
Instruments and appliances for aeronautical or space navigation (excl. compasses)	33201155	0.00157	Due to the high mass of products in this category, the factor adjusts the tantalum concentration assuming the functionality, and thus the tantalum content, of a single GPS device.
Semiconductor diodes, small transistors, thyristors, diacs, triacs & other devices	32105120, 32105125, 32105155, 32105157, 32105170, 32105250	0.01	1% of semiconductors contains tantalum, authors assumption

A2.4 Deriving tantalum concentrations

Table 2.3 in Chapter 2 contains indications of tantalum concentrations in products in kilograms tantalum per kilogram product. The indicated sources didn't always contain information on the tantalum content directly, but sometimes provided clues on the material composition, which needed further translation and interpretation. Below we provide the details to this translation for 6 products and components.

1) Glass lenses

Based on the average compositions of the 4 types of glass found in the patent of Kodak[10], we found that the described glass lenses contained 11.25 wt% tantalum oxide. Given the chemical composition of tantalum oxide in the form of Ta_2O_5, we derived that of the tantalum oxide, tantalum comprises only 82 wt%. This leads to 9.2 wt% tantalum, but since lenses are not all tantalum containing, we further assumed a 50% market share for tantalum-containing lenses, leading to an applied concentration of 0.046 kg of tantalum per kg of glass lenses.

2) Wave Filters

We found two sources containing clues to the tantalum composition of specific wave filters [11,12] and derived volumetric material compositions based on the cross-section drawing of the wave filters as indicated in Table A2.4 and A2.5 below. Then we applied the indicated densities to derive the weight percentage as also indicated.

Table A2.4. *Wavefilter material content based on Strijbos et al.*[12]*.*

	vol%	density (g/cm3)	wt%
Cu	12.5	8.96	16.9
Pt	12.5	21.45	40.4
AlN	25	3.26	12.3
SiO2	37.5	2.65	15.0
Ta2O5	12.5	8.25	15.5

Table A2.5. *Wavefilter material content based on Abbott*[11]*.*

	vol%	density (g/cm3)	wt%
Cu	2	8.96	3.7
SiO2	15	2.65	8.2
LiTaO3	45	7.46	69.7
Si	38	2.329	18.4

The subsequent application of tantalum weight of 82% for Tantalum Oxide and 77% for Lithium Tantalate lead to 12.7 wt% tantalum in one of the filters and 53.4 wt% in the other, thus leading to an average tantalum content in tantalum containing wavefilters of 33.05%. Mind that the market share was still applied. Mind that the market share given in Table A2.3 still has to be applied too this.

3) Computer Harddisk Drives (HDDs)

We assumed that tantalum was only contained in the harddisk platter (the disk actually storing the data), and that a harddisk platter accounts for 10,5% of the total harddisk weight, based on Yan et al.[13]. Furthermore, we used the average tantalum composition of the platters based on two studies [14,15]. In the study by Nunney et al.[14] we used the cross sectional drawing to derive volumetric material compositions based on the various layers that a harddisk platter contains. The elemental composition for each layer was given as a result of the x-ray analysis. Table A2.6 shows our interpretation of the study. Assuming that each layer has a similar density gives a tantalum composition of 45 wt% for the platter or 4.7 wt% considering the whole harddisk (including head motor, housing etc.).

Table A2.6. *Composition (wt%) of a harddisk platter according to Nunney et al. (2011)*[14]*.*

Layer name	**Layer**	Co	Pt	Ta	Cr	Ru	Ti	Ni	Al	Zr	C	O
Polymer	**4%**										90%	10%
Magnetic	**8%**	46%	13%		12%	30%						
nonmagnetic	**4%**	65%	18%		17%							
Magnetic	**8%**	46%	13%		12%	30%						
nonmagnetic	**4%**	65%	18%		17%							
seed layer	**10%**				90%		10%					
Tantalum	**3%**			90%	10%							
Buffer layer	**29%**			50%				50%				
Glass	**30%**								8%	2%		65%

A second source for the platter composition that we used was the Hitachi patent[15], which describes a layered structure that we interpreted according to Table A2.7 below. Similar to the case of wave filters and lenses, the weight percentage of the two layers containing tantalum was multiplied with the weight of tantalum in those layers based on their atomic description and then added, thus leading to a total tantalum content of 7.9 wt% in the data platter or 0.83 wt% in the total harddisk drive. This was combined with the numbers from Nunney et al. and averaged before applied in the main document.

Table A2.7. *Composition of a harddisk platter according to Hitachi (2007)*[15].

layer	Material	layer	density	weight %
coating	C/O	26%	3.9	13%
magnetic	(Co86Cr14)60Pt40	17%	15.175	34%
	Ta2O5	4%	8.25	4%
intermediate	Ru	3%	12.45	5%
	NiTa	4%	12.75	6%
	NiW	4%	14.15	7%
soft underlayer	CoNi	21%	8.9	24%
Substrate	glass	21%	2.6	7%

4) Artificial joints

The tantalum concentration in artificial joints is based on the materials mentioned in a study by Zardiackas et al.[16]. They mention 5 different types of alloying metals used in surgical applications. We also added a metal that we found repeatedly during a web-search, being a non-tantalum containing titanium alloy (Ti6Al4V), which together made 6 materials. Without information on the market shares of these alloys, we assume that all alloys were used in equal amounts. Thus, we can use the two materials that do contain tantalum, being Tantalum foam (Trabecular Metal) and a Ti-35Nb-7Zr-5Ta alloy (TiOsteum) alloy to derive the tantalum composition. We assume tantalum foam to be made a 100% out of tantalum, and we used a 5% tantalum content for the second alloy, thus leading to an estimated tantalum content of 17.5% by weight for artificial joints.

5) Semiconductors

The material composition was based on a study by Chaneliere et al.[17]. We used a visual representation of the components structure to derive material compositions by volume. Combining this with information on density lead to the composition by weight as elaborated in Table A2.8. The subsequent multiplication of the tantalum oxide weight with the 82 wt% tantalum (mentioned earlier) gives a total weight percentage of tantalum in semiconductors of 28,6 wt%, or 0,0286 kg tantalum per kg semiconductor.

Table A2.8. *Composition of a semiconductor according to Chaneliere et al.*[17]

	vol%	density (g/cm3)	wt%
Al	8	2.7	3.6
Ta2O5	25	8.25	34.9
HfO2	15	9.68	25.6
ZnS	23	4.09	16.2
ITO	6	7.16	7.6
AlO3	8	3.95	5.2
glass	15	2.6	6.9

6) Aerospace

As can be seen in Table A2.1, the only aerospace applications considered relevant to tantalum are aircraft engines. In fact, we assume the tantalum is only contained in the high temperature alloys of the turbine blades inside the aircraft engine. So, to find out how much tantalum is contained in aircraft engines, we started with a list of nickel-based superalloys for gas turbine blades as given by Muktinutalapati[18], out of the 17 materials listed, 6 contained tantalum. We used this indication to assume that 35% of high temperature alloys used actually contain tantalum. Of those materials containing tantalum we derived a tantalum weight as shown in Table A2.9 below, giving us an average tantalum content of 2.94% by weight.

Table A2.9. *Tantalum content in tantalum containing high temperature alloys based on Muktinutalapati*[18]*.*

Alloy type	Ta weight %
MAR-M246	1.5
IN 792	3.9
M 22	3
MAR-M246+Hf	1.5
IN 738	1.75
TMD-103	6

Because only the turbine blades were assumed to contain tantalum, we used a NASA engine weight model[19] to derive that the weight of the turbine is 18% of the complete engine based on the numbers given in Table A2.10 below.

Table A2.10. *Composition of an aircraft engine derived by NASA*[19]*.*

	volume	material	density (kg/ m3)	weight
inlet	10%	Aluminium	2723	4%
fan	29%	Titanium	4693	23%
compressor	17%	Titanium	4693	13%
burner	9%	Nickel alloy	8249	12%
turbine	13%	Nickel alloy	8249	18%
Nozzle	22%	Nickel Alloy	8252	30%

Finally, we assumed that 50% of the turbine weight is caused by the turbine blades, thus leading to an overall tantalum composition of 0.092% of the aircraft engine weight (35% of high temperature alloys containing tantalum, those that do contain 2.94 wt% tantalum in their turbine blades, which account for 50% of the turbine weight, which in turn accounts for 18% of the engine weight).

A2.5 Elaboration of Balancing Flow Allocations

In the Sankey diagram, Figure 2.2 in Chapter 2, we represent the flows of tantalum throughout various product stages, while respecting the conceptual representation as given in Figure A2.2 below, where A1 & A2 are the two steps requiring allocation of tantalum flows.

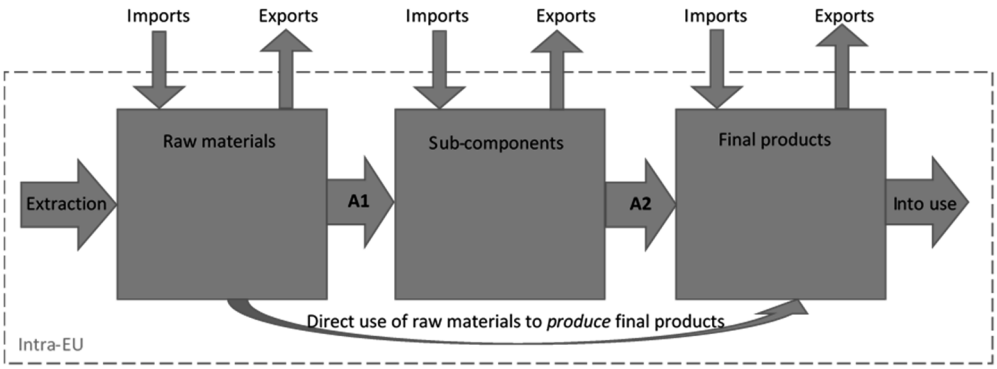

Figure A2.2. *Schematic overview of the tantalum flows considered in this study. A1 & A2 represent the flows that need further allocation, as described in the text.*

The allocation of tantalum flows between raw materials, subcomponents and final products is derived using an optimization as elaborated in the main document, except for the allocation of harddisks, which is based on literature. The use of this optimization in combination with exogenous allocation does not however guarantee a matching in demand and supply, nor does it guarantee a balanced system. To balance the system, the Sankey diagram contains balancing flows for both surpluses and shortages of tantalum supply. The actual mismatch in demand and supply for individual products is given in Table A2.11 and A2.12 below.

Table A2.11. *Does supply of tantalum raw material fulfill the demand for production of sub-components in Europe?*

From (Raw Material apparent consumption)	To (Sub-component production)	Fulfills production? (supply/ demand)
Tantalum carbides	Carbide Tools (F)	100% by assumption
Tantalum metal	Artificial joints (F)	100%
	HDDs	100%
Tantalum oxide	Vision correction lenses (F)	210%
	Camera lenses	245%
	Other lenses (F)	143%
	Wave filters	114%
Tantalum powder	Capacitors	100%
Tantalum ingots	Semi-conductors	100%
	High-temperature alloys	100%

	Fulfills production?
Mobile phones	56%
Cameras	99% (of Ta in camera bodies)
Desktop PCs	98%
Laptop PCs	432%
External HDD	*balancing factor*
Central storage	241%
DVD Players	100%
GPS devices	99%
TVs	99%
Hearing aid	94%
Pacemaker	98%
Vehicles	85%
Furnaces	100%
Aerospace	100%

Table A2.12. *Does supply of tantalum sub-components fulfill the demand for production of final products in Europe?*

References to Appendix 2

1. Eurostat. Europroms database of trade and production statistics. (2016). Available at: http://ec.europa.eu/eurostat/c/portal/layout?p_l_id=121328&p_v_l_s_g_id=0.
2. C.S.Aerotherm pvt. ltd. Biscuit baking oven. *Online sales information* (2014). Available at: http://www.csaerotherm.org/biscuit-baking-oven.html. (Accessed: 15th September 2014)
3. Wisconsin oven. WEWN Series Enhanced Walk-in oven 55 Sizes, gas or electric heat. *Online sales brochure* (2014). Available at: http://www.wisoven.com/sites/default/files/EWN Literature.pdf. (Accessed: 15th September 2014)
4. Ecoinvent. *Life Cycle inventories of electric and Electronic Equipment: Production, Use and Disposal.* (2007).
5. Guvendik, M. From Smartphone to Futurephone. (Delft University of Technology & Leiden University, 2014).
6. Beamont Orthopedics. Total Knee Replacement Surgery. (2014). Available at: http://orthopedics.beaumont.edu/total-knee-replacement. (Accessed: 15th September 2014)
7. Carver, E. Recreation GPS Reviews. (2016). Available at: http://gps.toptenreviews.com/recreation.
8. Epcos. *SAW Components, SAW RF filter, Automotive telematics*. (2010).
9. Coughlin, T. Perpendicular magnetic recording and other new technologies drive capital spending. (2006).
10. Kodak. Optical Glass. (1941).
11. Abbott, B. P., Chocola, J., Lin, K., Namenko, N. & Caron, J. Characterisation of Bonded Wafer for RF Filters with Reduced TCF. *Proc. 2005 IEEE Int. Ultrason. Symp.* 926–929 (2005).
12. Strijbos, R. C., Jansman, A., Lobeek, J. W. & Pulsford, N. Design and Characterisation of High-Q Solidly-Mounted Bulk Acoustic Wave Filters. in *IEEE Electronic Components and Technology Conference* 196–174 (2007).
13. Yan, G., Xue, M. & Xu, Z. Disposal of waste computer hard disk drive: data destruction and resources recycling. *Waste Manag. Res. J. a Sustain. Circ. Econ.* 31, 559–567 (2013).
14. Nunney, T. & Baily, C. *XPS Analysis of a Hard Disk Platter by Rapid Depth Profiling.* (2011).
15. Hitachi. Apparatus, system, and method for the selection of perpendicular media segregant materials. (2007).
16. Zardiackas, L. D., Kraay, M. J. & Freese, H. L. *Titanium, Niobium, Zirconium, and Tantalum for Medical and Surgical Applications.* (West Conshohocken: ASTM, 2006).
17. Chaneliere, C., Autran, J. L., Devine, R. A. B. & Balland, B. Tantalum pentoxide (Ta2Os) thin films for advanced dielectric applications. *Mater. Sci. Eng.* R22, 269–322 (1998).
18. Muktinutalapati. *Materials for Gas Turbines – An Overview*. (InTech, 2011).
19. NASA. Engine Weight model. (2015). Available at: http://www.grc.nasa.gov/WWW/k-12/airplane/turbwt.html. (Accessed: 5th January 2015)

Appendix 3

Based on the Supplementary Information provided with:
Deetman et al. (2018) - Scenarios for demand growth of metals in electricity generation technologies, cars and appliances – Environmental Science & Technology, Vol. 52, Issue 8, p. 4950–4959 https://doi.org/10.1021/acs.est.7b05549

A3.1 Assumptions on product compositions

Below we discuss the approach and assumptions used to derive the complete overview of product compositions for cars, appliances and electricity generation technologies. Together with the sources provided in Chapter 3, these provide the basis for Table A3.1.

A3.1.1 Cars

Table A3.1 presents the metal composition of cars based on the minimum and the maximum composition as found in following studies (Please note that if the study specifies multiple data points or sub-technologies, an average of the data points within each study is taken):

Internal Combustion Engines (ICE): Cullbrand & Magnusson[1], Habib[2] only for Nd, Alonso et al.[3], Widmer et al.[4], Hawkins et al.[5] only for Cu.

Hybrid Electric Vehicles (HEV): Cullbrand & Magnusson[1], Habib[2] only for Nd, Moss et al.[6], Elwert et al.[7], US Dept. Of Energy[8]

Plugin Hybrid Electric Vehicles (PHEV): Moss et al.[6], Elwert et al.[7], US Dept. of Energy[8]

Battery Electric Vehicles (BEV): Hawkins et al.[5] only for Cu, Moss et al.[6], Elwert et al.[7], US Dept. of Energy[8]

Fuel Cell Vehicles (FCV): Moss et al.[6] or similar to conventional ICE vehicle

A3.1.2 Consumer electronics

The following assumptions were applied to derive the metal content estimates for consumer electronics (appliances):

Air coolers & Fans: If no information was available, we assumed 50% or 15% of the metal composition of an air-conditioner, respectively (authors own estimate).

Tumbler dryers & Dishwashers: If no information was available, we assumed the same concentration as in washing machine, but adjusted for the weight ratio based on tumbler dryer weight: 43.2kg (dryer) OR 45.5kg (dish washer) over 71.4 kgs (washing machine).

Televisions (TVs): We assumed an average PCB weight in Flat Screen TVs based on Oguchi et al.[9], but using the tantalum content from PCBs of a PC according to Ewasteguide.info[10]

Personal Computers (PCs): average of Desktop & Laptop PCs in Oguchi OR average of available other studies.

Other small appliances: average of all other appliances in Oguchi OR average of available other studies.

A3.1.3 Electricity generation

The following assumptions were applied to derive the metal content estimates for energy generation technologies:

Off-whore wind: The minimum estimate of neodymium content in offshore windmills was based on the permanent magnet weight according to Alonso et al.[3] and the permanent magnet composition according to Long et al.[11]

Other renewables: The metal content of the IMAGE category "other renewables" was determined as the average of renewables

Oil-based technologies: The metal content of oil-based electricity generation was derived as the average of coal & gas based generation technologies.

Combined cycle power plants: Unless specific sources were available, we assumed the material use in conventional technology applies.

Carbon Capture and Sequestration (CCS): If no specific studies were available, the additional material use as specified by Moss et al.[6] is added to the metal content of conventional plants. The study by Moss et al. does not specify additional tantalum use for CCS, so in that case the conventional reference was taken.

Combined Heat and Power (CHP): Unless specific studies are available, we assumed that CHP uses the same amounts of metals per MW as the conventional plants. Only for the case of copper, we assumed an additional metal content of 1/10th of a CHP plant according to Moss et al.[6].

	Concentration data (in grams)										Weibull parameters			Categorization
	Cu		Co		Nd		Ta		Li		scale	shape	Source / comments	
Car types (g/product)	low	high	low	high	Low	high	low	high	low	high				
Internal Combustion Engine (ICE)	22,300[5]	27,333[1]	27[4]	35[1]	2[4]	415[2]	1.1[4]	8[1]	0[1]	17[4]	1.89	10.3	[12]	All ICE types in IMAGE
Hybrid Electric Vehicles (HEV)	42,188[6]	62,500[1]	118[6]	4,400[7]	118[6]	995[2]	3.47*	11[1]	120[6]	6,500[1]	1.89	10.3	[12]	All HEV types in IMAGE
Plugin Hybrid Electric Vehicles (PHEV)	41,797[7]	67,183[6]	995[6]	3,630[7]	473[7]	1,460[7]	3.47*	10.37*	988[6]	3,250[8]	1.89	10.3	[12]	All PHEV types in IMAGE
Battery Electric Vehicles (BEV)	53,373[7]	152,443[6]	4,400[8]	5,720[7]	567[7]	2,250[6]	3.47*	10.37*	3,598[7]	7,550[8]	1.89	10.3	[12]	All BEV types in IMAGE
Fuel Cell Vehicles (FCV)	22,300[5]	97,605[6]	27[4]	153[6]	2[4]	2,920[6]	1.1[4]	8[1]	0[1]	158[6]	1.89	10.3	[12]	All FCV types in IMAGE
Appliance types (g/product)														
Fan	129[13]	200[14]	0	0.3	3.5	22.5					1.3	9.4	2-01 in [15]	Cooling appliances
Air-cooler	3150	3300	0	1	11.5	75					2	13.5	1-06 in [15]	Cooling appliances
Air-conditioning	6301[9]	6600[14]	0	2[16]	23[16]	150[2]					2.8	12.3	[15]	Cooling appliances
Refridgerator	800[14]	1331[9]			1.5[17]	225[2]					2.2	16.5	[15]	Food appliances
Microwave	200[14]	1211[9]			33[2]						0.8	14.7	[15]	Food appliances
Washing Machine	1100[14]	2298[9]	0	3.2[16]	7.2[17]	312[2]					2.2	13.9	[15]	Washing appliances
Tumbler dryer	666	1391	0	1.9	4.3	189					2.6	16.5	[15]	Washing appliances
Dish washer	1250[18]	1465	0	2.0	4.6	199					1.6	13.1	[15]	Washing appliances
Television	500[14]	1260[19]					0.05[9]	0.19[9,10]*			2.1	12	4-08 in [15]	TV & video
VCR/DVD player	175[20]	196[9]			0.49[2]		0.01[9]	0.04[9]			1.7	10.5	4-04 in [15]	TV & video
PC & Laptop computers	245[9]	1070[14,19]	18.2[21]	70.4[9]	2.4[2]	2.8[22–24]	2.1[25,26]	2.6[9]	5.0[21]	8.4[9]	1.5	5.2	3-03 in [15]	Computers
Other small appliances	30[19,20]	129[9]	4.6[21]	5.5[9]	0.12[22]	0.54[2]	0.15[26]	0.97[9]	0.7[9]	1.3[21]	1.5	4	4-01 in [15]	Other small applainces
Power generation ** (g/kW)														
Solar PV	2,194[27]	10,490[28]												Solar
Concentrated Solar Power	2,300[27]	3,992[29]												Solar
Wind (onshore)	1,143[30]	4,318[29]			0	41[27]								Wind
Wind (offshore)	1,143[30]	10,000[31]			119[3,11]*	198[2]								Wind
Hydro	67[6]	3,331[32]												Hydro & other
Other Renewable	1,369	6,426			24	48	64[6]							Hydro & other
Nuclear	60[27]	1,470[33]	0	0.2[34]										Nuclear
Conv. Coal	792[35]	1,500[33]	30[36]	201[6]			0.5[6]	17[36]*						Fossil
Conv. Oil /Biomass	399	1,125	16	119			0.3	9.2						Fossil / Biomass
Conv. Natural Gas	6[37]	750[33]	2[6]	36[38]			0.07[2]	1.45[38]						Fossil
IGCC	792	1,500	30	201			0.5	17						Fossil
OGCC / Biomass CC	399	1,125	16	119			0.3	9.2						Fossil / Biomass
NG CC	1,003[39]	1,100[33]	2	36			0.07	1.45						Fossil
Coal + CCS	1,068[35]	2,192	37	209			0.5	17						Fossil+CCS
Oil/Biomass + CCS	1,091	2,192	23	126			0.3	9.2						Fossil+CCS / Biomass+CCS
Natural Gas + CCS	698	1,442	9	44			0.07	1.45						Fossil+CCS
CHP Coal	5,237	5,945	30	201			0.5	17						Fossil
CHP Oil	4,844	5,570	16	119			0.3	9.2						Fossil
CHP Natural Gas	4,451	5,195	2	36			0.07	1.45						Fossil
CHP Biomass	305[33]	5,570	16	119			0.3	9.2						Biomass
CHP Coal + CCS	5,929	6,637	37	209			0.5	17						Fossil+CCS
CHP Oil + CCS	5,536	6,262	23	126			0.3	9.2						Fossil+CCS
CHP Natural Gas + CCS	5,143	5,887	9	44			0.07	1.45						Fossil+CCS
CHP Biomass + CCS	997	6,262	23	126			0.3	9.2						Biomass+CCS

Table A3.1. *Assumptions on metal content and lifetimes for three product categories (in grams per car, grams per car appliance or grams per kW of peak electricity generation capacity). The categorization applies to the figures in the main text as well as the SI. ** PV = Photovoltaic cells, IGCC = Integrated gasification and combined cycle, OGCC = Oil Gassification & Combined Cycle, NGCC = Natural Gas Combined Cycle, CCS = Carbon Capture and Sequestration, CHP = Combined Heat and Power. Asterisks (*) indicate the use of an own estimation based on the indicated sources.*

A3.1.4 Additional assumptions for cars

Table A3.2 below provides the data used to translate passenger vehicle kilometers (IMAGE output) into the number of cars on the road, by means of kilometrage (cf. mileage) of an average car per year.

	Canada	**US**	**Europe**	**Australia**	**Japan**	**China**
Also applied to IMAGE region >	Mexico, Ukraine, Middle East, Afghanistan a.o., Russia		Central Amerika, Brazil, South America, South Afrika, Turkey		Indonesia, South-East Asia,	North-, West- and East Afrika, rest of south Afrika, rest of South Asia, India, Korea
Source & comments	[40]	[41]	[41] as an average of Finland, Belgium, Norway, the UK and Germany	[41]	[41]	[41]
1975	12638	14982	14392	15480	8851	27200
1980	11839	14183	14475	15167	8386	27200
1985	12816	15159	14436	15500	8610	27200
1990	14196	16539	15614	14667	9863	27200
1995	15292	17636	15700	14300	8978	27200
2000	16950	19294	15400	14300	8812	26400
2005	16000	19915	14989	14100	8406	26000
2008	15200	19783	15157	13900	8276	26000

Table A3.2. *The annual average passenger car kilometrage per region. The kilometrage (how many kilometers does an average car drive per year) applied is assumed to be constant at 2008 levels after this year.*

A3.1.5 Sensitivity analysis

Table A3.1 presents the high and the low assumptions on the content of five metals in almost all listed products. Only three entries remained for which only a single estimate of metal content could be made (highlighted in grey). To assess the importance of these three products in the overall outcomes, we tested for the effect of introducing a probable artificial range, based on the average range for the available products within each metal column. We did so only for the SSP2 baseline. So for the example of tantalum content in 'other renewables' we started with the estimate for geothermal energy by Moss et al.[6] and assumed it to be a medium estimate (64 g/kW, see Table A3.1). Subsequently, we calculated the average deviation from the medium value based on all other products with a tantalum content (on average 81% higher or lower). Applying this deviation to both sides of the assumed medium estimate by Moss et al. creates an artificial range for tantalum in the 'other renewables' product category (of 11.8 g/kW to 116 g/kW). Running the model with these numbers gives an average total annual tantalum demand between 2045 & 2050 that

is either 4% higher than the high baseline or 14% lower than the low baseline. When applying the same steps to the two missing estimates for neodymium products, we find a change in average annual neodymium demand that is either 1% higher than the high estimate or 9% lower than the low baseline, in the five last years of the scenario period. This indicates that excluding a range of estimates for the metal content of even a single product may in fact have a considerable effect on the outcomes in terms of total annual demand.

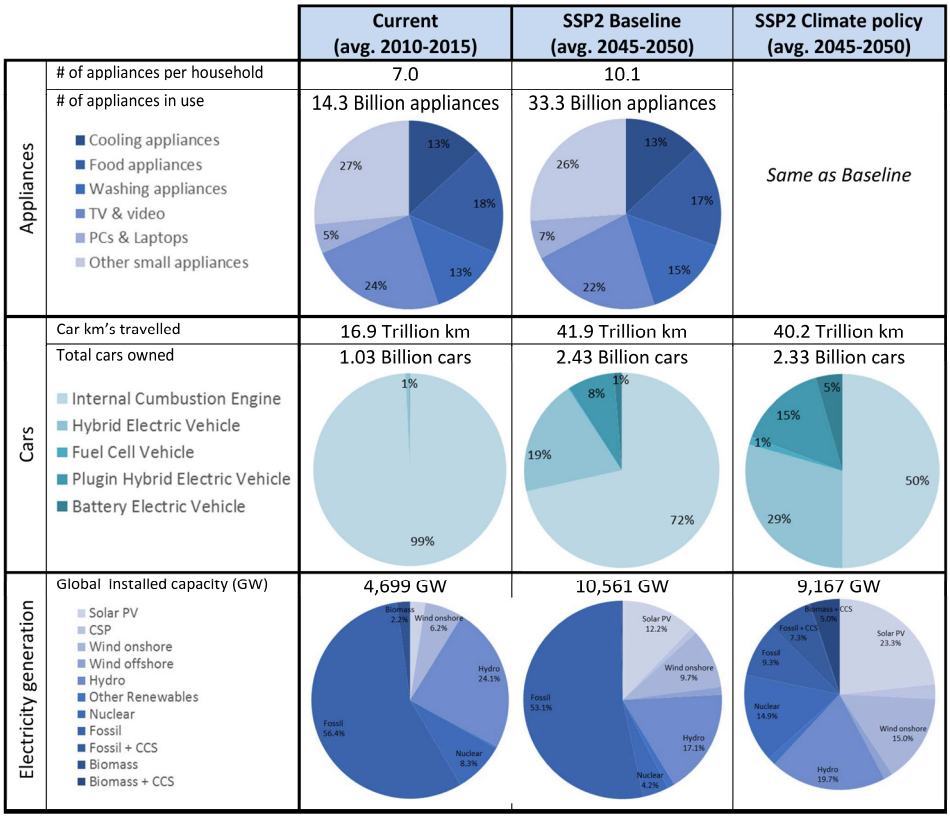

Figure A3.1. *Overview of scenario assumptions on in-use stocks of cars, appliances & electricity generation capacity.*

A3.2. Scenario assumptions and results

A3.2.1 Scenario assumptions

Figure A3.1 shows the assumptions on stocks-in-use of the three categories of applications. Though the numbers for electricity generation capacity are available independent of the

dynamic stock model, they are also provided for completeness. Because numbers on annual demand can fluctuate a lot, we decided to present all numbers as averages of recent years (2010 to 2015) and compare these to averages of the last available model years (being 2045 to 2050).

A3.2.3 Summary of metal demand under various scenarios

Below, the metal demand numbers are presented in Table A3.4. Annual metal demand (in kilotons per year) is provided for appliances, cars and energy technologies, as an average of the most recent years (2010-2015) and projections for the latest model years (2045-2050) given the SSP2 baseline and its corresponding 2-degree climate policy scenario. Numbers are rounded to 2 significant digits. Using these numbers the effect of the uncertainty in data on metal content on the scenario outcomes is depicted more visually in Figure A3.2.

Table A3.4. *Annual metal demand for appliances, cars and energy technologies.*

			Current (avg. 2010-2015)			**Baseline (avg. 2045-2050)**			**Climate policy (avg. 2045-2050)**		
			Low	**med**	**high**	**low**	**med**	**high**	**low**	**med**	**high**
Annual Metal demand (kt /yr) for selected applications	Cu	Appliances	930	1400	1800	2000	2800	3600	2000	2800	3600
		Cars	2800	3100	3500	7800	9400	11000	8900	12000	15000
		Energy tech	230	490	750	430	960	1500	520	1400	2200
		Total	**3900**	**5000**	**6000**	**10000**	**13000**	**16000**	**11000**	**16000**	**21000**
	Nd	Appliances	7.2	57	110	15	110	200	15	110	200
		Cars	2.3	27	53	33	110	180	62	160	260
		Energy tech	0.15	0.90	1.7	0.93	2.3	3.6	1.2	4.0	6.8
		Total	**10**	**85**	**160**	**49**	**220**	**380**	**78**	**270**	**470**
	Ta	Appliances	0.49	0.96	1.4	1.3	2.3	3.4	1.3	2.3	3.4
		Cars	0.14	0.56	1.0	0.48	1.5	2.4	0.61	1.5	2.5
		Energy tech	0.08	0.64	1.2	0.44	1.4	2.4	0.36	0.6	0.7
		Total	**0.71**	**2.2**	**3.6**	**2.2**	**5.2**	**8.2**	**2.3**	**4.4**	**6.6**
	Co	Appliances	7.5	12	17	18	30	45	18	31	45
		Cars	4.3	15	26	62	200	340	160	390	622
		Energy tech	2.0	8.5	15	3.4	14	25	0.91	3.3	5.6
		Total	**14**	**36**	**59**	**83**	**250**	**410**	**177.5**	**420**	**670**
	Li	Appliances	1.4	2.0	2.6	3.6	5.0	6.4	3.6	5.0	6.4
		Cars	1.3	17	33	52	249	450	140	470	800
		Energy tech	-	-	-	-	-	-	-	-	-
		Total	**2.7**	**19**	**36**	**55**	**250**	**450**	**140**	**480**	**810**

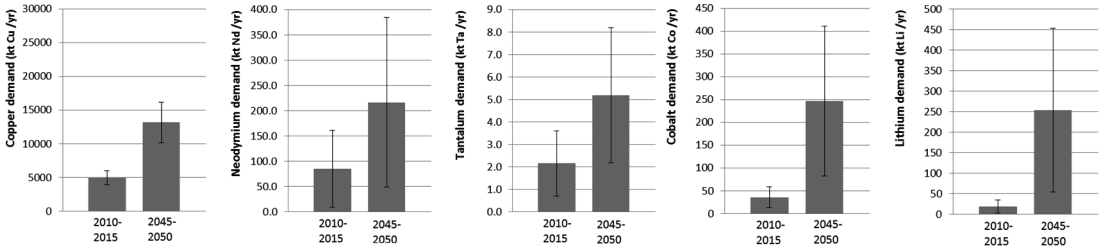

Figure A3.2. *Assessment of the effect of uncertainty for metal content data on scenario outcomes. Based on the SSP2 Baseline, presented in Table S4, the bar charts indicate the total demand of the three considered applications for each metal (in kt/yr), while the error bars show the outcomes using the low and the high metal content estimates.*

References to Appendix 3

1. Cullbrand, K. & Magnusson, O. The use of potentially critical materials in passenger cars. (2012).
2. Habib, K. Critical Ressources in Clean Energy Technologies and Waste Flows. (Syddansk Universitet, 2015).
3. Alonso, E. *et al.* Evaluating Rare Earth Element Availability: A Case with Revolutionary Demand from Clean Technologies. *Environ. Sci. Technol.* 46, 3406–3414 (2012).
4. Widmer, R., Du, X., Haag, O., Restrepo, E. & Wäger, P. A. Scarce metals in conventional passenger vehicles and end-of-life vehicle shredder output. *Environ. Sci. Technol.* 49, 4591–4599 (2015).
5. Hawkins, T. R., Singh, B., Majeau-Bettez, G. & Strømman, A. H. Comparative Environmental Life Cycle Assessment of Conventional and Electric Vehicles. *J. Ind. Ecol.* 17, 53–64 (2013).
6. Moss, R. L. *et al.* Critical metals in the path towards the decarbonisation of the EU energy sector. *Assessing rare metals as supply-chain bottlenecks in low-carbon energy technologies. JRC Report EUR* 25994, (2013).
7. Elwert, T. *et al.* Current Developments and Challenges in the Recycling of Key Components of (Hybrid) Electric Vehicles. *Recycling* 1, 25–60 (2015).
8. U.S. Department of Energy. Critical Materials Strategy. 194 (2011).
9. Oguchi, M., Murakami, S., Sakanakura, H., Kida, A. & Kameya, T. A preliminary categorization of end-of-life electrical and electronic equipment as secondary metal resources. *Waste Manag.* 31, 2150–2160 (2011).
10. Ewasteguide.info. Valuable Substances in e-waste. (2016).
11. Long, K. R., Van Gosen, B. S., Foley, N. K. & Cordier, D. The Principal Rare Earth Elements Deposits of the United States: A Summary of Domestic Deposits and a Global Perspective. in *Non-Renewable Resource Issues* 131–155 (Springer Netherlands, 2012). doi:10.1007/978-90-481-8679-2_7
12. Nomura, K. & Suga, Y. *Asset Service Lives and Depreciation Rates bas ed on Disposal Data in Japan*. (2013).
13. Schneider Electric. Product Environmental Profile of the ClimaSys CV. (2011).
14. Zhang, L., Yuan, Z. & Bi, J. Estimation of Copper In-use Stocks in Nanjing, China. *J. Ind. Ecol.* 16, 191–202 (2012).
15. Wang, F., Huisman, J., Stevels, A. & Baldé, C. P. Enhancing e-waste estimates: Improving data quality by multivariate Input-Output Analysis. *Waste Manag.* 33, 2397–2407 (2013).
16. Arai, Y., Koga, S., Hoshina, H., Yamaguchi, S. & Kondo, H. Recycling of Rare Earth Magnet from Used Home Appliances. *Mater. Cycles Waste Manag. Res.* 22, 41–49 (2011).
17. Seo, Y. & Morimoto, S. Comparison of dysprosium security strategies in Japan for 2010–2030. *Resour. Policy* 39, 15–20 (2014).
18. Truttmann, N. & Rechberger, H. Contribution to resource conservation by reuse of electrical and electronic household appliances. *Resour. Conserv. Recycl.* 48, 249–262 (2006).

19. Tickner, J., Rajarao, R., Lovric, B., Ganly, B. & Sahajwalla, V. Measurement of Gold and Other Metals in Electronic and Automotive Waste Using Gamma Activation Analysis. *J. Sustain. Metall.* 2, 1–8 (2016).
20. Namias, J. The future of electronic waste recycling in the United States: Obstacles and domestic solutions. (Columbia University, 2013).
21. Patrício, J., Kalmykova, Y., Berg, P. E. O., Rosado, L. & Åberg, H. Primary and secondary battery consumption trends in Sweden 1996–2013: method development and detailed accounting by battery type. *Waste Manag.* 39, 236–245 (2015).
22. Crock, W. D. Mapping stocks and flows of neodymium: An assessment of neodymium production and consumption in the Netherlands in 2010 and 2030. (TU Delft, Delft University of Technology, 2016).
23. Schulze, R. & Buchert, M. Estimates of global REE recycling potentials from NdFeB magnet material. *Resour. Conserv. Recycl.* 113, 12–27 (2016).
24. Sprecher, B. *et al.* Life Cycle Inventory of the Production of Rare Earths and the Subsequent Production of NdFeB Rare Earth Permanent Magnets. *Environ. Sci. Technol.* 48, 3951–3958 (2014).
25. Deetman, S., van Oers, L., van der Voet, E. & Tukker, A. Deriving European Tantalum Flows Using Trade and Production Statistics. *J. Ind. Ecol.* in press, (2016).
26. Chancerel, P., Marwede, M., Nissen, N. F. & Lang, K.-D. Estimating the quantities of critical metals embedded in ICT and consumer equipment. *Resour. Conserv. Recycl.* 98, 9–18 (2015).
27. Moss, R. L., Tzimas, E., Kara, H., Willis, P. & Kooroshy, J. *Critical Metals in Strategic Energy Technologies, Assessing Rare Metals as Supply-Chain Bottlenecks in Low-Carbon Energy Technologies*. *JRC Scientific and Technical Reports* (Publications Office of the European Union, 2011). doi:doi:10.2790/35716
28. Pihl, E., Kushnir, D., Sandén, B. & Johnsson, F. Material constraints for concentrating solar thermal power. *Energy* 44, 944–954 (2012).
29. BBF Associates; Kundig, K. J. A. Market study: Current and projected wind and solar renewable electric generating capacity and resulting copper demand. (2011).
30. Öhrlund, I. Future Metal Demand from Photovoltaic Cells and Wind Turbines–Investigating the Potential Risk of Disabling a Shift to Renewable Energy Systems. *Science and Technology Options Assessment (STOA)* 72 (2012).
31. Elshkaki, A. & Graedel, T. E. Dynamic analysis of the global metals flows and stocks in electricity generation technologies. *J. Clean. Prod.* 59, 260–273 (2013).
32. Flury, K. & Frischknecht, R. Life cycle inventories of hydroelectric power generation. *ESU-Services, Fair Consult. Sustain. Comm. by€ Oko-Institute eV* 1–51 (2012).
33. Dones, R. *et al. Sachbilanzen von Energiesystemen; Ecoinvent V2.0 report no. 6*. (2007).
34. Bhaduri, A. K. *et al.* Selection of hardfacing material for components of the Indian Prototype Fast Breeder Reactor. *J. Nucl. Mater.* 334, 109–114 (2004).
35. Singh, B., Bouman, E. A., Strømman, A. H. & Hertwich, E. G. Material use for electricity generation with carbon dioxide capture and storage: Extending life cycle analysis indices for material accounting. *Resour. Conserv. Recycl.* 100, 49–57 (2015).
36. Weitzel, P. S. *et al. Advanced Ultra-Supercritical Power Plant (700 to 760C) Design for Indian Coal*. *Proceedings of Power-Gen Asia, Thailand* (2012).
37. Meier, P. J. Life-Cycle Assessment of Electricity Generation Systems and Appliacations for Climate Change Policy Analysis. *Fusion Technology Institute* PhD, (University of Wisconsin - MAdison, 2002).
38. National Research Council. *Materials for Large Land-based Gas Turbines: Report of the Committee on Materials for Large Land-Based Gas Turbines, National Materials Advisory Board*. (National Academy Press, 1986).
39. S&T2 consultants. *A Review of GHG emissions from Plant Construction and DEcommissioning*. (Natural Resources Canada, 2006).
40. Natural Resources Canada. *Canadian Vehicle Survey 2009; summary report*. (2009). doi:ISSN 1927-4300
41. Pauliuk, S., Dhaniati, N. M. A. & Müller, D. B. Reconciling Sectoral Abatement Strategies with Global Climate Targets: The Case of the Chinese Passenger Vehicle Fleet. *Environ. Sci. Technol.* 46, 140–147 (2012).

Appendix 4

Based on the supplementary information provided with:
Marinova et al. (2020) - *Global construction materials database and stock analysis of residential buildings between 1970-2050* - Journal of Cleaner Production, Vol. 247, p. 119146 https://doi.org/10.1016/j.jclepro.2019.119146

A4.1 Corrigendum

The following corrigendum was reported to the journal of Cleaner Production, under ref. 119146: The authors regret to report that despite extensive efforts to review the work presented in this study, an error was made in the calculations. This has led to inaccurate reporting of the results for aluminium and glass in residential buildings detailed in Section 4.3.2.2. Results regarding floor space, other materials and service-sector buildings remain unchanged, and textual conclusions drawn from this work remain accurate. However, we feel the responsibility to provide the corrected figures and outcomes as detailed below. A corrected version of the model code can be found through the following link: https://github.com/SPDeetman/BUMA. Because the text in the manuscript remains unchanged, we only provide the corrected figures as shown below. The authors would like to apologise for any inconvenience caused.

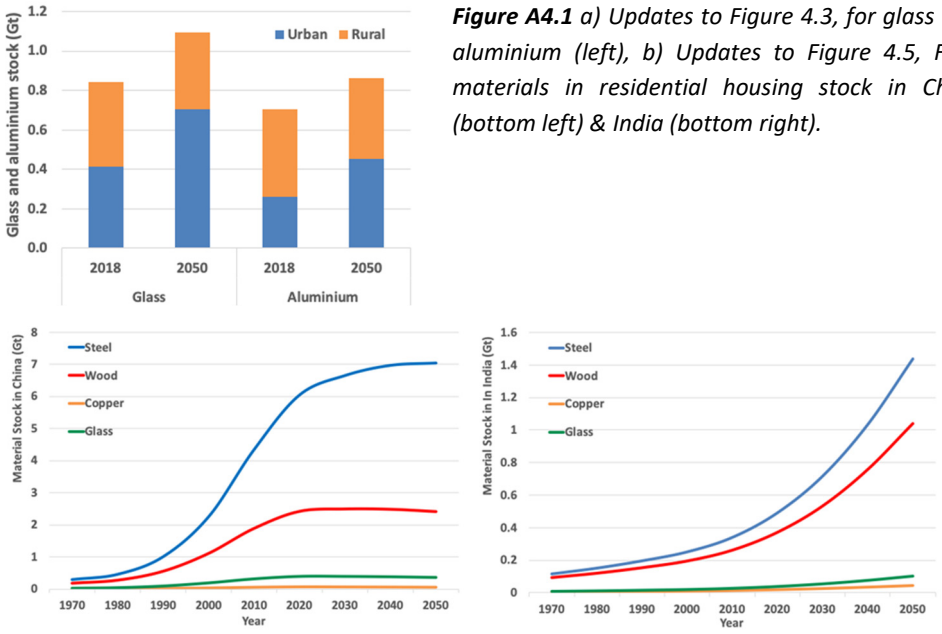

Figure A4.1 *a) Updates to Figure 4.3, for glass and aluminium (left), b) Updates to Figure 4.5, Four materials in residential housing stock in China (bottom left) & India (bottom right).*

A4.2 Usable floor area

In Table A4.1 we present detailed information on the average per capita floor space disaggregated in four dwelling types: detached house, row house, apartment buildings, high-rise buildings. The data is based on all available studies reviewed and presented in Chapter 4.

Due to lack of data we cannot provide accurate estimations of the average per capita square meters for certain regions and building types. In these cases, we apply global average values. The asterisk identifies the data directly available from the literature. The rest of the table is filled with the global average on all other available studies.

It is important to note that we use the global averages displayed in Table A4.1. solely to allocate the IMAGE data to the four building types. This approach is not ideal since our data is based mostly on developed regions and therefore it could be considered biased when applied to less developed countries. However, given the experimental nature of our model we believe that for the time being the numbers which we obtained are suitable to distribute the IMAGE data across the different building types. It is important to mention that future development of the data is necessary in order to provide as accurate as possible predictions for the development of the building stock.

Interestingly, the static data on per capita floorspace in the four building types suggests that urban housing, on average, provides a larger per capita floorspace than rural housing. This is in contrast to the IMAGE data, which assumes rural houses to be larger (even at a per capita basis, see Table A4.1). This difference is influenced by two data points from one individual study conducted by Bhochhibhoya et al. (2017)[1] included in the database. The paper focuses on the greenhouse gas emissions associated with three buildings located at rural area in Nepal. The data points display significantly lower value for per capita square meter (7.67 m^2/cap) in comparison to per capita floorspace values for rural buildings located in Turkey (22 m^2/cap) [2], India (32.63 m^2/cap) [3] and China (63.51 m^2/cap) [4]. Despite the fact that two data points are shifting the results, we decided to not exclude the study from the per capita floorspace calculations since Nepal is one of the few representatives for rural areas in Least Developed Countries (LDCs) [5]. In addition, we chose to not adjust our model for this discrepancy. However, we believe this issue should be explored and adjusted in future research, as elaborated in the discussion.

Table A4.1. *Average per capita floor space (m2/cap) (L). The asterisk (*) identifies the regional data directly available from the literature. The rest of the table is filled with the global average on all other available studies.*

Region	Area	Detached houses	Row houses	Apartments	High-rise buildings
1	Urban	42.88*	40.65	28.61	39.00*
1	Rural	33.00	32.61	22.00	31.40
2	Urban	50.98*	40.65	25.81*	20.90*
2	Rural	33.00	32.61	22.00	31.40
3	Urban	34.36	40.65	28.61	31.40
3	Rural	33.00	32.61	22.00	31.40
4	Urban	34.36	40.65	28.61	31.40
4	Rural	33.00	32.61	22.00	31.40
5	Urban	41.55*	40.65	28.61	13.93*
5	Rural	33.00	32.61	22.00	31.40
6	Urban	22.70*	35.00*	29.00*	31.40
6	Rural	33.00	32.61	22.00	31.40
7	Urban	34.36	40.65	28.61	31.40
7	Rural	33.00	32.61	22.00	31.40
8	Urban	17.12*	40.65	27.00*	31.40
8	Rural	33.00	32.61	22.00	31.40
9	Urban	34.36	40.65	28.61	31.40
9	Rural	33.00	32.61	22.00	31.40
10	Urban	13.67	40.65	13.67*	31.40
10	Rural	33.00	32.61	22.00	31.40
11	Urban	31.71*	28.13*	35.69*	34.50*
11	Rural	56.52*	32.61*	22.00	31.40
12	Urban	23.90*	40.65	37.00*	35.27*
12	Rural	33.00	32.61	22.00	31.40
13	Urban	34.36	40.65	28.61	65.00*
13	Rural	33.00	32.61	22.00*	31.40
14	Urban	34.36	40.65	28.61	31.40
14	Rural	33.00	32.61	22.00	31.40
15	Urban	34.36	40.65	28.61	31.40
15	Rural	33.00	32.61	22.00	31.40
16	Urban	34.36	40.65	28.61	31.40
16	Rural	33.00	32.61	22.00	31.40
17	Urban	57.52*	40.65	28.25*	31.40
17	Rural	33.00	32.61	22.00	31.40
18	Urban	13.27*	40.65	10.00*	28.04*
18	Rural	32.63*	32.61	22.00	31.40
19	Urban	34.36	40.65	16.32*	28.65*
19	Rural	33.00	32.61	22.00	31.40
20	Urban	17.50*	40.65	41.37	25.47*
20	Rural	35.20*	32.61	22.00	31.40
21	Urban	34.36	44.28*	27.77*	31.40
21	Rural	33.00	32.61	22.00	31.40
22	Urban	29.00	40.65	28.61	21.25*
22	Rural	33.00	32.61	22.00	31.40
23	Urban	31.34*	40.65	28.61	30.08*

23	Rural	33.00	32.61	22.00	31.40
24	Urban	38.25*	49.55*	36.85*	17.18*
24	Rural	33.00	32.61	22.00	31.40
25	Urban	34.36	40.65	28.61	31.40
25	Rural	7.67*	32.61	22.00	31.40
26	Urban	34.36	40.65	28.61	31.40
26	Rural	33.00	32.61	22.00	31.40

A4.3 Material content

Table A4.2 presents data on the material contents in each region across the four dwelling types. The building types are depicted by a code: 1 for detached houses, 2 for row houses, 3 for apartment buildings and 4 for high-rise buildings. The construction materials presented in this study we considered as commonly used in the built environment and are steel, cement, concrete, wood, copper, aluminium and glass.

Table A4.2. *Average material contents (kg/m^2) across the four different dwelling types and are separated into seven different construction materials: steel, cement, concrete, wood, copper, aluminium and glass. The asterisk (*) identifies the regional data directly available from the literature. The rest of the table is filled with the global average on all other available studies.*

Region	Building types	Steel	Concrete	Wood	Copper	Aluminium	Glass
1	1	32.31*	876.71*	48.75*	1.73	9.27*	2.68
1	2	32.89	1208.13	34.97	0.01	0.23	1.07
1	3	97.36	995.92	37.17	0.31	1.94	6.35
1	4	45.78*	1040.35*	28.66*	0.01	2.20	1.20*
2	1	7.26*	472.10*	48.45*	0.80*	1.84*	3.32*
2	2	32.89	1208.13	34.97	0.01	0.23	1.07
2	3	1.24*	57.69*	37.17	0.31	4.92*	6.35
2	4	61.48*	265.24*	54.48	0.01	3.05*	4.42
3	1	32.63	846.33	53.07	1.73	3.56	2.68
3	2	32.89	1208.13	34.97	0.01	0.23	1.07
3	3	97.36	995.92	37.17	0.31	1.94	6.35
3	4	116.98	910.21	54.48	0.01	2.20	4.42
4	1	35.50*	735.00*	90.00*	1.73	3.56	2.68
4	2	27.00*	1315.00*	40.00*	0.01	0.23	1.07
4	3	97.36	995.92	37.17	0.31	1.94	6.35
4	4	116.98	910.21	54.48	0.01	2.20	4.42
5	1	32.63	897.65*	868.96*	1.73	3.56	0.80*
5	2	32.89	1208.13	34.97	0.01	0.23	1.07
5	3	97.36	995.92	37.17	0.31	1.94	6.35
5	4	116.98	611.19*	20.63*	0.01	2.20	0.66*
6	1	35.15*	607.64*	19.78*	1.73	3.56	1.18*
6	2	39.29*	894.86*	17.68*	0.01	0.23	1.07*

Region	Building types	Steel	Concrete	Wood	Copper	Aluminium	Glass
6	3	37.50*	933.00*	2.70*	0.31	1.94	1.80*
6	4	116.98	910.21	54.48	0.01	2.20	4.42
7	1	32.63	846.33	53.07	1.73	3.56	2.68
7	2	32.89	1208.13	34.97	0.01	0.23	1.07
7	3	97.36	995.92	37.17	0.31	1.94	6.35
7	4	116.98	910.21	54.48	0.01	2.20	4.42
8	1	8.93*	675.66*	6.89*	1.73	2.89*	0.04*
8	2	32.89	1208.13	34.97	0.01	0.23	1.07
8	3	26.73*	995.92	42.06*	0.31	1.94	6.35
8	4	116.98	910.21	54.48	0.01	2.20	4.42
9	1	32.63	846.33	53.07	1.73	3.56	2.68
9	2	32.89	1208.13	34.97	0.01	0.23	1.07
9	3	97.36	995.92	37.17	0.31	1.94	6.35
9	4	116.98	910.21	54.48	0.01	2.20	4.42
10	1	32.63	846.33	53.07	0.77*	3.56	2.68
10	2	32.89	1208.13	34.97	0.01	0.23	1.07
10	3	97.36	995.92	37.17	0.39*	1.94	6.35
10	4	116.98	910.21	54.48	0.01	2.20	4.42
11	1	47.90*	1507.04*	77.29*	3.11*	0.93*	2.51*
11	2	24.63*	796.02*	35.77*	0.01	0.23*	1.07
11	3	76.24*	567.99*	49.88*	0.15*	0.46	11.21*
11	4	142.30*	850.70*	27.00*	0.01*	2.20	4.75*
12	1	32.63	1892.83*	99.36*	1.73	3.56	33.54*
12	2	32.89	1208.13	34.97	0.01	0.23	1.07
12	3	97.36	810.86*	22.71*	0.31	1.94	6.35
12	4	116.98	902.59*	2.54*	0.01	2.20	4.42
13	1	32.63	846.33	53.07	1.73	3.56	2.68
13	2	32.89	1208.13	34.97	0.01	0.23	1.07
13	3	75.50*	1507.64*	9.57*	0.31	1.94	6.35
13	4	40.65*	768.27*	8.08*	0.01	2.20	4.42
14	1	32.63	846.33	53.07	1.73	3.56	2.68
14	2	32.89	1208.13	34.97	0.01	0.23	1.07
14	3	97.36	995.92	37.17	0.31	1.94	6.35
14	4	116.98	910.21	54.48	0.01	2.20	4.42
15	1	32.63	846.33	53.07	1.73	3.56	2.68
15	2	32.89	1208.13	34.97	0.01	0.23	1.07
15	3	97.36	995.92	37.17	0.31	1.94	6.35
15	4	116.98	910.21	54.48	0.01	2.20	4.42
16	1	32.63	846.33	53.07	1.73	3.56	2.68
16	2	32.89	1208.13	34.97	0.01	0.23	1.07
16	3	97.36	995.92	37.17	0.31	1.94	6.35
16	4	116.98	910.21	54.48	0.01	2.20	4.42
17	1	102.55*	1641.98*	11.88*	1.73	0.73*	2.72*
17	2	32.89	1208.13	34.97	0.01	0.23	1.07
17	3	335.19*	1926.32*	37.17	0.31	1.94	6.35

Region	Building types	Steel	Concrete	Wood	Copper	Aluminium	Glass
17	4	116.98	910.21	54.48	0.01	2.20	4.42
18	1	20.77*	1069.50*	17.41*	2.02*	3.56	2.60*
18	2	32.89	1208.13	34.97	0.01	0.23	1.07
18	3	21.16*	1005.80*	37.17	0.31	1.94	6.35
18	4	121.21*	1733.60*	54.48	0.01	2.20	4.42
19	1	32.63	846.33	53.07	1.73	3.56	2.68
19	2	32.89	1208.13	34.97	0.01	0.23	1.07
19	3	106.51*	2319.18*	37.17	0.73*	1.94	6.35
19	4	63.31*	932.62*	54.48	0.01	2.20	9.25*
20	1	25.80*	2613.94*	36.92*	1.73	10.21*	7.82*
20	2	32.89	1208.13	34.97	0.01	0.23	1.07
20	3	374.30*	995.92	15.04*	0.25*	1.94	6.35
20	4	128.95*	295.01*	61.89*	0.01	3.43*	1.97*
21	1	32.63	846.33	53.07	1.73	3.56	2.68
21	2	37.93	2729.51	54.65	0.01	0.23	1.07
21	3	33.95*	1164.02*	11.26*	0.31	0.44*	0.78*
21	4	116.98	910.21	54.48	0.01	2.20	4.42
22	1	28.39*	25.78*	107.15*	1.73	3.56	1.60*
22	2	32.89	1208.13	34.97	0.01	0.23	1.07
22	3	97.36	995.92	37.17	0.31	1.94	6.35
22	4	116.98	910.21	54.48	0.01	0.33*	0.73*
23	1	57.22*	224.67*	76.00*	1.73	1.50*	4.00*
23	2	32.89	1208.13	34.97	0.01	0.23	1.07
23	3	97.36	995.92	37.17	0.31	1.94	6.35
23	4	304.33*	1871.00*	18.00*	0.01	2.00*	2.00*
24	1	21.05*	627.84*	67.25*	1.14*	1.90*	1.06*
24	2	35.58*	795.98*	29.49*	0.01*	0.23	1.07
24	3	49.41*	701.25*	37.17	0.01*	1.94	6.35
24	4	120.72*	1136.39*	176.66*	0.01	2.20	7.30*
25	1	32.63	846.33	34.04*	1.73	3.56	2.68
25	2	32.89	1208.13	34.97	0.01	0.23	1.07
25	3	97.36	995.92	37.17	0.31	1.94	6.35
25	4	116.98	910.21	54.48	0.01	2.20	4.42
26	1	32.63	846.33	53.07	1.73	3.56	2.68
26	2	32.89	1208.13	34.97	0.01	0.23	1.07
26	3	97.36	995.92	37.17	0.31	1.94	6.35
26	4	116.98	910.21	54.48	0.01	2.20	4.42

A4.4 Steel in residential buildings in China: literature comparison

The Chinese in-use steel stock data coming from our model show very high values in comparison with the rest of the world regions. We therefore performed a sanity check of

our results by comparing them with steel stock estimations from the literature (see Table A4.3).

Pauliuk et al. (2013b) [6] developed a dynamic stock model to estimate the present in-use stock of the steel on a global level. The in-use stock is divided into four product categories (transportation, machinery, construction and products) within ten regions. In addition, Pauliuk et al. (2013a) [7] modeled the in-stock and future demand of the steel on a global level. Table A4.3 shows that our estimates are in the same order or magnitude as ours. Compared to our results Pauliuk et al. (2013a and b) [6,7] show a smaller initial steel stock, but a larger stock in 2050 compared to our estimates.

Hatayama et al. (2010) [8] analysed global steel use using a dynamic MFA. The steel in-use stock and future demand is estimated for three categories (buildings, civil engineering (infrastructure) and vehicles). The future building stock is modelled by a logistic function including parameters such as GDP, population density and saturation value per capita. Hatayama shows results for the whole of Asia, of which China is an important part. According to Hatayama et al. (2010) [8], Asia's steel stock will be at the level of 35 Gt in 2050, 21 of which will reside in buildings. Our estimate for Asia as a whole is around 11 Gt. Note that our estimates include residential buildings only.

Table A4.3. *Comparison of steel in-use stock estimates for China.*

	Pauliuk et al. (2013a), 2000-2005, China [7]	Pauliuk et al. (2013b), 2050, China [6]	Hatayama et al. (2010) 2050, Asia [8]
Steel stock from literature (Gt)	2.6 in total, 1.6 in buildings*	17 in total, 10 in buildings*	35 for whole of Asia, 21 in buildings
Our estimated steel stock in residential buildings (Gt)	2.2	7	11 for whole of Asia

*calculated from Pauliuk et al. estimate of 2 tons/cap in the early 2000s and 13 ton/cap in 2050, and a population of 13 million in both 2000 and 2050 in accordance with SSP2.

A4.5 Sensitivity analysis

A4.5.1 Description

In order to estimate the uncertainties related to the material intensity parameter and its influence on the model outcomes, we performed a sensitivity analysis using three different alternative values for the material content in terms of kg/m2 UFA. The effect on the modelled material stock development is estimated under these three "sensitivity scenarios". As the number of measurements for the individual regions is often too low, we performed this analysis at the global level only and disregarded the regional specificity of the material intensities of residential buildings. In addition, we aggregated over the four different building types, for the same reason.

In sensitivity scenario 1, we estimate the global material stock considering the mean global value for each material. Sensitivity scenario 2 is based on the values representing the 20th percentile, and sensitivity scenario 3 considers the values depicting the 80th percentile. In that way, we have some idea of the variability of the results.

A4.5.2 Outcomes and discussion

The outcomes from the sensitivity analysis are presented in Table A4.4 and Figure A4.3. Table A4.4 displays the mean, the 80th percentile, 20th percentile and the median scenarios compared to the model outcome based on averages for the period between 2045-2050, as specified in Chapter 4. The numbers in Table A4.4 represent differences in the outcome compared to the modelling results in Chapter 4 in percentages. The red numbers represent lower modelling outcomes while the green numbers show an increase in the stock in relation to the original results. The outcomes presented in Table A4.4 show that assuming a global mean material intensity does not lead to very different results for the materials stock estimates near the end of the modelled period. Only for copper, using mean values lead to slightly higher stock estimates while the other material stocks show lower values.

This can be explained with the fact that the material content of copper for square meter for certain building types (e.g. copper in row houses and apartment buildings) is relatively low as shown in Table 4.2 in Chapter 4. In addition, the same table shows that the global average of copper for detached houses is rather high in comparison with the rest of the dwelling types.

Table A4.4. *Effects of the sensitivity variants on selected material demand indicators. The percentages indicate the change with respect to the same indicators under the default analysis presented in Chapter 4. The* ***bold*** *numbers indicate an increase in the stock, while the italic numbers indicate a decrease.*

Indicator	Year	Mean MI	80th Percentile	20th Percentile	Median
Steel stock	2045 - '50	*-14%*	**8%**	*-67%*	*-35%*
Concrete stock	2045 - '50	*-16%*	**4%**	*-60%*	*-22%*
Glass stock	2045 - '50	*-18%*	**22%**	*-72%*	*-41%*
Wood stock	2045 - '50	*-10%*	**34%**	*-64%*	*-34%*
Aluminium stock	2045 - '50	*-17%*	**21%**	*-73%*	*-57%*
Copper stock	2045 - '50	**2%**	**35%**	*-86%*	*-53%*

Thus, applying the global mean and disregarding of the different regions results in a higher value for building types which in reality contain low amount of the material. Copper and glass are the construction materials showing the smallest difference between the applied and the mean scenario. This might indicate that the intensity of the materials is rather standard and the fluctuations in the data range are limited. The lower mean values for the stock of the rest of the materials might be explained by a very high values for material intensities, for instance the amount of concrete in detached houses in China. The value for concrete used for detached houses in this region are two times higher than the global mean value which could lead to decline in the mean variant compared to the applied scenario, as China represents an important share of the global stock. This outcome suggests the importance of using (and collecting) regional specific data.

The 80th percentile variant shows significantly higher stock estimations for the period between 2045-2050, as expected. The only exception is concrete (4%). This once again can be explained with the significantly higher mean value of the material intensity of the concrete in detached houses in China in relation to the global average, that contribute so much to the global stock.

The stock estimates based on the 20th percentile values for material content are much lower than either the applied, the mean or the median scenarios, by 60-70% for most materials and by over 80% for copper. We explain that with the wilder range of the data for copper resulted from the differences in the material intensity in the different regions and dwelling types. One reason could be the limited amount of data for copper, another could be the actual differences in the amount of copper used in buildings given that the material has a various purposes and the amount used could significantly vary across residential buildings [9,10].

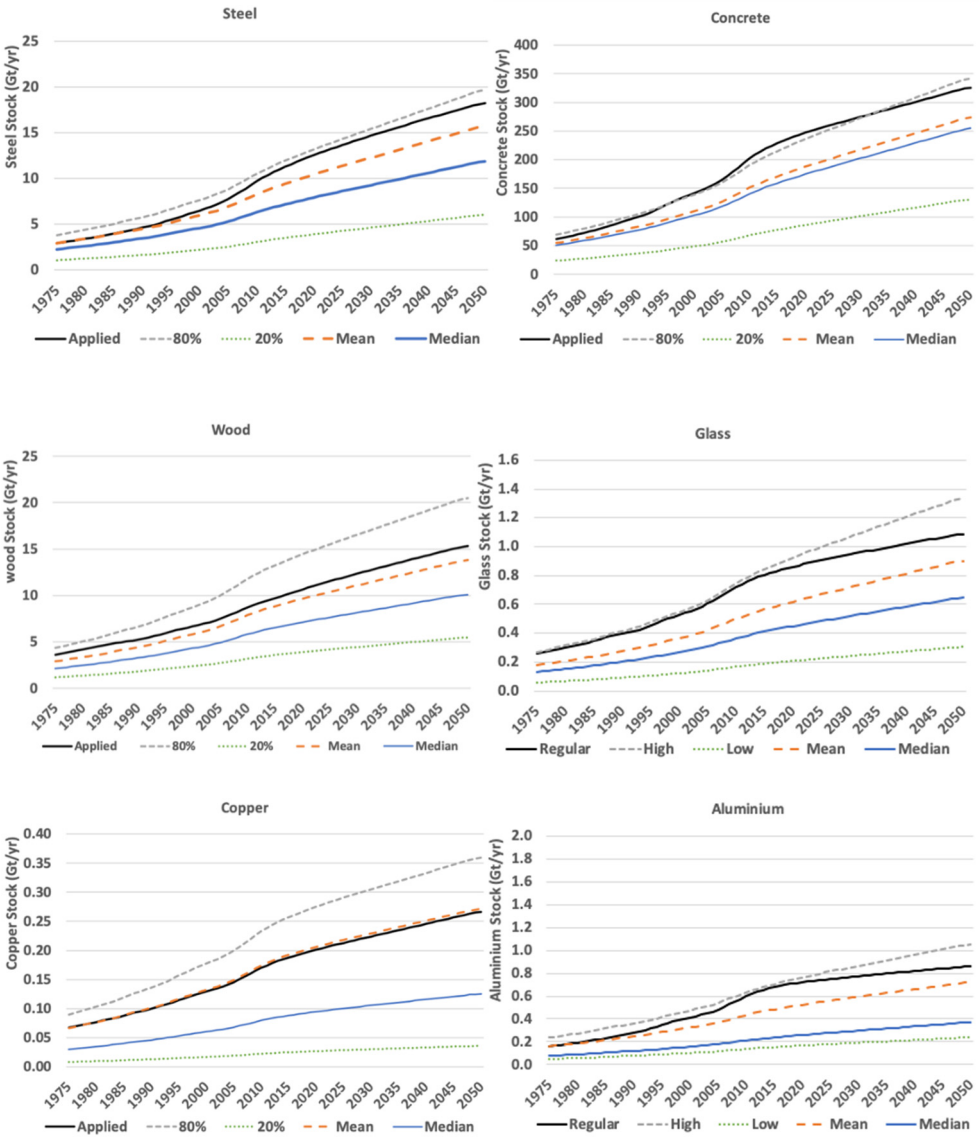

Figure A4.3. *Annual global stock development under four sensitivity variants. "Applied" shows the original data and the results as described in Chapter 4. The "Mean" depicts the global mean material content. The "Median" shows the "middle" value for each material. The "20%" assumes the global values for 20th percentile and "80%" represents the global values for 80th percentile as identified in Figure 4.2 in Chapter 4.*

The median scenario shows lower stock estimation in comparison with the applied, mean and 80th percentile scenarios. This can be explained with the fluctuation of the range of data and having extreme values for certain regions. This fact once again highlights the importance of the regional desegregation as the different regions are characterised by different architectural styles and preferred materials.

The 20th and 80th percentile values could be interpreted as the range of modelling outcomes based on data variability. The range is considerable: in most cases, a factor 4 difference between highest and lowest values is visible in the results, and a higher factor difference for materials with fewer data points. This indicates there is a high variability in the material content of dwellings. It also points to the need for a more consistent collection, as well as typology of buildings. Another interesting observation is that both the mean and the applied values are much closer to the 80th percentile values than to the 20th percentile values. Apparently, the bulk of the measurements are closer to the higher values, indicating the lower values might represent atypical situations.

In all, we can conclude that the database on material contents for doing such stock assessments is sufficient to arrive at order-of-magnitude credible values, but still is limited and lacks a lot of detail regarding regional differentiation and differentiation over the housing types. The sensitivity for reginal differentiation is large and the database not always allows regional differentiation. This is a challenge to be taken up by researchers, but especially by architects, construction companies and demolishers. We hope the database will be further developed to allow more robust outcomes.

References to Appendix 4

1. Bhochhibhoya, S. *et al.* The global warming potential of building materials: an application of life cycle analysis in Nepal. *Mt. Res. Dev.* 37, 47–55 (2017).
2. Atmaca, A. & Atmaca, N. Life cycle energy (LCEA) and carbon dioxide emissions (LCCO2A) assessment of two residential buildings in Gaziantep, Turkey. *Energy Build.* 102, 417–431 (2015).
3. Sharma, A. & Marwaha, B. M. A methodology for energy performance classification of residential building stock of Hamirpur. *HBRC J.* (2015). doi:10.1016/j.hbrcj.2015.11.003
4. Yang, X., Hu, M., Wu, J. & Zhao, B. Building-information-modeling enabled life cycle assessment, a case study on carbon footprint accounting for a residential building in China. *J. Clean. Prod.* (2018). doi:10.1016/j.jclepro.2018.02.070
5. Least Developed Country Category: Nepal Profile | Economic Analysis & Policy Division. *Nations, Development Policy & Analysis Division | Dept of Economic & Social Affairs | United* (2019).
6. Pauliuk, S., Wang, T. & Müller, D. B. Steel all over the world: Estimating in-use stocks of iron for

200 countries. *Resour. Conserv. Recycl.* 71, 22–30 (2013).

7. Pauliuk, S., Milford, R. L., Müller, D. B. & Allwood, J. M. The steel scrap age. *Environ. Sci. Technol.* 47, 3448–3454 (2013).
8. Hatayama, H., Daigo, I., Matsuno, Y. & Adachi, Y. Outlook of the world steel cycle based on the stock and flow dynamics. *Environ. Sci. Technol.* 44, 6457–6463 (2010).
9. Rathi, M. K. & Patil, A. K. Use of Aluminium In Building Construction. 1–7 (2013).
10. Gontia, P., Nägeli, C., Rosado, L., Kalmykova, Y. & Österbring, M. Material-intensity database of residential buildings: A case-study of Sweden in the international context. *Resour. Conserv. Recycl.* 130, 228–239 (2018).

Appendix 5

Based on the supplementary information provided with:
Deetman et al. (2020) - Modelling global material stocks and flows for residential and service sector buildings towards 2050 - Journal of Cleaner Production, Volume 245, pages 118658 - https://doi.org/10.1016/j.jclepro.2019.118658

A5.1 Corrigendum

The following corrigendum was reported to the journal of Cleaner Production, under ref. 118658: The authors regret to report that despite extensive efforts to review the work presented in this study, an error was made in the calculations. This has led to inaccurate reporting of the results for aluminium and glass in residential buildings detailed in Section 5.3.3 and 5.4.1 and the Supplementary Information. Results regarding floor space, other materials and service-sector buildings remain unchanged, and textual conclusions drawn from this work remain accurate. However, we feel the responsibility to provide the corrected figures and outcomes as detailed below. A corrected version of the model code can be found through the following link: https://github.com/SPDeetman/BUMA. The authors would like to apologize for any inconvenience caused.

With regard to Section 5.3.3, the total annual demand for glass by the end of the scenario period (2045-2050) changes to 61Mt (89Mt before), and the demand for aluminium changes to 39Mt (instead of the 52Mt reported before). This also affects the reported growth rates between 2015 and 2050, which increase to 35% for glass and to 9% for aluminium (up from 22% and 5%, respectively). The corresponding maximum fraction of the inflow that could theoretically be fulfilled by the outflow decreases to 60% for glass and to 68% for aluminium (down from 64% and 71% respectively). The latter is also mentioned in the abstract and the conclusions. Finally, the sensitivity analysis, reported in Section 5.4.1, indicated that assuming a mean global material intensity would lead to 18% lower demand for aluminium, which should have been 21%, given the model corrections. Per capita stocks for aluminium reported by our model, displayed in Table 5.4, should read 0.19 t/cap (globally by 2030) and 0.13 t/cap (for Japan, 2010). The corrected figures are shown below.

A5.2 Regression analysis for service sector floorspace

As indicated in Chapter 5, the starting point for our analysis is the 2017 data on service-related floor space in 231 countries, according to the Navigant Global Building Stock Database[2]. Because this is a commercial database, we cannot provide the original data. This

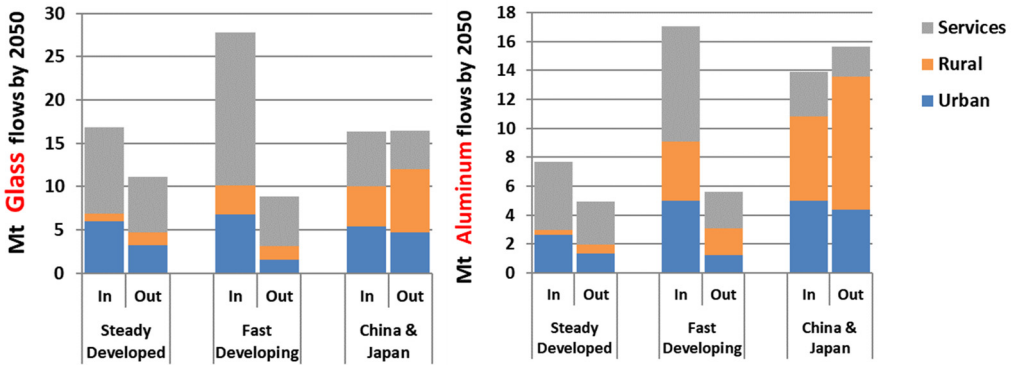

Figure A5.1 *Updates to Figure 5.5, for aluminium and glass*

section just explains the steps taken in the regression analysis, while providing additional detail.

First, we excluded countries for which we could not find the Gross Domestic Product (GDP) in Purchasing Power Parity (PPP) or the Service Value Added (SVA) fraction in the United Nation statistics[3,4]. The following countries were excluded for this reason:

Greenland, Andorra, Faeroe Islands, Gibraltar, Holy See, Isle of Man, Liechtenstein, Monaco, American Samoa, Cook Islands, French Polynesia, Guam, North-Korea, Mayotte, New Caledonia, Niue, Northern Mariana Islands, Taiwan, Tokelau, Wallis and Futuna Islands, Anguilla, Aruba, Belize, Cuba, Falkland Islands, French Guiana, Guadeloupe, Martinique, Montserrat, Saint Helena, Saint Kitts and Nevis, Saint Lucia, Saint Pierre and Miquelon, Saint Vincent and the Grenadines, Sint Maarten (Dutch part), Suriname, Turks and Caicos Islands, Venezuela, British & US Virgin Islands, Bahrain, Oman, Syrian Arab Republic, Djibouti, Eritrea, Libya, Rwanda, Somalia, Sudan, Western Sahara.

Secondly, we excluded another group of countries which represented outliers in terms of per capita service sector floorspace, because they are island states, or typical city states. Because the model resulting from the regression is applied to 26 large global regions, we feel that calibrating a model to such atypical cases should be avoided. For this reason, the following countries were omitted in the regression analysis:

Cyprus, Bhutan, Brunei Darussalam, Comoros, Fiji, Hong-Kong, Kiribati, Macau, Maldives, Marshall Islands, Micronesia, Nauru, Palau, Samoa, Singapore, Solomon Islands, Tonga, Tuvalu, Vanatu, Antigua and Barbuda, Bahamas, Barbados, Caribbean Netherlands, Cayman Islands, Grenada, Puerto Rico, Trinidad & Tobago, Kuwait, Qatar, United Arab Emirates, Cabo Verde, Mauritius, Sao Tome and Principe, Seychelles

The remaining 147 countries yield data points which are used in the regression analysis, for which the results are shown in Figure A5.2. These figures show the resulting unweighted models as well as the population weighted model, using a Gompertz function (also see the main text):

$$y = \alpha \cdot e^{-\beta \cdot e^{-\gamma x}}$$

y being the service sector floor space demand in square meter per capita, and *x* the Service Value Added per capita in 2016-US$ for a particular country/yr, in Purchasing Power Parity. The coefficients α, β and γ were estimated using the Sequential Least Squares Programming (SLSQP) algorithm from the scipy package implemented in a python script (See Section S.6). We choose the SLSQP routine because as a sequential quadratic programming routine it has been shown to perform well (in terms of both efficiency and accuracy) for constrained non-linear optimization problems, such as ours[5,6]. The model is used to project the global floor space demand by applying the SVA for 26 IMAGE regions. As the SVA in IMAGE is expressed in 2005 US$ (PPP), we correct for inflation based on the inflation calculator of the United States Bureau of Labor Statistics[7].

A5.2.1 Weighted regression

As explained in Chapter 5, the model validation based on unweighted regression did not lead to a suitable fit with the 2017 data. The unweighted model (black line) would underestimate the known total global floorspace for 2017. This mismatch is addressed by means of a 'fit' indicator, ϕ, which represents the total modelled floor space over the total observed floor space in 2017, when multiplied with the population size for the 147 countries used in the regression:

$$\phi = \frac{\sum_{i=1}^{147}(y(x_i) \times p_i)}{\sum_{i=1}^{147}(y_i \times p_i)}$$

Here, $y(x_i)$ is the modelled per capita floor space, for country *i*, as derived from the estimated regression model, and using information on the Service Value Added per capita, x_i per country. y_i is the per capita floor space according to the data and p_i is the population in a country, according to the data. As indicated in Figure A5.2a, the total service-related floor space demand based on unweighted regression analysis would have a fit of $\phi = 0.67$. In other words, the model predicts a total service sector floor space demand that would be off by 33% in 2017.

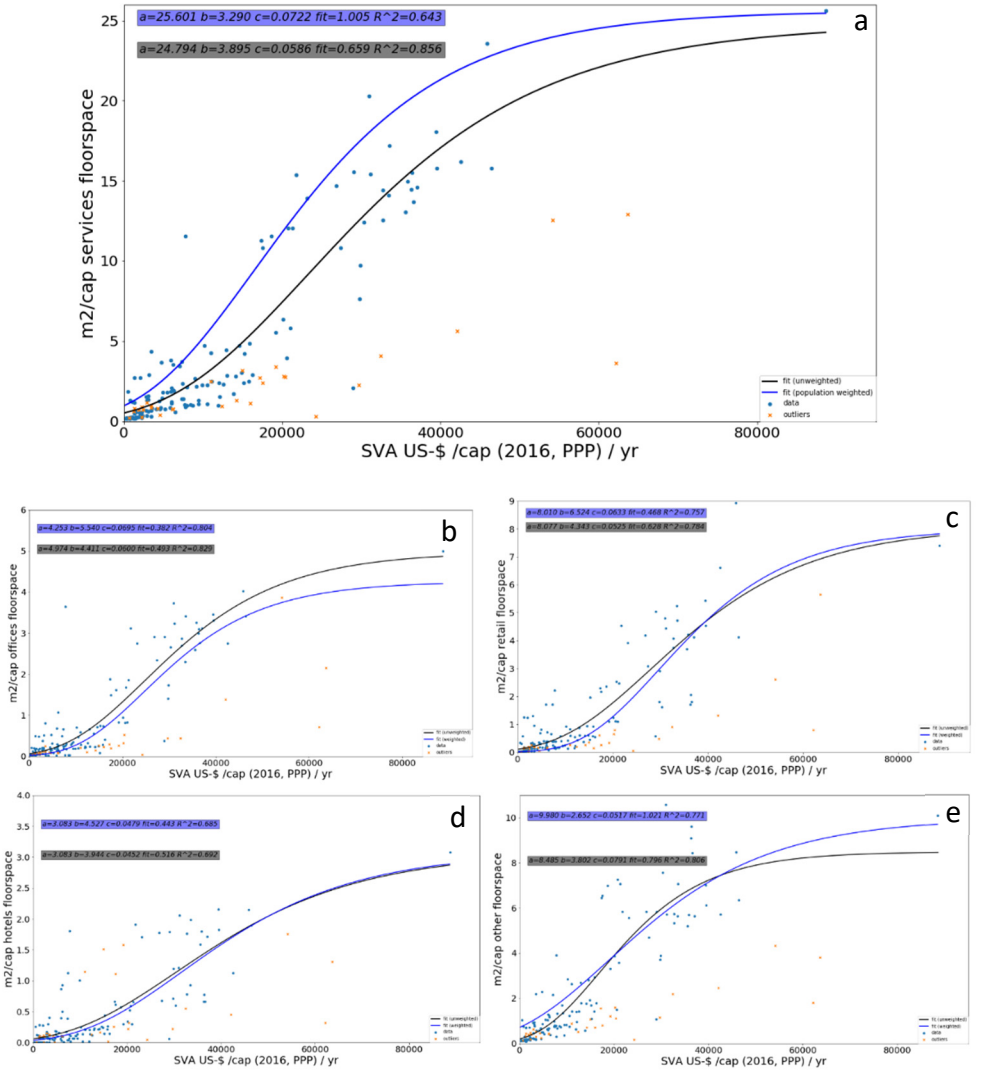

Figure A5.2a-e. *Development of per capita service sector floorspace demand, according to the unweighted regression (black) and a population weighted regression (blue). a) represents the total service sector floorspace (data points represent the sum of the data points in panel b-e). b) shows the office space, c) shows the floorspace for retail, shops & warehouses, d) shows hotels & restaurants & e) shows the per capita demand for other buildings (educational buildings, hospitals, governmental buildings, buildings for assembly and public transportation).*

This is caused by the fact that many countries with a large population size lie above the unweighted curve, while many countries with a small population size are below the curve. It was thus decided to use a population weighted regression model for the floor space demand from the service sector as a whole (top line in Figure A5.2a). This was done by minimizing the goodness-of-fit parameter, or the χ^2, according to Bevington & Robinson [8]:

$$\chi^2 = \sum_{i=1}^{147} \left\{ \frac{1}{\sigma_i^2} [y_i - y(x_i)]^2 \right\}$$

Here, x_i is the Service Value Added in US$ (2016, PPP) and σ_i is the uncertainty of the y_i, so of the per capita floor space of country i, measured in terms of a standard deviation. An unweighted model assumes an equal (but possibly unknown) σ_i for all countries. There is no information on the value of these σ-values. We decided to construct them based on the (population or GDP per capita weighted) per capita floorspace y and a country-specific uncertainty weight w_i as follows:

$$\sigma_i = y \times w_i$$

Here the uncertainty weight w_i is assumed to decrease linearly (with population size or GDP/cap) until a maximum reached (200 million people or $40,000 GDP/cap, see Figure A5.3):

$$w_i(population\ weighted) = \begin{cases} -1.4 \cdot 10^{-9} \times p_i + 0.3 \text{ if } p_i \leq 2 \cdot 10^8 \\ 0.015 \text{ if } p_i \geq 2 \cdot 10^8 \end{cases}$$

$$w_i\left(\frac{GDP}{cap} weighted\right) = \begin{cases} -7.125 \cdot 10^{-6} \times p_i + 0.3 \text{ if } p_i \leq 4 \cdot 10^4 \\ 0.015 \text{ if } p_i \geq 4 \cdot 10^4 \end{cases}$$

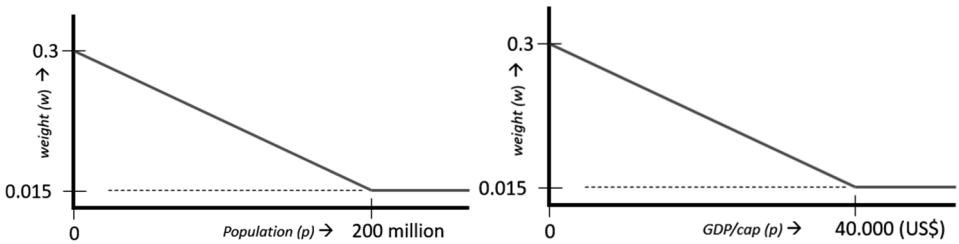

Figure A5.3. *Graphical representation of the uncertainty weighting factors (w) used in the weighted regression analysis. Left: population weighted regression; Right: regression weighted by GDP per capita.*

This means that we introduce a relatively large uncertainty weight (w), and resulting relative standard deviation of the service-related floor space (of 30%) for countries with a small population size (p), while countries with a population size beyond 200 million people are assumed to have a smaller relative standard deviation of the service-related floor space (of 1.5%). When implemented, these settings ensure that the model fit becomes more accurate, because it allocates more weight to data points representing countries with a larger population (since these have a lower uncertainty weight). Using the estimated Gompertz parameters resulting from the weighted regression leads to a much better fit of $\phi = 1.005$ for the year 2017, representing a mismatch of total global floor space of only 0.5%. A more accurate model verification in the year 2017, however, comes at the cost of lower R^2 values as can be seen from Figure A5.2.

While the total service-sector floorspace is represented using a population weighted regression, thus ensuring an appropriate model fit, it was decided to follow a different approach regarding the disaggregation of floorspace demand across the four service building types (Figure A5.2b-c). One reason being the lower resulting R^2 values from a population weighted regression. Another reason is that if the total service floorspace ensures a proper representation of the current situation, the need for population-based weighting diminishes for the specific building types. Instead we applied a more common weighting approach based on the reliability of the data. Here, we assume that reported data from countries with a higher per capita income have a higher reliability than data from countries with a lower income per capita. This could be defended by the common view that affluent countries tend to have better statistical offices for example. To translate a countries affluence into a proxy for the data reliability we used the per capita GDP (2016 US$/cap, PPP). Similar to the population weighted approach we use a high uncertainty weight of 30% at low income levels, and assume a linear decrease to 1.5% at high levels of GDP per capita (beyond 40.000 US$/capita yr^{-1}), as shown in Figure A5.3.

The disaggregation of the total commercial floor space demand (based on the weighted regression) was done based on the relative contribution according to the GDP/cap weighted regression fits for the four service-related building types, as can be found in Figure A5.4 a&b.

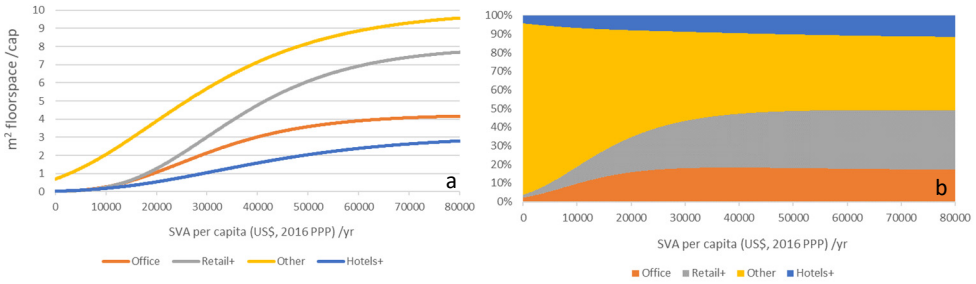

Figure A5.4a-b. *Per capita floor space demand for four service sector building types, used to disaggregate the total service-related floorspace demand (blue line in Figure A5.2a). a) Four regression models used for the four commercial building types (the corresponding Gompertz parameters for these curves can be found in Table 5.1). b) Relative contribution of the four service building types to the total service sector floorspace demand, at different levels of Service Value Added (in US$/capita yr^{-1}).*

A5.2.2. Reflection on model specification

In the current model specification, we use national data on per capita service value added to derive the development of the per capita floorspace for non-residential buildings. However, this does not mean that service value added is the only possible independent variable to explain the development of non-residential floorspace demand. From literature we know, for example, that the amount of some shops seems to be correlated with population density at the local level[9]. To see if this is true for our data, we displayed the per capita floorspace demand for four non-residential building types in relation to the population density in Figure A5.5. Using the figure one can identify some of the city-states, but other than that, the figures do not suggest any clear relationship between non-residential floorspace demand and population density.

That does not mean, however, that such relationship does not exist. If data on non-residential floorspace demand would be specified for smaller regions, or if it would distinguish between urban and rural areas, one may expect to find not only a better regression, but perhaps a better model by incorporating a second independent variable such as population density. The current model specification is therefore chosen based on data-availability, given the global scope of our research.

Furthermore, in the definition of a global model describing a generic development path we inevitably lose sight of exceptional regional factors such as culture and lifestyle, which surely play a role in floorspace demand. We would like to emphasize that therefore careful interpretation is required when using regional model outcomes. For this exact reason we

provide both the data and the model used, which should make it easy to build and improve upon our work, for example by improving the regional representation.

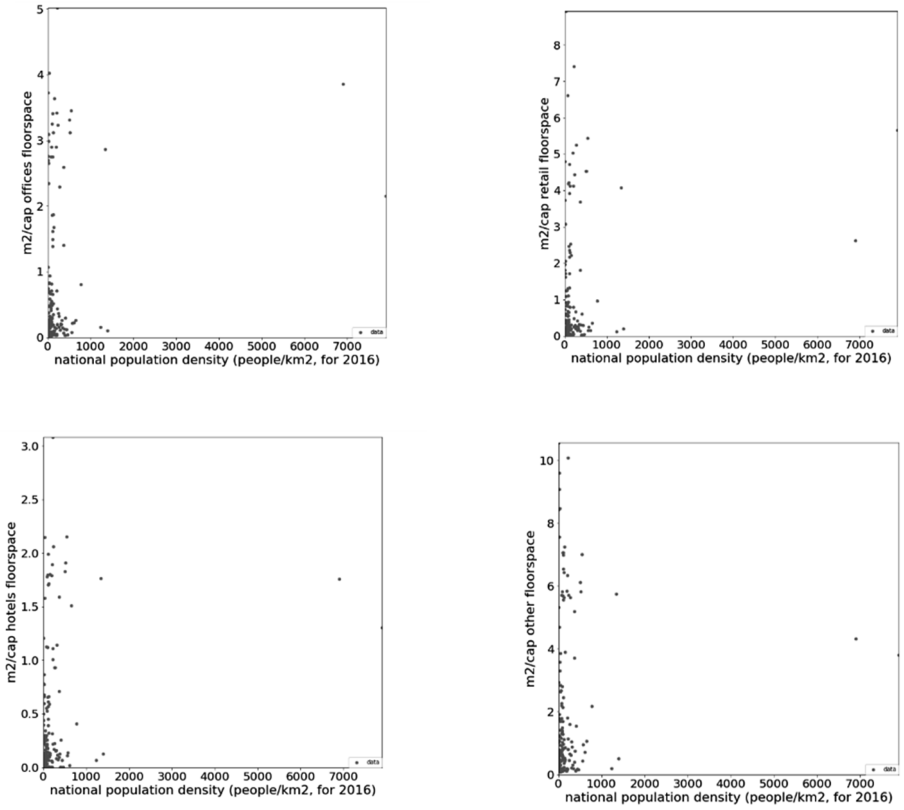

Figure A5.5. *Per capita floorspace demand in 4 non-residential building types (top-left: offices; top-right: retail+; bottom-left: hotels+; bottom-right: other) versus the population density. Data points represent countries, including outliers (N=176).*

Finally, the assumption of a fixed relation between demand (floor-space) and income (SVA) is only valid under a presumption of a 'business as usual' development. This is a legitimate assumption under the SSP2 scenario, as it explicitly assumes a "path in which social, economic, and technological trends do not shift markedly from historical patterns" according to Riahi et al.[10]. However, implementation of our model under different scenarios (SSP or other) could mean that this relation between service sector floorspace demand and SVA needs to be revisited.

A5.3 Dynamic stock modelling for service sector floorspace

A5.3.1 Lifetime assumptions

The dynamic stock model used was originally developed by Pauliuk and co-contributors[11], and was applied in this study using a stock-driven approach. This requires lifetime assumptions for the buildings in our model, which were based on the Weibull distribution parameters as found in literature. Table 5.3 shows the averaged Weibull parameters used, but as indicated in Chapter 5, we used building-specific Weibull parameters where possible. Table A5.1 shows the parameters used.

Averaging lifetime distributions based on given Weibull parameters cannot simply be done by averaging the available shape parameters and the available scale parameters. Therefore, we used a python least squares optimization routine to find the closest representation of the average, given multiple Weibull curves. In case we used an average to represent the multiple Weibull parameters found in literature, we indicate the coefficient of determination for the fitted curve with respect to the average of multiple curves (2 to maximum 5 curves) in brackets. Thus, representing how well our parameter settings matches the average of the lifetimes found in literature. For an example, please see Figure A5.6.

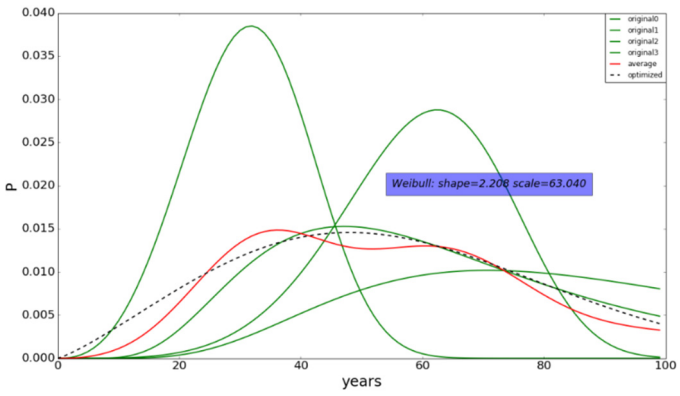

Figure A5.6. *Example of fitting a Weibull distribution to an average of multiple Weibull curves found in literature. This example shows the four literature-based Weibull curves for Western Europe in green, the red line is the resulting average for the 4 curves, and the dotted line is the fitted curve used in our model, which fits the average with an* R^2 *of 0.965.*

Region	Building type	shape	scale	Comment
Japan	Detached	1.88	41.23	Building Specific Weibull parameters according to the average found in two studies [12,13] (R^2 = 0.99)
	Semi-detached	1.89	42.58	
	Apartments	1.90	43.95	
	High-rise	2.56	34.05	
China	Urban: detached	2	33.85	Region specific shape parameter and building specific scale parameter according to the mean indicated in Wang et al.[14]
	Urban: semi-detached	2	39.49	
	Rural: (semi)-detached	2	31.03	
	Apartments	2	53.60	
	High-rise	2	56.42	
Eastern Europe	(semi)-detached	2.5	73.26	Region specific shape parameter according to Novikova et al.[15,16]
	Appartments	2.5	101.43	
	High-rise	1.97	67.36	Global Average (see below)
United States	All	4.16	85.19	Region specific parameters according to average [17–19] (R^2 = 0.951)
Western Europe	All	2.95	70.82	Region specific parameters according to average [19–21] (R^2 = 0.965)
Canada	All	1.97	57.53	Global shape, regional mean [22,23]
Mexico	All	1.97	63.17	Global shape, regional mean [23,24]
Brazil	All	1.97	112.80	Global shape, regional mean [25]
Rest of South Amerika	All	1.97	68.24	Global shape, regional mean according to the average of Argentine, Chile, and South-Amerika in [22–24,26]
Southeastern Asia	All	1.97	56.40	Global shape, regional mean [22]
Oceania	All	1.97	94.00	Global shape, regional mean according to Buyle et al. [22] and Stephan et al.[27]
Global Average	All	1.97	67.34	These lifetime parameters are applied when no information is available, it is a constructed average of parameters from 5 regions, being Japan, China, US, East & Western Europe. (R^2 = 0.994)

Table A5.1. *Weibull parameters describing the lifetime distributions used. Where possible, we used lifetime estimates specific to the building type.*

A5.3.2 Historic stock development

Since we have no data on the age distribution of the initial stock, we needed to extend the historic time series to derive the age-distribution of buildings based on historic inflow. We did so using the historic population dating back to 1820 based on Bolt et al. [28], and an additional 100 years of linear increase in population from 0 in 1720. During this model-setup period, we also assumed that the per capita floor space increased at the average global rate found in the first ten years of the IMAGE data (about 1% per year). For the development of the share of urban population before 1971 a similar approach was used, but based on regionally specific annual growth-rate. Both for the per capita floor space and the urban population fraction a minimum was maintained based on the lowest regional value in 1971. To assess the viability of these historic model assumptions, we checked whether our model was able to re-create the known age-distribution of the building stock in two European test-cases (See Figure A5.7 for an elaboration). The model managed successfully, but to ensure a proper fit, both test-cases required relatively high lifetimes, compared to those found in Table 5.3. This suggests that some of the mean building lifetimes found in literature could be rather low.

A5.3.3 Lifetime verification

We performed a model verification exercise, in which we tested assumptions on the historical model setup (Section 5.2.2.2) as well as the lifetime assumptions for residential buildings. We were able to find two sources describing the age distribution of residential buildings in great detail. One for the Netherlands in the year 2018 [29] and the other for Western Europe as a whole in the year 2010 [30]. Given the age-structure of the building stock for these regions and years, we were able to see whether the model is able to re-create these numbers. We thus run our model given the historic assumptions as described in the main text , lifetimes as found in the literature and historic population development based on Bolt et al. [28] . The Weibull parameters for Western Europe are the same as used in the main model (see Table 5.3), while for the Netherlands we used the same shape parameter, but an adjusted scale parameter, corresponding to an average lifetime of 120 years for residential building, based on Sandberg et al. [31]. Furthermore, in this test-case, we assume the historic development of per capita floorspace to be similar to that of Western Europe. Figure A5.7 shows the resulting model outcomes, compared to the available statistics. It shows that for the Netherlands the model is able to re-create the age-structure of the residential building stock quite well, based only on GDP and Population as a driver. Perhaps with the exception of historical artefacts such as a relatively high share of remaining houses from before 1900 (which could be explained by policies aimed at preservation of historical & monumental buildings in the Netherlands) and some noticeable historic abnormalities, such as the effect of the second world war on housing construction activities.

However, using the regular lifetime assumptions for Western Europe (i.e. a Weibull distribution with a mean lifetime of 63 years) seems to lead to an over-estimation of recent building activities (Figure A5.7b), because the model projects the demolition of buildings that in reality have remained in stock. Only when we assume a much higher average lifetime of 130 years, the model is able to match the known age-distribution of the stock in the year 2010 (Figure A5.7c). This suggests that the literature-based lifetimes of Western European residential buildings could be lower than in reality. Another factor that may explain the mismatch between our model and the available statistics for these two test-cases is the fact that we do not account for the lifetime dynamics of monumental buildings. The latter may be quite relevant for Western Europe, given the fact that historic and monumental buildings make up a large part of the (urban) building stock [32].

Though this highlights two important paths for future research and model improvement (introducing more realistic lifetime distributions and accounting for stock dynamics for monumental buildings specifically), we are currently unable to adjust our model for these findings. Given that we aim to develop a global model we currently lack the data and the time to perform a similar verification for all 26 regions in our model.

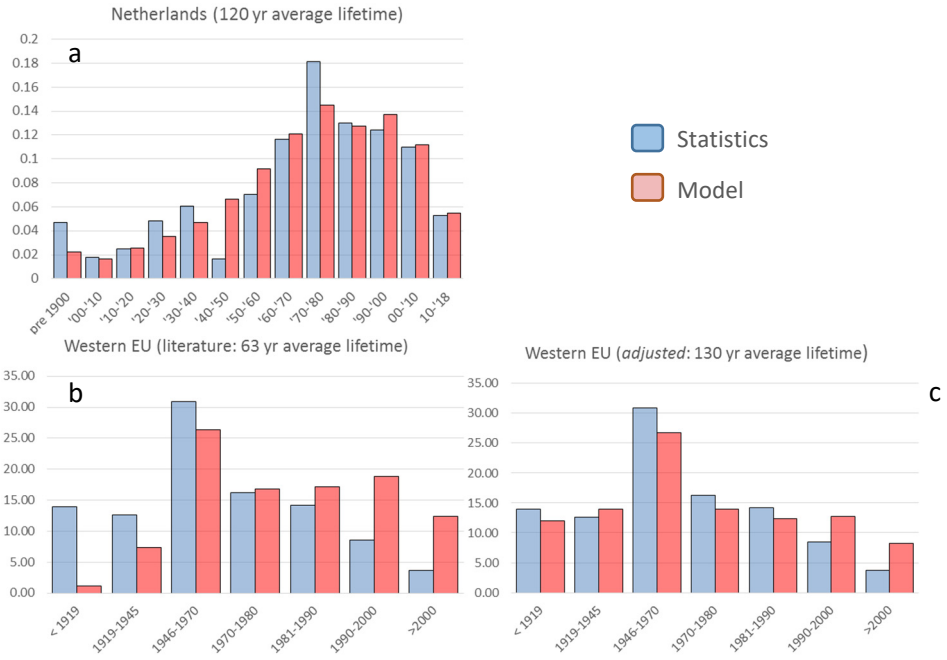

Figure A5.7. *Model verification results. Showing the fraction of residential buildings by age-cohort on the y-axis, according to the available statistics (blue), and according to our model (red). Data for the Netherlands (a) represents the year 2018 based on [29], while data for Western Europe (b&c) represents the year 2010 based on [30].*

	Source	Description	Region	Steel	Concrete	Aluminium	Copper	Wood	Glass
Offices	Ecoinvent [34]	Multi-storey building	-	24	393	8.5	8.5	24.7	3.1
	Kashkooli [35]	High-rise office building	Mexico	124	425		2.7	3.0	1.0
	Kofoworola [36]	Typical office building	Thailand	256	2118	0.3		1.5	9.6
	Oka [37]	Offices	Japan	158					
	Reyna [38]	Offices (low & high)	USA	42	533	9.7		0.2	4.6
	Schebek [39]	Offices	-	87	1057	0.6	0.7	4.2	13.9
Retail+	Ecoinvent [34]	Hall-type building	-	26	785	1.2		18.2	1.8
	Reyna [38]	Warehouse, department store & small store	USA	83	658	2.1			1.9
	Schebek [39]	Warehouse	-	85	349	1.1	0.7	4.2	13.9
	Gruhler* [40]	Wholesale & Car-shop	Germany	121	1009	5.2	3.9	11.0	
Hotels+	Reyna [38]	Hotel	USA	89	93	5.2			2.7
	Rossello-Batle [41]	Hotel	Spain	51	1007	3.0	3.3	12.0	5.1
	Gruhler* [40]	Hotel/guesthouse	Germany	113	1073	4.9	3.7	25.0	
Other	Kumanayake [42]	University	Sri Lanka	132	1543	5.0			7.6
	Reyna [38]	School & Hospital	USA	132	835	7.9			4.9
	Gruhler* [40]	Nursing-home & Emergency services	Germany	104	1037	4.5	3.4	25.5	
	Marcellus-Zamora [43]	Civic/Institutional	USA	40	702				31.0
Avg.				**97.9**	**850.9**	**4.2**	**3.3**	**11.8**	**7.8**

Table A5.2. *Material content of service-related building types in kg/m^2. Corresponding to the use in the main text, 'Retail+' refers to the combination of retail, shops and warehouses, 'Hotels+' refers to hotels and restaurants and 'Other' refers to other buildings such as hospitals, educational buildings, governmental buildings, buildings for assembly and transport-related buildings. *The study by Gruhler reports metals as a single category, we used an assumption on the share of 93% steel, 4% aluminium and 3% copper to disaggregate the three metals.*

A5.4 Material assumptions

All of the assumptions on material content of residential buildings (in kg per m^2) is described by Marinova et al. [33]. The material content estimates for service-related buildings applied in our calculations are summarized in Table 5.2. Table A5.2 shows how these averages were derived from the individual sources.

The Ecoinvent database gives the material use during the assumed lifetime of a building, and thus incorporates the replacement of some building elements with shorter lifetimes, such as the window-frames for example. As indicated in the main text, we adjusted the material use per m^2 to reflect the materials contained in the building, so not accounting for the maintenance & refurbishment. We adjusted for this using the indicated lifetimes of the building components which are replaced during the lifetime of the entire building. To give an example; if the Ecoinvent database indicated 3 kgs of Aluminium window-frame, with an expected service life of 25 years, per square meter of a hall-type building with an expected 50 yr lifetime, we assumed a 1,5 kg/m2 Aluminium demand based on our 'one-time-built' approach.

Other conversion factors used to derive the material content for service sector buildings as displayed in Table A5.2 are shown in Table A5.3. Figure A5.8 shows the distribution of the data on material intensities for buildings in the service sector as a whole (4 building types combined). The mean values displayed in this figure are used in the sensitivity analysis, where they are applied to all 4 building service-related types.

Table A5.3. *Conversion factors used in calculating the material intensities of service sector buildings*

Conversion factor	**value**	**source**
kg per m2 glass	10	[44]
kg per m2 corrugated steel roof plate	10	Appendix 1 in [45]
kg per cement block	12.25	'standard' according to [46]
kg per m2 steel cladding	3.66	26 Gauge according to [47]
kg per ft2 of concrete brick	18.07	3.4 kg per brick acc. to [48]

.

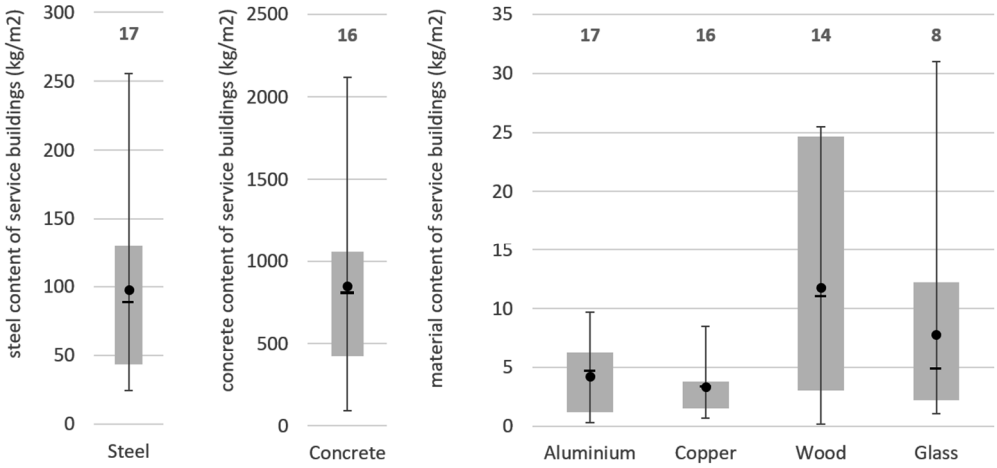

Figure A5.8. *Distribution of the data points on material intensity for buildings in the service sector. The boxes represent the 20th to 80 percentile interval range, while the whisker indicate the maximum and minimum values for each of the six materials. Numbers above the plots indicate the number of data points. Though our analysis applies average material intensities per service sector building type based on Table A5.2 (not shown here), these graphs are meant to give an impression of the overall data variability. Furthermore, the mean values displayed here are used in the sensitivity analysis.*

A5.5 Detailed results

A5.5.1 Per capita floorspace demand

Figure 5.2 shows the development of the global building stock in terms of floor space (in m^2) as a consequence of the development of population as well as affluence. To show the effect of increased affluence only, Figure A5.9 shows the development of the average per capita floor space (in-use stock) between 2000-2015 and 2035-2050, for both rural and urban residential purposes and for service-related purposes. The per capita floorspace demand in the service sector remains well below the residential floor space demand. It can also be seen that the per capita floor space for urban housing is slightly lower than the per capita floor space in rural areas, as elaborated by Daioglou et al.[49]. Though this seems to be a logical consequence of compact urban living, driven by scarcity of space in areas with a high population density, the available data on per capita floor space in our database for materials in residential buildings seems to suggest the opposite. For a more elaborate discussion about this interesting finding and possible future model improvements, please see Marinova et al.[33].

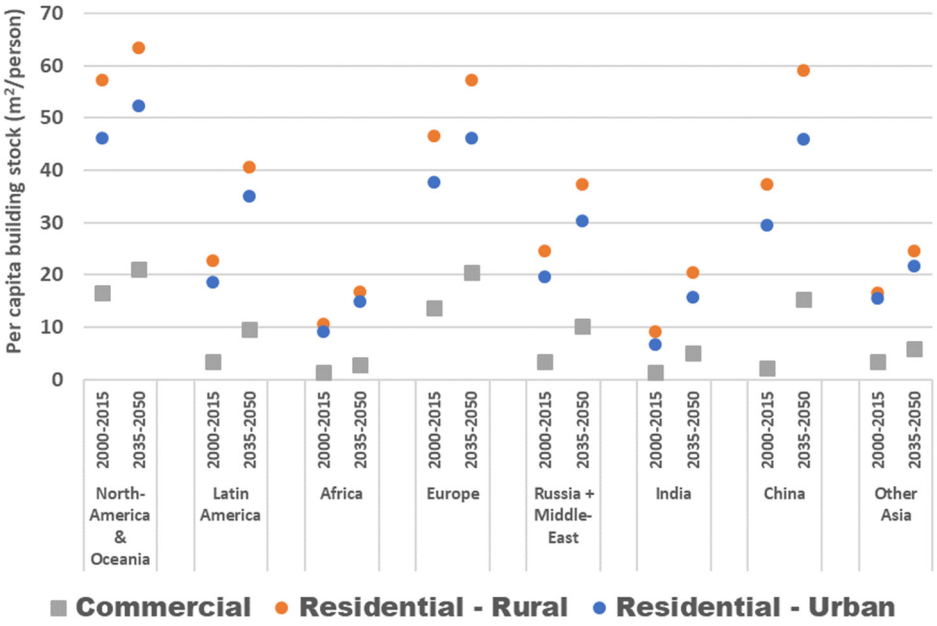

Figure A5.9. *Development of the average per capita floor space stock by region, for the period 2000-2015 and 2035-2050. Urban residential buildings are shown in blue, rural residential buildings in orange and service sector floor space in grey.*

Figure A5.9 shows the growth of the residential and service-related per capita floor space demand. As discussed in the main text, the latter grows more rapidly. As a consequence of the regression analysis and the resulting demand curves as shown in Figure A5.4a, some service sector building types grow more rapidly than others. Table A5.4 provides the relative contribution of each building type to the total commercial building stock and the resulting growth factors between 2018 and 2050. It shows that demand for retail and offices is expected to grow faster than the demand for other service-related building types.

Table A5.4. *The share of service sector building types in the total service-related building stock, and the resulting growth factors per building type. Using the same definition of building types as in Table A5.2.*

	Share		
	2018	2050	Growth
Hotels+	8%	9%	2.71
Offices	13%	16%	2.96
Other	63%	54%	2.10
Retail+	17%	22%	3.15

A5.5.2 Detailed model outcomes

The full set of model outcomes is available from the Supplementary Data, which provides data for the entire modelling period (1970-2050), for all 26 IMAGE regions, for 4 residential building types as well as 4 service sector building types, and for floorspace (in m^2) as well as material demand (in kgs), it contains the model outcomes for the building stock, but also for the inflow and outflow as derived from the stock. As discussed in the main text, it is not advisable to use detailed regional outcomes without critical reflection. We present a first attempt to model the global building stock, with regional detail. All assumptions are listed transparently where possible, but we cannot guarantee that the results make sense at the highest level of detail. We decided to provide the detailed results so that priorities for model improvement can be identified. We encourage people to use and expand this model as they see fit. Therefore, the model and the associated data are made available on Github, under a creative commons license[50].

To show the contribution of different building types on the demand of construction materials and the consequential outflow of scrap building materials, Figure A5.10 below shows the material flows by the end of the modelling period (average of 2045-2050) for each building type, and for all six materials.

A5.6 Sensitivity analysis

A5.6.1. Description of four sensitivity variants

1. Mean Material Intensity (Mean MI)

Based on the material intensity database as described by Marinova et al.[33] we defined a sensitivity variant in which we ignore the regional detail on material intensities of residential buildings, but instead assume a global mean material intensity for each of the four residential building types and the six materials, based on all available studies. Here, we further explore the effects on inflow and outflow related indicators. Please note that when no literature was available on the residential material intensities of a particular region, a global average was already used in the default analysis (main text). This means that for the residential buildings, this alternative assumption can be used to identify the sensitivity of overall outcomes to the regional assumptions on material intensities.

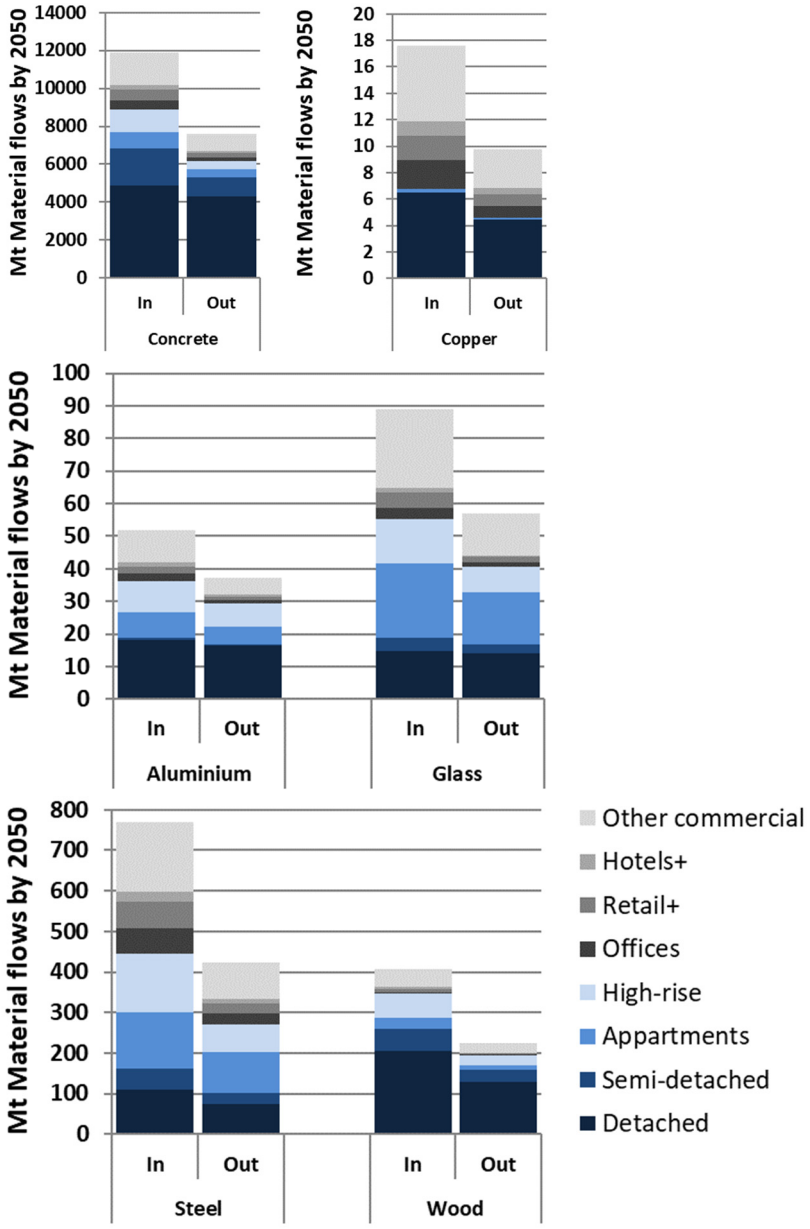

Figure A5.10. *Ratio between the total inflow and outflow of building materials by the end of the modelling period (average of the period 2045-2050). The contribution of service sector building types (in grey) and residential building types (in blue) is shown. For the definition of residential building types, please see* [33]*. The definition of service building types is similar to Table A5.2.*

Material intensities in service sector buildings, however, are not regionally specified to begin with. So, to come up with a sensitivity variant based on the material intensities described in this paper, we defined the mean material intensities for service sector buildings based on all available studies describing the service-related building types. The mean values used are shown in Figure A5.8 and represent the assumption that all service-related building types would have a similar material demand.

2. Normal distribution for building lifetimes

Stock dynamics in both residential and service sector buildings are based on the assumed Weibull lifetime distributions. To see the effect of different lifetime profiles, we defined a sensitivity variant based on a normal distribution.

We assumed the same mean lifetimes as in the regular analysis, but defined the normal lifetime distribution using a standard-deviation that would make sure that the distribution would be above zero (as opposed to the Weibull distribution, the normal distribution continues below zero, leading to unrealistic assumptions). To this end we linearly increased the standard deviation from 10 at a mean lifetime of 35 years to 20 at a mean lifetime of 60 years, leading to an increasing spread of the lifetime distribution at higher expected lifetimes (based on literature, see Table A5.1). The resulting lifetimes can be seen in Figure A5.11. To avoid disregarding the mass balance by any remaining 'tail' of the distribution before the building's actual lifetime, we actually deploy a folded normal distribution, which presents only a very slight deviation from the normal distribution during the first few years after construction. This method was applied for both residential and service sector buildings.

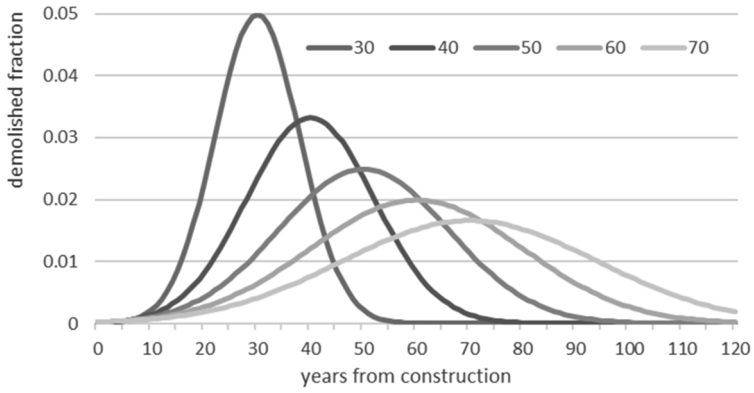

Figure A5.11. *Normal lifetime distributions used in the sensitivity variant. We assumed that an increasing mean lifetime leads to an increasing standard deviation as shown here.*

3. Increasing Alpha with 10%

The Gompertz parameters resulting from the regression analysis are key in determining the demand for service sector buildings. In particular the value of alpha, as it determines the maximum value for the per capita demand of service-related floor space. In the regular analysis the value of alpha was maximized to represent the highest value in the available data in the Global Building Stock Database by Navigant Research[2]. Our model thus assumes that demand for service sector buildings will grow towards what is currently known to be the highest value. However, wealthy regions like the United States seem to be approaching that maximum already[51]. To assess the effect of allowing a higher per capita service sector floorspace demand we defined a sensitivity variant that allows for a 10% higher value of alpha for the overall service sector. Mind that we only change the alpha for the total service sector, while keeping the original Gompertz parameters for the individual building types. As such, we assume that the sub-division of service-related building types remains the same.

If we only increase the value of alpha by 10%, the service-related building stock would simply increase by 10%, leading to a corresponding 10% increase in annual demand for each of the materials. This shows a high dependency of the outcomes on the value of alpha, but it does not make a very interesting sensitivity analysis. Therefore, we decided to change the assumptions in the regression by finding a new set of Gompertz parameters based on a regression in which alpha was maximized to the maximum in the data, plus 10%. This gives a slightly better population weighted R^2 of 0.685, based on the resulting parameters of alpha: 28.161, beta: 3.191 and gamma: 6.06*10^-5

4. Replacing the Gompertz model with an Exponential Decay function

Another key factor prescribing the development of service sector floorspace demand is the assumed Gompertz curve. To assess the effect of a different regression model, we implemented a sensitivity variant based on an Exponential Decay function:

$$y = \alpha - \beta e^{-\gamma x}$$

Similar to the model described in the main text, y is the service floor space demand in square meter per capita, and x is the Service Value Added per capita in 2016-US$ for a particular country, in PPP. While α, β and γ are the regression parameters. The method performing the regression remained the same as described in the main text. Again, we only change the model describing the total service related floorspace demand, thus using a population weighted regression. The sub-division of the total floorspace across the 4 service-related building types was unaltered.

The regression leads to the following alpha: 25.601, beta: 28.431 and gamma: 4.15*10^-5. This leads to a somewhat lower R^2 of 0.514 at a fit (ϕ) of 0.995, suggesting a somewhat

inferior model than used in the regular calculations. Furthermore, the exponential decay function leads to negative values at lower levels of Service Value Added. To avoid this, we minimized the function below 0.542 m^2/cap, which represents the 25th percentile of the original data.

To understand the effects of choosing an alternative model function, we plot the development of service sector floorspace demand based on the regular model as well as the two sensitivity variants in Figure A5.12 below.

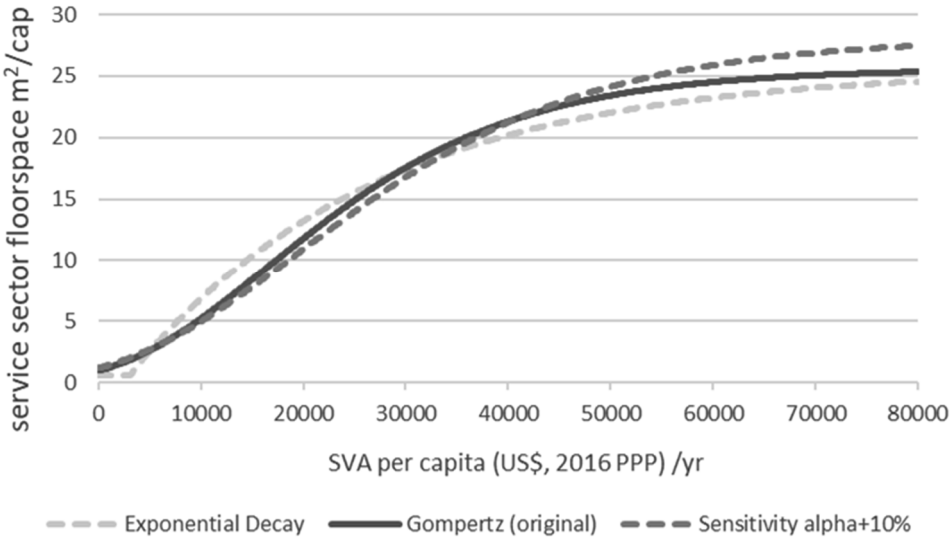

Figure A5.12. *Development of the service sector floorspace demand (expressed per capita).*

A5.6.2 Outcomes of the sensitivity analysis

The outcomes of the sensitivity analysis are displayed in Table A5.5 and Figure A5.13. Table A5.2 shows the changes in 3 different material demand indicators by 2045 (based on a 5-yr moving average) on 6 materials with regards to the regular analysis presented in the main manuscript. Two of the sensitivity variants only have an effect on the demand for materials in service-related buildings, while the other two sensitivity variants also affect the demand of materials in residential buildings.

Since Chapter 5 elaborates on the gap between inflow and outflow of construction materials by the end of the scenario period (2045-2050) in Figure 5.5, the sensitivity analysis also explores the effect of changing assumptions on the mismatch between inflow & outflow

(thus, the potential for reaching a circular material flows). We do not display the ratio between inflow and outflow itself, but the extent by which this ratio changes. A positive number means that the mismatch between inflow and outflow becomes even larger, while a negative number means that the outflow of construction materials covers a larger fraction of the new demand for construction materials, compared to the analysis in the main text. Figure A5.13 shows the development of the annual demand for the six materials under investigation for service sector buildings only.

A5.6.3 Discussion on the sensitivity analysis

Looking at the outcomes of the sensitivity data in Table A5.5 it seems that the largest deviations from the regular outcomes arise when assuming global mean material intensities (in kg/m^2). This sensitivity variant can lead to both slightly higher or lower annual material demand by the end of the scenario period, depending on the material and the focus on either residential or service sector buildings.

For service sector buildings, the demand for glass and wood is most affected, given that the most important building type (being the 'other' service-related buildings, a.o. based on governmental and institutional buildings) has a relatively high material intensity for glass and wood according to the literature used (Table 5.2, or Table A5.2). Assuming a mean material intensity for all service-sector buildings leads to a lower value, and thus to a lower demand for wood and glass. On the one hand this may indicate that more data has to be acquired on the use of these materials, especially in service-related building types that are not offices, retail or catering related. However, building materials like wood and glass and aluminium are often non-structural and therefore their material intensities may simply have a wider range, leading to larger deviations based on alternative assumptions.

The effect of assuming a global mean material intensity for residential buildings is most noticeable for concrete and aluminium. This can be mostly explained the relatively high material intensities found for detached houses in China. Both aluminium and concrete intensities for detached houses in China are over 2 times the global mean, thus leading to a considerable drop in material demand in the sensitivity variant. As can be seen in Table A5.5 this translates to a decrease in the global demand of around 18-20% for both materials. As mentioned before, this sensitivity analysis highlights the importance of proper material intensity data, especially for dominant regions like China.

Interestingly, Table A5.5 also shows that a drop in the annual demand for concrete and aluminium in residential buildings under the assumption of a mean material intensity causes an increase of the Inflow-to-Outflow (I/O) ratio at the global level.

Sub selection	Indicator	year	**Mean MI** Mean of all service building types & Mean of all regions for residential buildings	**Normal distr. (lifetimes)** For all buildings, including residential	**Alpha + 10%** Only affects service sector floorspace demand	**Exponential Decay** Only affects service sector floorspace demand
Service sector buildings	Steel demand	2045-'50	**1%**	*-13%*	*-2%*	**7%**
	Concrete demand	2045-'50	*-6%*			**7%**
	Glass demand	2045-'50	*-23%*			**9%**
	Wood dem.	2045-'50	*-35%*			**9%**
	Aluminium demand	2045-'50	*-10%*			**8%**
	Copper demand	2045-'50	**2%**			**7%**
Residential	Steel demand	2045-'50	*-10%*	**5%**	0%	0%
	Concrete demand	2045-'50	*-20%*	*-8%*		
	Glass demand	2045-'50	*-2%*	*-9%*		
	Wood dem.	2045-'50	**2%**	*-5%*		
	Aluminium demand	2045-'50	*-18%*	*-10%*		
	Copper demand	2045-'50	*-0.3%*	*-8%*		
All (Services & Residential)	Steel I/O ratio	2045-'50	**8%**	**2%**	**0.03%**	**1%**
	Concrete I/O ratio	2045-'50	**36%**	**2%**	*-0.6%*	**2%**
	Glass I/O ratio	2045-'50	*-1%*	**1%**	*-1.0%*	**3%**
	Wood I/O ratio	2045-'50	*-13%*	**2%**	*-0.4%*	**1%**
	Aluminium I/O ratio	2045-'50	**23%**	**1%**	*-0.7%*	**2%**
	Copper I/O ratio	2045-'50	**2%**	*-0.3%*	*-1.3%*	**4%**

Table A5.5. *Effects of the four sensitivity variants on selected material demand indicators. See text for a description of the sensitivity variants. 'I/O ratio' stands for the Inflow-to-Outflow ratio. Please note that the numbers indicate the change with respect to the same indicators under the regular analysis presented in the main document.* ***Bold*** *numbers indicate an increase in demand or I/O ratio, while red numbers indicate a decrease.*

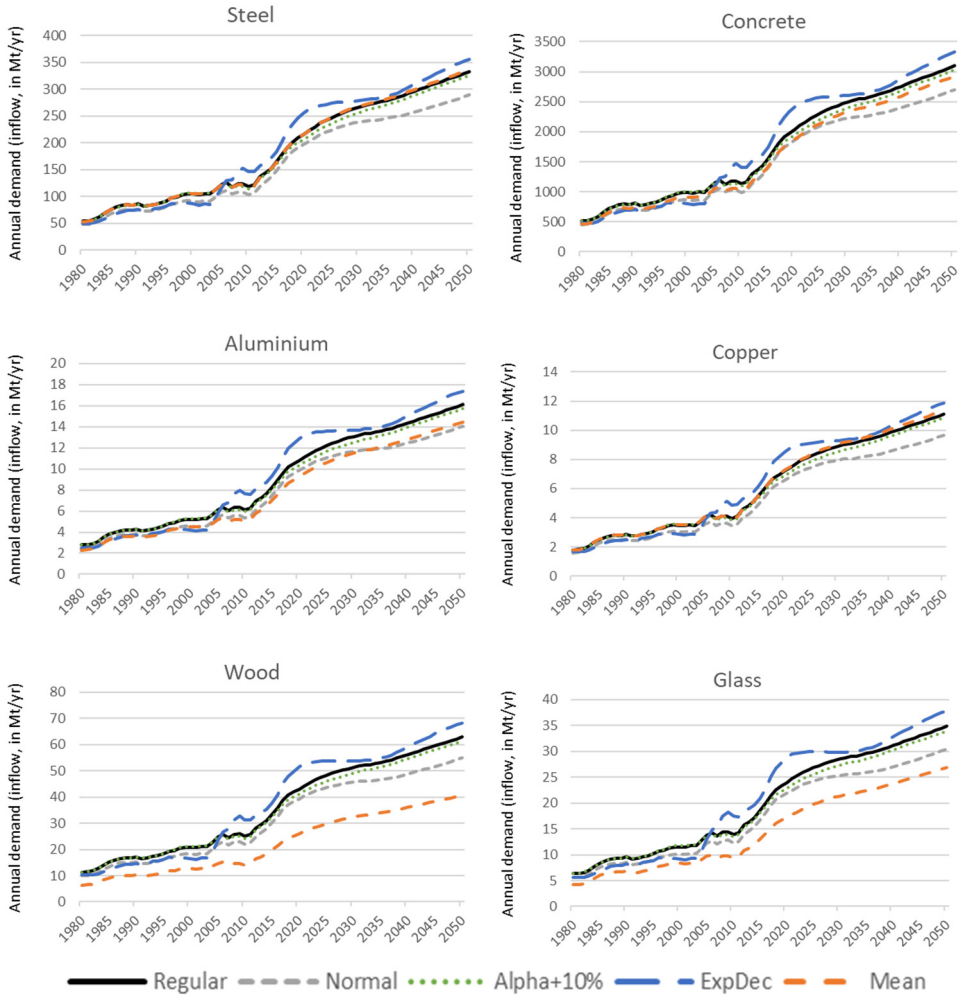

Figure A5.13. *Annual material demand in service sector buildings under the four sensitivity variants (5-yr moving average). 'Regular' indicates the regular (or default) assumptions as described in the main document. 'Normal' refers to the assumption of a normal lifetime distribution as opposed to a Weibull distribution. 'Alpha+10%' is the result of allowing a 10% higher maximum per capita floorspace demand in the regression describing the development of service sector building stock. 'ExpDec' refers to an alternative regression model for service-related floor space demand based on an Exponential Decay function as opposed to a Gompertz function. 'Mean' assumes global mean material intensities; the results for service-related buildings as shown here are the result of assuming a single global material intensity for all service sector buildings, based on the mean in the available data as shown in Figure A5.8.*

So, even though material demand from construction of residential buildings is lower, the gap between inflow & outflow increases. This has to do with a combination of stock dynamics and regional material intensities.

While the demand for concrete is lower in China under the mean material intensity assumptions, so is the Chinese outflow, which due to a relatively short lifetime is considerable towards 2050 as can be seen in Figure 5.4c. At the global level, the inflow (annual demand) of concrete towards 2050 is mostly determined by fast developing regions (see Figure 5.4b). Because the material intensities of most fast developing regions remain mostly the same as in the regular analysis, the inflow remains high in the sensitivity variant, while the outflow (mainly from China) is lower. Thus, leading to an increase in the Inflow-to-Outflow Ratio.

Replacing the Weibull lifetime distribution with a normal distribution has a slightly smaller effect on the annual demand. For service sector buildings it consistently decreases the annual material demand by 13%. As a consequence of a skewed probability density function (PDF) of the Weibull distribution, which leads to faster building replacement and higher inflow, compared to the normal distribution (which therefore has the effect of lowering material demand). This effect is temporary, as we use the same mean lifetimes. The Weibull distribution has a higher spread and consequentially offsets this higher inflow rates due to early decommissioning by lower inflow rates due to a larger surviving fraction at higher building lifetimes, as can be seen in Figure A5.14. A higher spread represents the real-life possibility that a building lasts longer than its envisioned service-life. However, in our model, the continuously expanding commercial stock leads to a larger emphasis on the short term effects than on the long term effects of considering a different lifetime distribution. Assuming a normal lifetime distribution thus causes less service sector buildings to be replaced in the short term.

The effect of implementing a normal lifetime distribution is similar for residential buildings, but there the regional stock dynamics also play a role. Global residential stock increases rapidly during the period 2000-2020, mostly as a consequence of Chinese stock expansion. Since Chinese buildings are assumed to have a relatively short lifetime, a large fraction of the residential cohorts built in this period is already demolished by the end of the scenario period (2045-2050), while most of these buildings are demolished a bit later under the assumption of a normal lifetime distribution, thus leading to an (additional) decrease in demand for most materials in residential buildings compared to the default model. Interestingly, the lower annual demand for materials in residential and service sector buildings does not translate to a smaller gap between inflow and outflow (I/O ratio), which actually increases slightly due to the same stock dynamics.

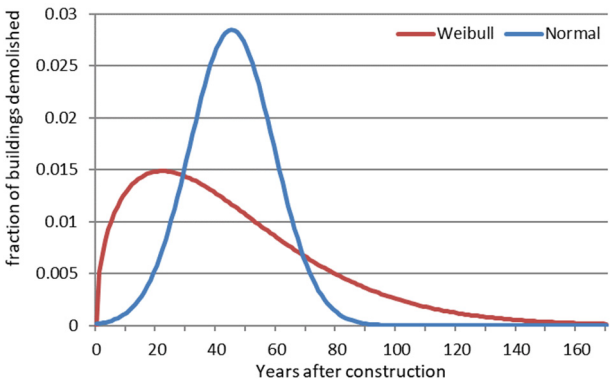

Figure A5.14. *Comparison of building lifetimes in the service sector under two lifetime distributions. The default analysis uses the Weibull distribution, while the sensitivity variant uses the normal distribution.*

The effects of increasing the maximum per capita floorspace demand for service sector buildings may seem counter-intuitive at first sight. One would intuitively expect that a higher maximum floorspace demand would lead to a higher material demand for service sector buildings. However, because of the implementation of this sensitivity variant the entire regression was changed. This means that not only the maximum per capita floorspace demand was increased, but also the beta and gamma parameters of the Gompertz function were changed. Together they lead to a higher demand for service-related floorspace at higher levels of per capita Service Value Added, but to slightly lower demand for service-related floorspace at lower income levels (<40.000 US$ SVA/capita yr^{-1}). Because most regions in the IMAGE model remain below that level, the overall effect is a slight decrease of annual demand for materials in service sector buildings by about 2%.

Finally, the effect of implementing a different regression model for the service sector floorspace demand can also be seen in the right-most column of Table A5.5. Replacing the default Gompertz curve for an Exponential Decay function results in a slight (7-9%) increase in material demand for service sector buildings. This is a consequence of the fact that the Exponential Decay function behaves opposite to the sensitivity variant on increasing alpha. As can be seen from Figure A5.12. This means that the function yields slightly higher per capita demand of floorspace for service sector buildings in the mid-range income regions (with an SVA between 5.000 to 30.000 US$/capita yr^{-1}). As most regions are moving up within this range during the scenario period, the Exponential Decay function leads to slightly increased floorspace demand and a subsequent increase in the use of building materials for buildings in the service sector.

A5.7 Model code

The code of the regression analysis is available in the supplementary information to the original article, the main model is available from Github at https://github.com/SPDeetman/BUMA

References to Appendix 5

1. Stehfest, E., van Vuuren, D., Bouwman, L. & Kram, T. *Integrated assessment of global environmental change with IMAGE 3.0: Model description and policy applications*. (Netherlands Environmental Assessment Agency (PBL), 2014).
2. Machinchick, T. & Freas, B. *Global Building Stock Database, Commercial and Residential Building Floor Space by Country and Building Type: 2017-2026*. (2018).
3. UNData. Per capita GDP at current prices. *National Accounts Estimates of Main Aggregates, United Nations Statistics Division* (2018). Available at: http://data.un.org/Data.aspx?q=GDP&d=SNAAMA&f=grID%3A101%3BcurrID%3AUSD%3BpcFlag%3A1#SNAAMA.
4. UNData. GVA by kind of economic activity. *National Accounts; United Nations Statistics Division* (2018). Available at: http://data.un.org/. (Accessed: 19th November 2018)
5. Kraft. A software package for sequential quadratic programming. (1988).
6. Perez, R. E., Jansen, P. W. & Martins, J. R. R. A. pyOpt: a Python-based object-oriented framework for nonlinear constrained optimization. *Struct. Multidiscip. Optim.* 45, 101–118 (2012).
7. US Bureau of Labor Statistics. CPI Inflation Calculator. (2019). Available at: https://www.bls.gov/data/inflation_calculator.htm. (Accessed: 23rd January 2019)
8. Bevington, P. R. & Robinson, D. K. *Data Reduction and Error Analysis for the Physical Sciences*. *McGraw-Hill* (2003). doi:10.1063/1.4823194
9. Jensen, P. Network-based predictions of retail store commercial categories and optimal locations. *Phys. Rev. E* 74, 035101 (2006).
10. Riahi, K. *et al.* The Shared Socioeconomic Pathways and their energy, land use, and greenhouse gas emissions implications: An overview. *Glob. Environ. Chang.* 42, 153–168 (2017).
11. Pauliuk, S. & Heeren, N. Open Dynamic Material Systems Model. (2018).
12. Daigo, I., Iwata, K., Oguchi, M. & Goto, Y. Lifetime Distribution of Buildings Decided by Economic Situation at Demolition: D-based Lifetime Distribution. *Procedia CIRP* 61, 146–151 (2017).
13. Nomura, K. & Suga, Y. *Asset Service Lives and Depreciation Rates bas ed on Disposal Data in Japan*. (2013).
14. Wang, T., Tian, X., Hashimoto, S. & Tanikawa, H. Concrete transformation of buildings in China and implications for the steel cycle. *Resour. Conserv. Recycl.* 103, 205–215 (2015).
15. Novikova, A., Csoknyai, T. & Szalay, Z. Low carbon scenarios for higher thermal comfort in the residential building sector of South Eastern Europe. *Energy Effic.* 11, 845–875 (2018).
16. Novikova, A. *et al. The typology of the residential building stock in Albania and the modelling of*

its low-carbon transformation. (2015).

17. Olson, B. D. *Residential Building Material Reuse in Sustainable Construction*. (Washington State University, 2011).
18. Kapur, A., Keoleian, G., Kendall, A. & Kesler, S. E. Dynamic Modeling of In-Use Cement Stocks in the United States. *J. Ind. Ecol.* 12, 539–556 (2008).
19. Hatayama, H., Daigo, I., Matsuno, Y. & Adachi, Y. Assessment of the Recycling Potential of Aluminum in Japan, the United States, Europe and China. *Mater. Trans.* 50, 650–656 (2009).
20. Heeren, N. *et al.* Environmental Impact of Buildings—What Matters? *Environ. Sci. Technol.* 49, 9832–9841 (2015).
21. Davis, J. *et al.* Time-dependent material flow analysis of iron and steel in the UK: Part 2. Scrap generation and recycling. *Resour. Conserv. Recycl.* 51, 118–140 (2007).
22. Buyle, M., Braet, J. & Audenaert, A. Life cycle assessment in the construction sector: A review. *Renew. Sustain. Energy Rev.* 26, 379–388 (2013).
23. Murakami, S., Oguchi, M., Tasaki, T., Daigo, I. & Hashimoto, S. Lifespan of Commodities, Part I. *J. Ind. Ecol.* 14, 598–612 (2010).
24. OECD & Eurostat. *Eurostat-OECD Survey of National Practices in Estimating Net Stocks of Structures*. *OECD* (2015).
25. Condeixa, K., Haddad, A. & Boer, D. Material flow analysis of the residential building stock at the city of Rio de Janeiro. *J. Clean. Prod.* 149, 1249–1267 (2017).
26. Olaya, Y., Vásquez, F. & Müller, D. B. Dwelling stock dynamics for addressing housing deficit. *Resour. Conserv. Recycl.* 123, 187–199 (2017).
27. Stephan, A. & Athanassiadis, A. Quantifying and mapping embodied environmental requirements of urban building stocks. *Build. Environ.* 114, 187–202 (2017).
28. Bolt, J., Inklaar, R., Jong, H. de & van Zanden, J. L. Maddison Project Database, version 2018. (2018). Available at: www.ggdc.net/maddison. (Accessed: 26th November 2018)
29. Kadaster. Basisadministratie Adressen en Gebouwen. (2018). Available at: https://zakelijk.kadaster.nl/basisregistratie-adressen-en-gebouwen. (Accessed: 23rd January 2019)
30. Dol, K. & Haffner, M. *Housing Statistics in the European Union 2010*. *Delft University of Technology* (2010). doi:10.1002/hep.21180
31. Sandberg, N. H., Sartori, I. & Brattebø, H. Sensitivity analysis in long-term dynamic building stock modeling—Exploring the importance of uncertainty of input parameters in Norwegian segmented dwelling stock model. *Energy Build.* 85, 136–144 (2014).
32. Lodi, C., Magli, S., Contini, F. M., Muscio, A. & Tartarini, P. Improvement of thermal comfort and energy efficiency in historical and monumental buildings by means of localized heating based on non-invasive electric radiant panels. *Appl. Therm. Eng.* 126, 276–289 (2017).
33. Marinova, S., Deetman, S. & Van der Voet, E. Construction materials database and stock analysis of the global residential built environment: 1970-2050. *J. Clean. Prod.* in review, (2019).
34. Kellenberger, D. *et al.* Life Cycle Inventories of Building Products. *ecoinvent report No. 7* (2007). doi:10.1109/SECON.2017.7925283
35. Kashkooli, A. M. S., Vargas, G. A. & Altan, H. A semi-quantitative framework of building lifecycle analysis: Demonstrated through a case study of a typical office building block in Mexico in warm and humid climate. *Sustain. Cities Soc.* 12, 16–24 (2014).
36. Kofoworola, O. F. & Gheewala, S. H. Life cycle energy assessment of a typical office building in Thailand. *Energy Build.* 41, 1076–1083 (2009).

37. Oka, T., Suzuki, M. & Konnya, T. The estimation of energy consumption and amount of pollutants due to the construction of buildings. *Energy Build.* 19, 303–311 (1993).

38. Reyna, J. L. & Chester, M. V. The Growth of Urban Building Stock: Unintended Lock-in and Embedded Environmental Effects. *J. Ind. Ecol.* 19, 524–537 (2015).

39. Schebek, L. *et al.* Material stocks of the non-residential building sector: the case of the Rhine-Main area. *Resour. Conserv. Recycl.* 123, 24–36 (2017).

40. Gruhler, K. & Deilmannl, C. Materialaufwand von Nichtwohngebäuden – Teil II. in (Fraunhofer IRB Verlag, 2017).

41. Rosselló-Batle, B., Moià, A., Cladera, A. & Martínez, V. Energy use, CO2 emissions and waste throughout the life cycle of a sample of hotels in the Balearic Islands. *Energy Build.* 42, 547–558 (2010).

42. Kumanayake, R., Luo, H. & Paulusz, N. Assessment of material related embodied carbon of an office building in Sri Lanka. *Energy Build.* 166, 250–257 (2018).

43. Marcellus-Zamora, K. A., Gallagher, P. M., Spatari, S. & Tanikawa, H. Estimating Materials Stocked by Land-Use Type in Historic Urban Buildings Using Spatio-Temporal Analytical Tools. *J. Ind. Ecol.* 20, 1025–1037 (2016).

44. Leadbitterglass. How To Calculate The Weight Of Glass. (2019). Available at: http://www.leadbitterglass.co.uk/glassroom/calculate-weight-of-glass/. (Accessed: 23rd January 2019)

45. Porteus, J. & Kermani, A. *Structural Timber Design to Eurocode 5*. (John Wiley & Sons, Ltd, 2007). doi:10.1002/9780470697818

46. Brown's. Standard and Lightweight Concrete Block / Architectural Block Cube Sizes and Weights. (2019). Available at: https://www.brownsconcrete.com/images/Resources/Building/Product_Info/Block_Weight_Cube_Size.pdf. (Accessed: 23rd January 2019)

47. Ted Pella inc. Standard Gauge for Sheet and Plate Iron and Steel. (2019). Available at: https://www.tedpella.com/company_html/gauge.htm. (Accessed: 23rd January 2019)

48. National Masonry. Masonry Blocks & Bricks. (2019). Available at: https://www.nationalmasonry.com.au/wp-content/uploads/National_Masonry_Design_Guide_Book_2_SQLD.pdf. (Accessed: 23rd January 2019)

49. Daioglou, V., van Ruijven, B. J. & van Vuuren, D. P. Model projections for household energy use in developing countries. *Energy* 37, 601–615 (2012).

50. Deetman, S. repository for the building materials model. (2019). Available at: https://github.com/SPDeetman/BUMA.

51. IEA. Commercial Buildings Energy Consumption Survey (CBECS). (2012). Available at: https://www.eia.gov/consumption/commercial/.

Appendix 6

Based on supplementary information with:
Deetman et al. (2021) - *Projected material requirements for the global electricity infrastructure – generation, transmission and storage* - Resources, Conservation and Recycling, Vol. 164, p. 105200 - https://doi.org/10.1016/j.resconrec.2020.105200

A6.1 Detailed assumptions on electricity generation capacity

The development of generation capacity is one of two main drivers of our material model and is given as an output of the IMAGE/TIMER model [1] based on the SSP2 scenario used in this study [2]. Corresponding to the total global generation capacity as provided in the main text (Figure 6.3), Figure A6.1 provides some more regional detail with respect to the development of generation capacities by technology.

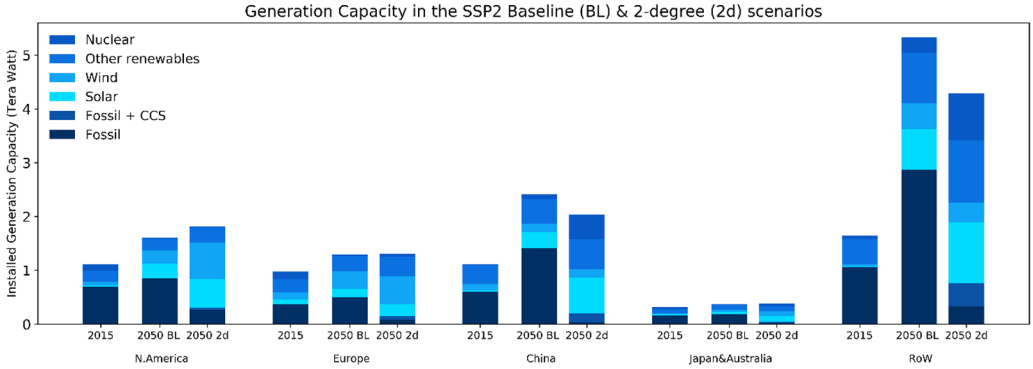

Figure A6.1. *Electricity Generation Capacity in the SSP2 Baseline and 2-degree scenarios according to the IMAGE model [1], [2]. More information on assumptions underlying the SSP scenarios, such as the development of population, economic indicators, land-use etc. can be found in the online at https://tntcat.iiasa.ac.at/SspDb based on [3].*

With generation capacity given, we came up with the corresponding material use as detailed in the results of the main manuscript. To do so, we required data on the materials per unit of generation capacity for each of the 27 generation technologies in the IMAGE/TIMER energy model, which is given in Table A6.2, below.

Even though the IMAGE/TIMER uses a vintage stock model based on fixed lifetimes to derive annual additions to stock (newly installed generation capacity) as described in [4], we also

wanted to provide the outflow of scrap materials from electricity generation technologies, so we decided to apply a dynamic stock model, as part of an open source software platform developed & described by [5], to derive both the inflow and outflow of materials. The lifetimes are derived from [4], and are applied in combination with a standard-deviation of 0.214 times the mean lifetime, based on [6]. This translates to a relatively low spread in the lifetime distribution, which is typical for industrial capital as it is subject to standard maintenance & decommissioning contracts.

Technology	Technical lifetime (yrs)
Solar PV	25
CSP	25
Wind onshore	25
Wind offshore	25
Hydro	80
Other Renewables	30
Nuclear	60
Fossil Fuel Based	40

Table A6.1. *Technical lifetime assumptions for generation technologies, based on [4]. These are used in the calculation of the inflow and outflow of materials.*

A6.2 Electricity transmission, the grid

A6.2.1 Grid lengths

Using a preprocessed version of Open Street Maps for the year 2016, available from http://osm2shp.ru/#Data and the power_ln files, we extracted the length of the grid lines according to the IMAGE region definition detailed in Appendix 1. Because underground lines are typically not identified or distinguished, the resulting line lengths were interpreted as being overhead high voltage (HV) lines, given their typically prominent visibility. Unless this was counter-indicated by any of the sparse national statistics, as displayed in Table A6.4 below. It shows that the OSM data provides a reasonable estimate of HV line lengths in quite a few cases. However, it also shows cases of possible overreporting (e.g. Ukraine) or underreporting (e.g. China) compared to national studies.

Table A6.2. *Material intensities for electricity generation technologies in ton/MW peak (or kg/kW peak capacity), corresponding to the 27 generation technologies in the IMAGE/TIMER energy model [4]. * For offshore wind farms, more information was available on steel monopile base structures, we assumed that only 10% of the base structures are composed of concrete monopiles. ** assumed to be the same as an onshore windmill. Material intensities for copper, cobalt and neodymium are based on the medium estimates found in [7].*

						Based on [7]			
Technology	Con-crete	Steel	Al	Pb	Glass	Cu	Co	Nd	Sources & Comments
Solar PV		150	10.2	0.122		6.34			[8–11]
CSP	1351.8	576	5.50		156	3.15			[8,11–13]
Wind onshore	434	121	0.87			2.73		0.02	[8,14–21]
Wind offshore	509*	158	1.44			5.57		0.16	[8,9,17,19,20,22–24]
Hydro	2833	71		0.005		1.70			[11,25,26] & 10% run-off river
Other Renewables	1026	216	3.6	0.03	31	3.90		0.04	Assumed: Average of above
Nuclear	235	43	0.08	0.034		0.76	1.2^{E}-4		[11,27], table 24 & 25 in [28]
Conv. Coal	352.8	84.6	0.504			1.15	0.12		[29–31]
Conv. Oil	213.4	72.9	0.6			0.76	0.07		[32] *or avg. of Conv. Coal/NG CC*
Conv. Natural Gas	43.0	4.0	0.4			0.38	0.02		[33] *or avg. of Conv. Coal/NG CC*
Waste	213.4	72.9	0.6			0.76	0.07		Assumed: same as Conv. Oil
IGCC	165	34.9	0.504			1.15	0.12		[12] or if no data: same as Coal
OGCC	213.4	72.9	0.6			0.76	0.07		Assumed: same as Conv. Oil
NG CC	64.6	29	0.65			1.05	0.02		[26,33]
Biomass CC	89.2	33.4	0.3			0.76	0.07		[12,26]
Coal + CCS	352.8	109.2	0.504			1.63	0.12		[31], or Conv. Coal if no data
Oil/Coal + CCS	213.4	94.1	0.6			1.45	0.07		Based on 29% more steel & [31]
Natural Gas + CCS	43.0	5.2	0.4			1.07	0.03		Based on 29% more steel & [31]
Biomass + CCS	89.2	43.1	0.3			1.45	0.07		Based on 29% more steel & [31]
CHP Coal	352.8	84.6	0.5			5.59	0.12		Mn: added 10% of CHP in [34]
CHP Oil	213.4	72.9	0.6			5.21	0.07		Mn: added 10% of CHP in [34]
CHP Natural Gas	43.0	4.0	0.4			4.82	0.02		Mn: added 10% of CHP in [34]
CHP Biomass	243.8	6.2	0.05			2.94	0.07		Table 8.3 in [35]
CHP Coal + CCS	352.8	109.2	0.5			6.28	0.12		Assumed: Same as CCS variant
CHP Oil + CCS	213.4	94.1	0.6			5.90	0.07		Assumed: Same as CCS variant
CHP Nat. Gas + CCS	43.0	5.2	0.4			5.52	0.03		Assumed: Same as CCS variant
CHP Biomass + CCS	243.8	43.1	0.3			3.63	0.07		Assumed: Same as CCS variant

Table A6.3. *Projected global average material intensities of the generation capacity (in ton/MW installed capacity) for 7 materials. These are a result of combining the changes in installed capacity (from IMAGE, see Figure 6.3a in Chapter 6) with the material intensities by technology as provided above (Table A6.2).*

	2015	2050, Baseline	2050, 2-degree
Steel	65	84	101
Aluminium	0.6	1.7	2.8
Concrete	859	691	741
Glass	0.10	1.5	3.8
Cu	1.7	2.2	2.9
Nd	0.0015	0.0044	0.006
Co	0.041	0.041	0.012
Pb	0.007	0.017	0.035

This highlights the importance of further improving the data in the lengths of transmission lines. For now, however, the data used was deemed adequate, given that we were able to check the majority of the global circuit kilometers against at least one national study. In fact, only 12.6% of the total global circuit length used in this study (Table A6.4) could not be validated against national studies. This indicates that the possible underestimation or (most likely) overestimation of the data for these countries represents a small fraction of the global line length.

Once we derived the HV voltage line lengths from Table A6.4, we continue by calculating the length of lower voltage transmission lines based on a static ratio between high voltage and medium voltage (MV) or low voltage (LV) according to [37] and [38] as detailed in Table A6.5. It shows that national studies provided more information on the MV network than on the length of the LV network. It is difficult to determine whether this is a realistic representation, or a definition issue due to the use of different sources for example. So, this might be an area for future research.

A6.2.2 Undergrounding of power lines

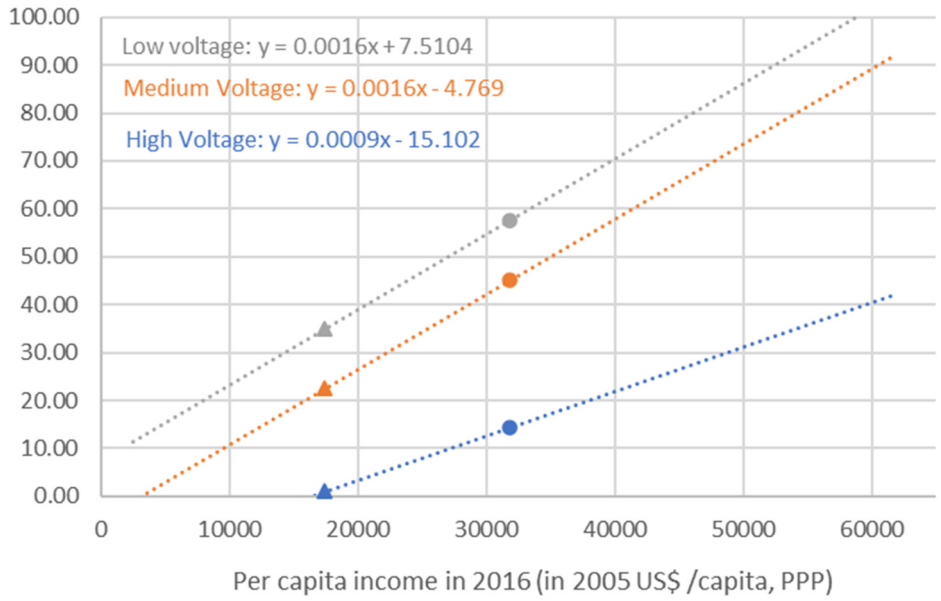

Figure A6.2. *Assumed relation between income levels and percentage undergrounding of transmission lines of different voltage levels, based on the indicated data points for Western Europe (circles) and Eastern Europe (triangles) as reported by [37].*

Table A6.4. *Length of grid lines in several studies, in km. Data in the first column is copyrighted by OpenStreetMap (OSM) contributors and available from https://www.openstreetmap.org. If available, the second column gives an indication of the grid length from national studies. Similar to [38] we assume that most of the OSM coverage represents high-voltage lines (overhead + underground). Highlighted cells indicate the numbers used in this study (average of the highlighted cells per row). Data was selected (highlighted) based on the following rationale: by default, we use the average between our own calculations and the Arderne study, unless the study by Arderne et al. reported a HV line length more than 3 times the value from national statistics (indicated with an asterisk *), in that case we chose to ignore the values from Arderne (as we expected over-reporting of the HV network in these cases) and incorporate the national estimates in the average used. In other cases where we suspected over reporting of HV lines in the OSM data (USA, Europe, India & Oceania), we used the two lowest available values. In cases where we expected under-reporting of HV line lengths (Mexico, China, Korea, Indonesia & Rest of South Asia), we chose to ignore the two highest available estimates. For National studies, voltage levels are defined as follows: LV: <1kV, MV: 1-135kV, HV: >135kV. For the study by Arderne et al. Voltage classifications deviate slightly for the Medium & High Voltages (LV: <1kV, MV: 1-75 kV, HV: >75kV), which may explain slightly higher numbers for HV transmission line lengths.*

	Open Street Maps	**National Studies**			**Nature Scientific Data**		
Sources:	*Calculation by the Authors*	*globaltransmission.info,* [36, 37]			*(Arderne at al.)*		
Year of data:	*2016*	*2013-2017*			*2019*		
	HV	**HV**	**MV**	**LV**	**HV**	**MV**	**LV**
Canada	95,100	96,500	37,500		114,000	180,700	713,800
USA	641,400	441,900	171,900		647,700	959,800	8,647,400
Mexico	48,000	51,200	52,900	749,400	49,600	171,000	1,666,600
Central America	8,900	7,600	8,166		16,700	79,800	626,700
Brazil*	94,335	67,200			232,900	370,700	3,105,800
Rest of South America	66,800				111,300	335,600	2,462,700
Northern Africa	86,700				96,300	150,800	2,012,500
Western Africa	20,700				41,100	232,500	130,800
Eastern Africa	18,900				27,200	90,800	41,300
South Africa*	54,200	15,200			57,200	89,600	58,600
Western Europe	560,300	251,200	2,857,800	4,894,000	491,500	706,000	8,871,000
Central Europe	165,100	67,100	716,100	1,072,600	175,700	291,200	2,662,900
Turkey	45,100				55,200	171,400	1,057,000
Ukraine region*	126,400	10,400			131,500	130,300	1,301,300
Central Asia	40,600				60,600	156,100	916,100
Russia Region*	322,900	69,200			388,800	631,300	2,783,600
Middle East	123,100	123,400	94,500		135,900	337,900	2,516,300
India	319,800	273,500	298,600		422,400	693,100	604,400
Korea	9,300				14,400	36,400	536,100
China	183,900	646,500			284,500	827,000	17,508,600
South Eastern Asia	22,700				68,900	237,500	2,817,800
Indonesia Region	12,100				24,100	143,500	3,324,200
Japan*	43,800	18,800			62,700	68,600	2,122,800
Oceania	57,900	26,100			73,500	73,900	651,100
Rest of South Asia	18,700	21,900	12,200		50,700	142,700	1,952,400
Rest of Southern Africa	15,200	16,400			50,900	137,700	36,300

Table A6.5. *Transmission line length ratios. The values indicate the length of Medium Voltage lines (MV) or Low Voltage (LV) per km of High Voltage (HV) line. If multiple values are available, we apply an average. See Table A6.4 for sources and the lengths of HV lines. This table excludes regions with expected under-reporting or over-reporting as discussed with Table A6.4, except when a national statistics on MV/HV or LV/HV ratio were available.*

Region	**Km MV per km HV line**		**Km LV line per km HV line**	
Source	National studies	Arderne et al. [38]	National Studies	Arderne et al. [38]
Canada	0.39	1.58		6.3
USA	0.39	1.48		13.4
Mexico	1.03	3.45	14.6	33.6
Central America	1.07	4.77		37.5
Rest of South America		3.02		22.1
Northern Africa		1.57		20.9
Western Africa		5.66		3.2
Eastern Africa		3.34		1.5
Western Europe	11.4	1.44	19.5	18.0
Central Europe	10.7	1.66	16.0	15.2
Turkey		3.10		19.1
Central Asia		2.58		15.1
Middle-East	0.77	2.49		18.5
India	1.09	1.64		1.4
South East Asia		3.45		40.9
Rest of south Asia	0.56	2.82		38.5
Rest of Southern Africa		2.70		0.7
Average	3.04	2.65	16.7	18
Average used (for other regions)	**2.85**		**17.35**	

A6.2.3 Substations and transformers

To incorporate additional electricity transmission infrastructure, our analysis covers the material contents of substations and transformers. To do so, we first needed to derive the demand for these elements in units per kilometer of transmission line, specified for three different voltage levels as detailed in Table A6.6, below.

Table A6.6. *Assumptions on the number of substations and transformers per km of transmission line.*

(units/km)	**High**	**Medium**	**Low**
Sources →	[39]	[39,40]	[40]
Substations	0.0169	0.085	1.107
Transformers	0.0532	0.103	1.107

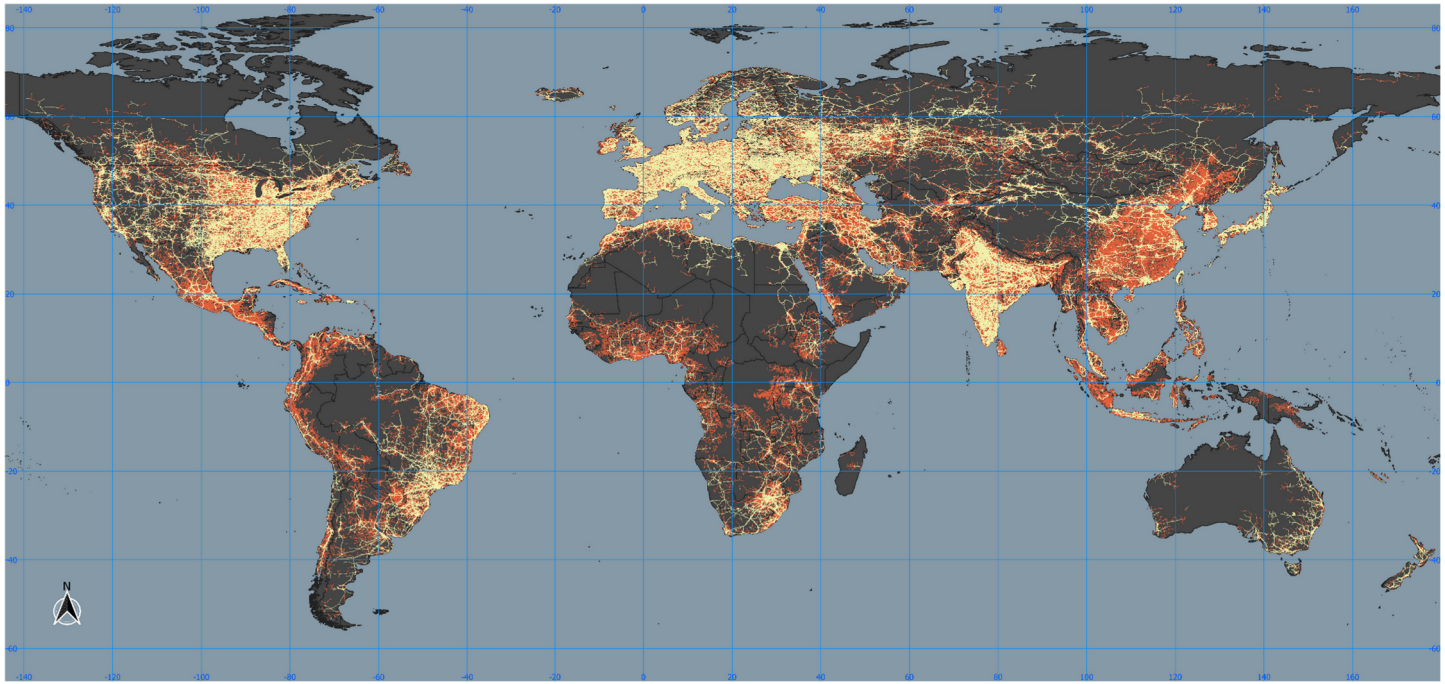

Figure A6.3. *Global High Voltage & Medium Voltage Transmission Lines. Data displayed here is based on the work by Arderne et al. [39], High Voltage lines are based on OpenStreetMap and displayed in yellow, Medium Voltage lines are modelled by Arderne et al. as published online at https://gridfinder.org/*

A6.2.4 Lifetimes of grid elements

To account for the lifetimes of power lines, substations and transformers, we applied the same dynamic stock model as described in section A6.1. We even apply the same standard-deviation, but on grid-specific mean lifetimes as detailed in Table A6.7.

Table A6.7. *Mean lifetimes applied to the grid elements. Numbers are based on [39–42].*

	Lifetime (in years)
transformers	30
lines	40
substations	40

A6.2.5 Material intensities of grid elements

Now that we have an indication of the length of the transmission line as well as the number of substation and transformers, we apply a fixed, but voltage-level specific, material intensity for each of the grid elements in Table A6.8 and Table A6.9, below.

Table A6.8. *Material intensities for substations and transformers (in kg/unit). These numbers are derived using our interpretation of data from [39,40,42].*

kg/km	Concrete	Steel	Aluminium	Cu	Pb	Glass
HV overhead	209138	52266	12883			1097
HV underground	17500			11650	14050	
MV overhead		802.3		1488		
MV underground		0	823.6	662.9		
LV overhead		0	981			
LV underground		177	531			

Table A6.9. *Material intensities for power lines, including towers/poles (in kg/km line). These numbers were derived using the following sources: [40,41,43].*

kg/unit	Concrete	Steel	Aluminium	Cu	Glass
Hv Substation	123900	14652	33204	4611	0.05
Mv Substation	127021	1815	1228	279.2	
Lv Substation	476	38	1228	1	
Hv Transformer	648000	296000	497	76047	
Mv Transformer	46826	22659	21	6877	
Lv Transformer	176	480	85	13	

A6.3 Electricity storage

A6.3.1 Electricity storage demand

Total electricity storage demand is the second main driver of the material model described in the main text and is provided as an output from the IMAGE model. Within the IMAGE model, it is calculated using a relation between the penetration of wind and solar in the mix as shown in Figure A6.4. Here, we show the demand for storage capacity expressed as a fraction of the installed generation capacity as an (unweighted) average of the 8 region specific residual load duration curves (RLDCs) available from [44]. It is important to note that these RLDCs were constructed using a fixed storage price based on flow-batteries of 100$/kWh and a round-trip efficiency of 76% [44]. This is a rather low price estimate compared to our price assumptions as detailed in Table A6.13, which might mean that the assumed storage demand is on the high side.

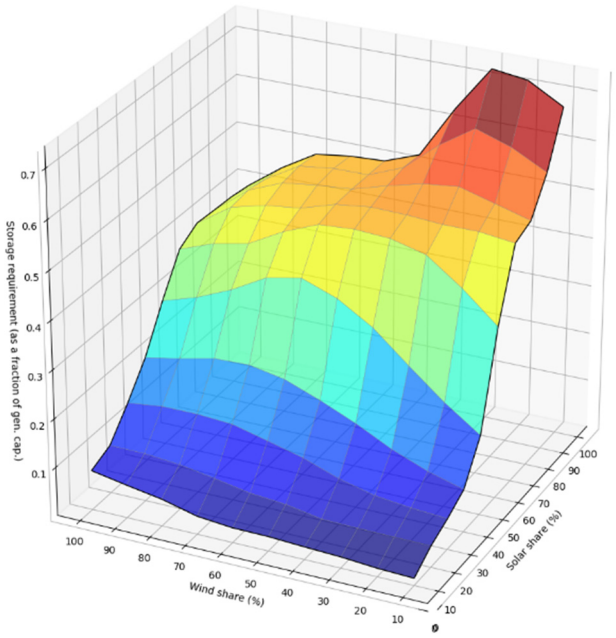

Figure A6.4. *Storage demand as a fraction of peak generation capacity, given different levels of solar and wind energy penetration, based on data from [44]. The numbers are an (unweighted) average of multiple regions, and only serve as an illustration of the approach to determining storage demand. Combined solar and wind shares of more than 100% are possible, because at high renewable penetration, peak demand can only be supplied by a surplus generation capacity.*

A6.3.2 Pumped hydro storage

Our analysis assumes a tiered approach to electricity storage deployment, in which pumped hydro storage is the first and default option. We use projections on pumped hydro storage availability according to [45], as shown in Figure A6.5.

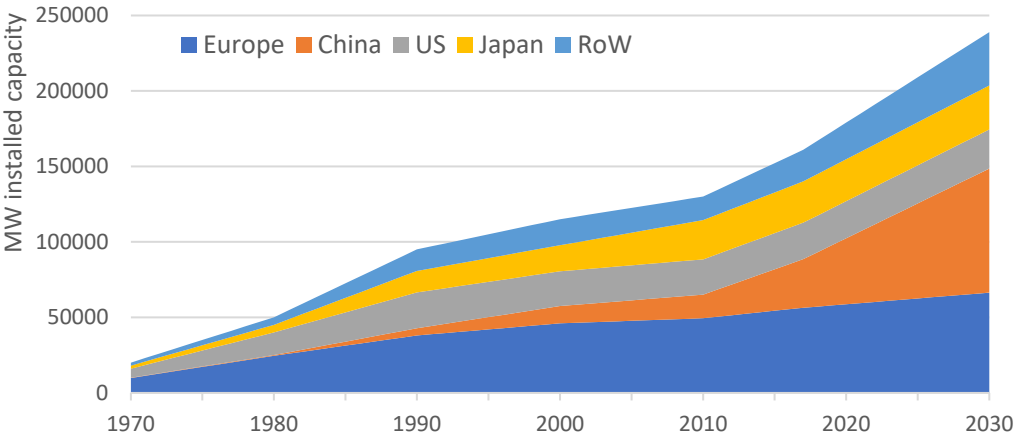

Figure A6.5. *Expected development of Pumped Hydro Storage availability (in MW installed capacity) according to [45]. We assume a regional disaggregation according to the IMAGE relative hydro-power capacity, and a continued growth of pumped hydro capacity according hydro-power expansion within regions [46].*

A6.3.3 Electricity storage in electric vehicles

In order to determine the availability of electricity storage in the electric vehicle (EV) fleet we first determined the number of cars based on the IMAGE model projections described by [47] and a dynamic stock model, including lifetime assumptions, in the same way as described by [7]. Secondly, we determine the average storage capacity in current electric cars based on a review of currently available plugin- and full battery EV models according to ev-database.org, as can be seen in Table A6.10.

The average battery capacity of full battery electric vehicles (BEVs) and plugin hybrid electric vehicles (PHEVs) found in Table A6.10. is used to represent the recent situation and applied for the year 2018. However, battery density is expected to increase, while battery costs are expected to go down over the coming years (see Table A6.13), which could lead to a variety of possible changes to the available Vehicle to Grid (V2G) storage capacity over time. Here, we assume that the weight (and not necessarily the costs) are the limiting factor for battery deployment in EVs. This means that an increase in battery density would allow for more storage capacity, without affecting the weight of the battery unit or the car. We therefore apply a fixed battery weight, which results in a changing total battery capacity per vehicle as can be seen in Figure A6.6. The figure also indicates the assumed penetration rate of vehicle to grid as a technology, which increases from 0% for 2025 (based on [48]) before reaching the maximum available percentage of the storage capacity of 10% (PHEVs) or 12% (BEVs) by 2040. Reiterating from the main text that these model settings may perhaps look

optimistic regarding the adoption of vehicle to grid as a common practice, but is rooted in the idea that most of the perceived obstacles to its adoption (such as 'range anxiety') [49] are expected to become less of a problem given the expected increase in battery capacity as indicated in Table A6.13.

Table A6.10. *Battery capacity of recent BEV and PHEV car models, according to ev-database.org (accessed 11-11-2019). The average from all models is used to represent the current battery capacity in our analysis.*

BEVs			PHEVs		
Brand	**Model**	**Capacity (kWh)**	**Brand**	**Model**	**Capacity (kWh)**
Tesla	Model3, LR, Dual	75	Porsche	Panamera Sport Tur. 4 E-hybrid	14.1
Mercedes	EQC 400 4MATIC	85	Porsche	Cayenne E-hybrid	14.1
VW	e-Golf	35.8	Land Rover	Rover Sport p400e	12.4
Audi	e-tron 55 quattro	95	BMW	225xe iPerformance	7.6
Tesla	Model3, std range plus	55	Mitsubishi	Oultander	13.8
Kia	e-Niro	64	Mini	Countryman Cooper SE All4	7.6
MG	ZS EV	44.5	Hyundai	IONIQ	8.9
Nissan	Leaf	40			
Nissan	Leaf e+	62			
Tesla	Model3, LR, Perform.	75			
Hyundai	IONIQ	38.3			
BMW	i3 120Ah	42.2			
Jaguar	I-Pace	90			
Renault	Zoe ZE50 R110	55			
Hyundai	Kona	67.1			
Tesla	Model S	100			
Opel	Ampera-e	60			
Renault	Zoe ZE50 R135	55			
Tesla	Model X, LR	100			
Tesla	Model S, Perform.	100			
Nissan	e-NV200 Evalia	40			
Citroen	C-Zero	16			
BMW	i3s 120Ah	42.2			
Renault	Kangoo Maxi ZE33	33			
Peugeot	iOn	16			
Tesla	Model X, Perform.	100			
Peugeot	Partner Tepee	22.5			
Average		**59.6**	**Average**		**11.2**

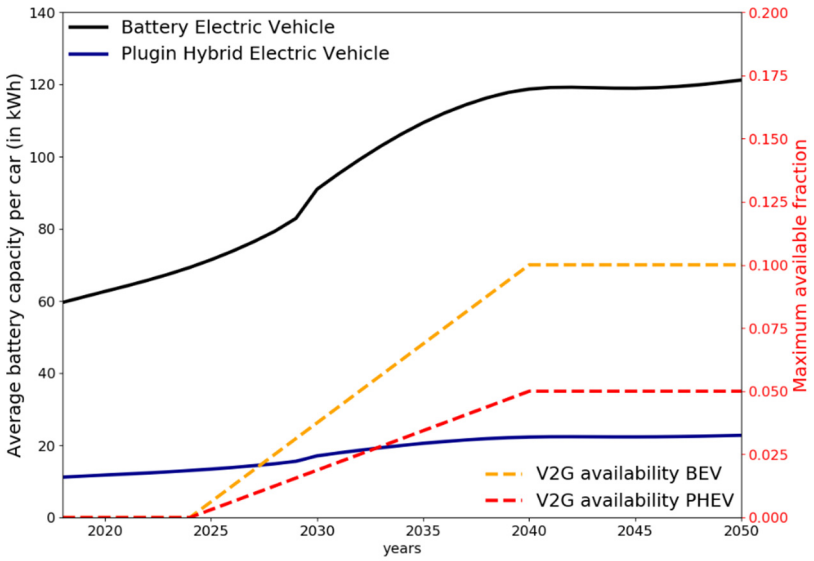

Figure A6.6. *development of EV & PHEV storage capacity (kWh), given a fixed battery weight assumption. Due to increased energy density of EVs, the average battery capacity will double from about 60 kWh to 120 kWh by 2040. The secondary axis displays the slow adoption of vehicle to grid technology from 2025 onward, ensuring a maximum of 12% of the vehicles battery capacity is available for energy storage.*

A6.3.4 Dedicated storage demand

Dedicated storage demand is the result of the tiered approach of the regional availability of pumped-hydro storage and electric vehicles for vehicle-to-grid storage as described in the main text. The sensitivity to regional circumstances is depicted in Figure A6.7. Which shows that in many regions there is no demand for additional storage capacity, even in the SSP2 2-degree climate policy scenario, because the growth of pumped hydro and electric vehicle availability is enough to fulfill the total storage demand. Only in the regions labeled as 'Rest of the World' a dedicated storage capacity is required. The resulting regional deployment of dedicated storage capacity is detailed in Figure A6.8.

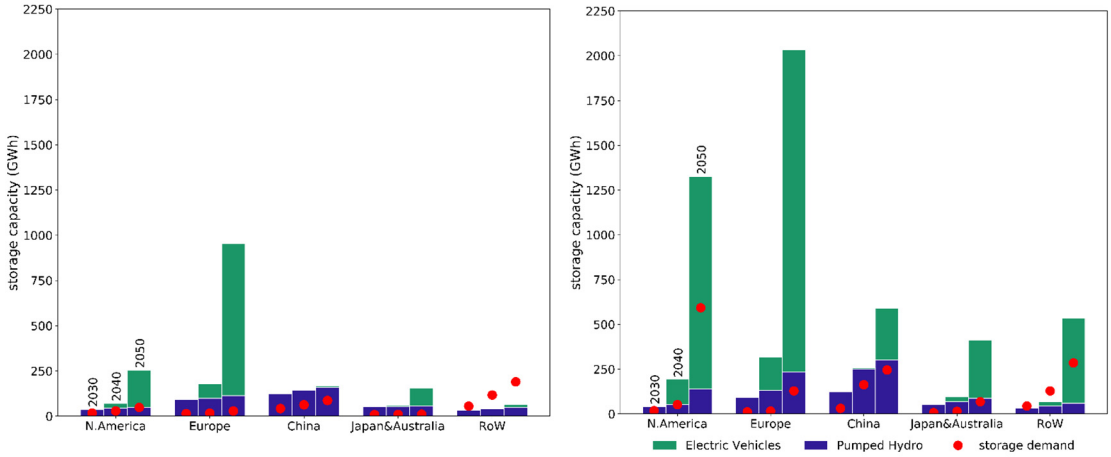

Figure A6.7. *Demand & supply of electricity storage capacity in 2030, 2040 and 2050, in 5 world regions, under the SSP2 Baseline (left) and under a climate policy scenario (SSP2 2-degrees, right). RoW: Rest of the World.*

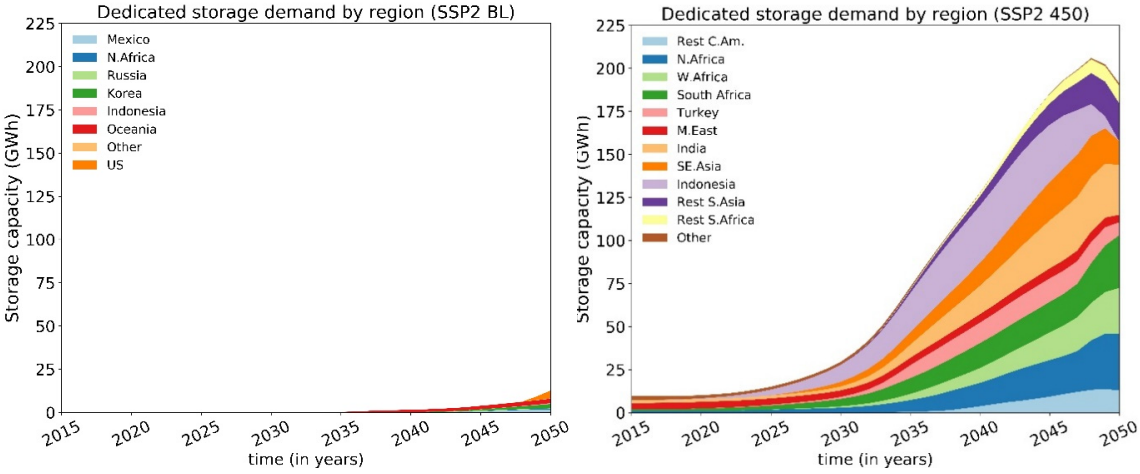

Figure A6.8. *Total demand for dedicated storage, by region. Results are given for the SSP2 baseline (left) and the SSP2, 2-degrees climate policy scenario (right).*

A6.3.5 Market shares of storage technologies

Once the size of the 'dedicated' storage demand has been determined as the remainder of the total storage demand minus the available capacity in pumped hydro and EVs, we need to determine the market share of individual technologies to fulfill the last tier of storage. This is done based on the basis of the lowest costs per kWh (cycled, not capacity) using a multinominal logit model, as detailed in the main text. Calibration of the logit parameter uses cost data from Table A6.13 and is checked against data by the IEA for the year 2016 [50] (p. 63), leading to a logit parameter (λ) setting of 0.2. A further set of cost penalties was applied to enhance the fit with the available literature by the IEA, as shown in Figure A6.9. These penalties are reduced towards 2030, but the implied cost-reduction of lithium- and nickel-based batteries is maintained beyond 2030 (due to an expected second hand market for batteries from former EVs as stationary storage). The combination of a low logit parameter and the need for high cost penalties (e.g. high for Compressed Air) needed to match historic markets suggest that the energy storage sector does currently not deploy technologies according to the cost-optimality principle.

Table A6.11. *Cost penalties (multipliers) applied to the costs of some energy storage technologies. These multipliers are applied to the costs in Table A6.13 in order to ensure a reasonable representation of the current market.*

	2018	2030
Flywheel	1.5	1
Compressed Air	18	1
NiMH	0.6	0.4
LMO	0.5	0.4
NMC	0.5	0.4
NCA	0.5	0.4
Zinc-Bromide	3	1
Vanadium Redox	3	1
Sodium-Sulfur	1.5	1
ZEBRA	1.5	1

The development of the market shares over time, of both the newly installed storage capacity as well as the resulting development of the technology shares within the stock are given in Figure A6.10a &b, below. The share of the stocks is based on two additional model assumptions, being: 1) that all dedicated electricity storage pre-1990 is based on deep cycle Lead-Acid batteries, and 2) a changing lifetime assumption by technology as detailed in Table A6.12.

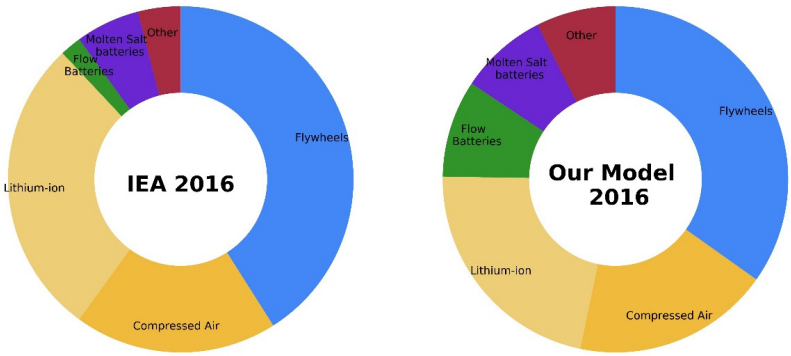

Figure A6.9. *Current market fit of our model compared to IEA 2017* [50].

Table A6.12. *Lifetime assumptions for storage technologies used in dedicated electricity storage (in yrs). The lifetime is based on 150% of the indicated cycle life given in Table A6.13, assuming a diurnal use or the shelf-life in years given by* [51] *(whichever comes first). The cycle life is extended by 50% to represent the idea that dedicated energy storage is subject to enormous capital investments and the fact that the cycle life is determined using the technical lifetime, beyond which about 80% of the storage capacity remains usable.*

	Lifetime (yrs)	
	2018	**2030**
Flywheel	20	30
Compressed Air	50	50
Hydrogen FC	4.1	9.6
NiMH	4.1	6.2
Deep-cycle Lead-Acid	6.2	12.3
LMO	2.1	3.3
NMC	6.2	8.2
NCA	2.1	3.3
LFP	10.3	20
LTO	15	23
Zinc-Bromide	12	20
Vanadium Redox	10	17
Sodium-Sulfur	17.0	22.0
ZEBRA	15.0	22.0
Lithium Sulfur	2.15	4.11
Lithium Ceramic	2.00	10.00
Lithium-air	2.98	4.44
PHS	60	60

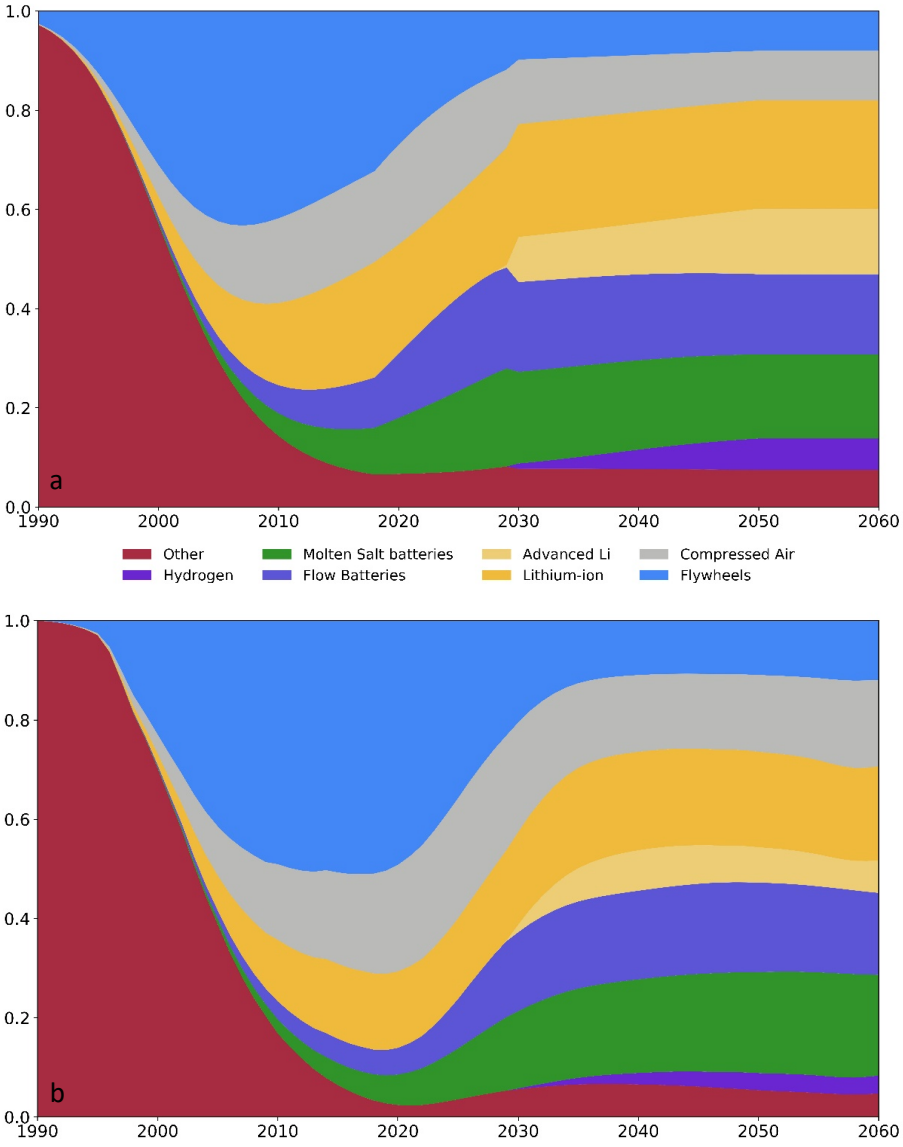

Figure A6.10a-b. *Market shares of the dedicated electricity storage technologies (a) & shares of the technologies within the stock (b).*

Now that the share of the dedicated electricity storage technologies (both stock & purchases) is known, they can be multiplied with the weights (using energy densities in Table A6.13) and the weight composition as shown in Table A6.14.

		Technology ↓	Energy density		(dis)charge cycles		Investment costs		Round trip efficiency		
		Unit →	Wh/kg		Nr. of cycles before end of life (@80% cap.)		USD/kWh (storage capacity)		%		
Grouping		Time →	**2018**	**2030**	**2018**	**2030**	**2018**	**2030**	**2018**	**2030**	**Sources**
Batteries	Nickel	NiMH	75	100	1000	1500	300	300	70%	80%	52,53
	Lead-acid	Deep-cycle Lead-Acid	40	40	150	150	150	150	70%	80%	51
	Li-ion	LMO	121	160*	500	800	400	225	96%	98%	51,54
		NMC	185	283*	1500	2000	420	225	96%	98%	51,54,55
		NCA	230	300*	500	800	350	200	96%	98%	51,54
		LFP	120	212*	2500	5000	580	230	94%	96%	51,54,55
		LTO	65	211	7500	20000	800*	400*	98%	99%	51,54,56,57
	Flow	Zinc-Bromide	40	67	10000	10000	538	250	70%	80%	51,58,59
		Vanadium Redox	25	35	15000	15000	475	131	70%	80%	51,58,60
	Molten-salt	Sodium-Sulfur	200	250	6000	8000	463	145	80%	85%	51,61
		ZEBRA	186	300	4500	7500	525	110	84%	87%	59,62
	Lithium-metal (/advanced Li)	Lithium Sulfur	328	750	523	1000	375	250	91%	98%	63,64
		Lithium Ceramic	299	740	600	6000	800*	110	70%	90%*	65,66,67
		Lithium-air	200	250	725	1080	700	275	50%	85%	68,69,70,71,72
Other	Mechanical	Pumped-Hydro	1	1	50000	50000	63	63	80%	80%	51
		Flywheel	100	100	112500	140000	4500	2000	85%	88%	51,73
		Compressed-Air	4	5	30000	40000	86	45	52%	63%	51,73
	Fuel-cells	Hydrogen FC	157	157	1000	2333*	747	133	25%	45%	51,74

Table A6.13. *Cost and performance indicators for electricity storage technologies between 2018 and 2030, based on various sources. * Some values indicated with an asterisk include estimates by the authors. Only highlighted battery types are assumed to be available for mobile applications such as electric vehicles.*

Grouping		Technology	Steel	Al	Plastics	Glass	Cu	Co	Ni	Pb	Mn	Nd	Sources & comments
Batteries	Nickel	NiMH	10%	0.26%	21%		1.77%	0.26%	44.3%		0.26%	4.7%	[52]
	Lead-acid	Deep-cycle Pb-Acid			10%	2%				61%			[34]
	Li-ion	LMO	21.5%	3.7%	8.4%		10 %				16.7%		[75]
		NMC	21.5%	3.7%	8.4%		10%	7.6%	7.6%		7.1%		[75]
		NCA	0.7%	24.4%			12.5%	3.1%	9.4%		2.9%		[76]
		LFP	14.1%	5%	10%*		5%						[77]
		LTO	4.5%*	14%	6.2%						7.7%		[78] and assuming: same wt% of anode as in LFP & Pure LTO as in [79]
	Flow	Zinc-Bromide	15%		4.3%		1%						[60]
		Vanadium Redox	10.6%		4.3%		0.8%						[60]
	Molten-salt	Sodium-Sulfur	30.4%		2.2%		3.5%						[80]
		ZEBRA	30.4%	11.1%	2.2%		3.5%		17.6%				[59]
	Lithium-metal (/advanced Li)	Lithium Sulfur	0.53%	18.4%	4.1%		7.82%						[64]
		Lithium Ceramic	0.53%	18.4%	4.1%		7.82%		16.8%		1.96%		Assumed: same as Li-S, but with NMC811 as cathode & wt% acc. to [78]
		Lithium-air			30.6%		9.4%						[69]
Other	Mechanical	Pumped-Hydro	94.8%	0.32%			2.17%		1.94%				Additional materials comp. to a hydro dam (Table S.2) based on [81]
		Flywheel	60.9%	20.2%			1.36%					0.64 %	[82] and own calculations based on: [83], [84] and [85]
		Compressed-Air	98.4%	0.77%			0.8%						[34,82]
	Fuel-cells	Hydrogen FC	96.2%	0.47%			1.77%						Table 34 in [34]

Table A6.14. *Weight composition (as a % of the total weight) of electricity storage technologies. Values indicated with an * were derived using assumptions by the authors.*

A6.4 Comparison to other sectors

In order to get a feeling for the importance of the electricity sector compared to other material demand sectors, such as buildings, we compare the growth rates of these sectors in Figure A6.11. It shows that the rate of expansion of infrastructure in the electricity sector towards 2050 is larger than the growth in housing stock, and comparable to the rate of growth in commercial buildings.

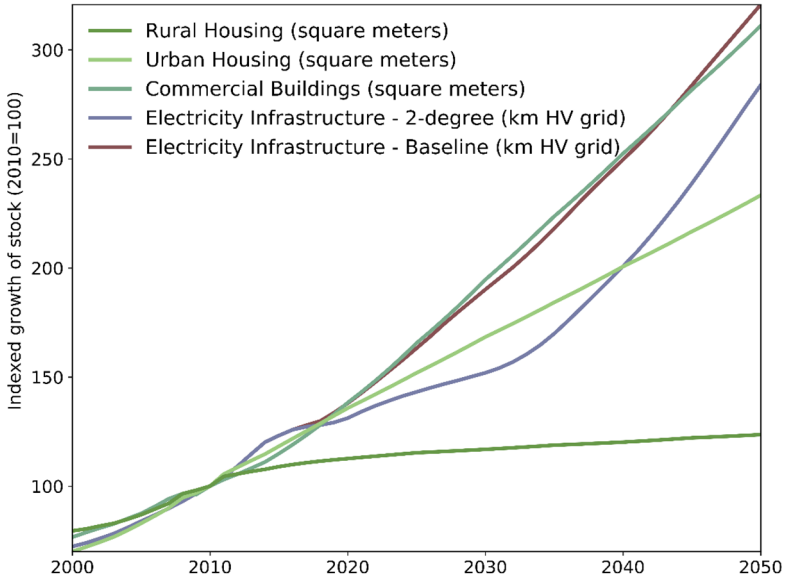

Figure. A6.11. *Indexed growth of buildings and electricity related infrastructure (2010=100). The indicators are based on the total kilometers of high-voltage (HV) grid lines discussed in this study, the development of floorspace in buildings is based on [86].*

A6.5 Sensitivity analysis

In order to better understand the uncertainties regarding some of the assumptions and their impact on the outcomes of the presented model, we perform a sensitivity analysis. In addition to the default model outcomes presented in the main text, we define three alternative model setting to represent a range of possible future developments with relevance to the material use in the electricity sector. We focus on three key uncertainties, being 1) the development & deployment of electricity storage, 2) the extent to which the transmission infrastructure requires expansion, and 3) the uncertainty regarding future

material composition of several technologies. We start by explaining the alternative model settings on transmission and storage in conjunction.

A6.5.1 Alternative assumptions on drivers: transmission and storage

It is often highlighted that high shares of variable renewable energy such as solar and wind pose a challenge to relialably provide electricity to consumers, due to their intermittent nature [87,88]. Backup generation capacity, energy storage technologies, grid expansion and load-shifting practices are typically propsed as options to stabilize the grid, because they may all help to alleviate the temporary imbalance between electricity supply and demand. The difficulty with defining scenarios on future energy systems is that it remains highly uncertain to which extent these stabilizing technologies will be deployed, given that they may be used interchangeably and depending on local conditions.

To account for a wider range of possible future developments of infrastructure in the electricity sector, we define two so called sensitivity variants. The first sensitivity variant is focussed on the application of additional storage capacity and the second on additional expansion of transmission capacity. It is worth noting that most of the literature that we consulted on this topic stated that storage and grid expansion are considered to be interchangeable balancing solutions in cost-optimal models (grid expansion seems to reduce the need for storage and vice versa) [87–90]. This is why we define the first two sensitivity variants to be mutually exclusive.

Please mind that quantitative scenarios on global deployment of transmission infrastructure or storage capacity are scarce and the few studies that exist present a wide range of possible outcomes [87]. For example, the need for storage capacity in Europe towards 2050 could be much higher than our default model [89], but could also be negligible [91]. Therefore, we often had to define the sensitivity variants based on our own judgement and some proxys from data on Europe. We present and explore the effects on the model results only to get a better understanding of the sensitivities of the model and to identify materials for which the demand is highly dependent on the scenario storyline, and therfore more uncertain.

A6.5.1.1 Sensitivity variant 1: high storage, low V2G, low PHS

The first sensitivity variant assumes a higher storage demand by doubling the required storage capacity towards 2050. This alternatve assumption could be justified by [91], who find that the European storage requirements as reported by the IMAGE model might be low compared to other models. Combined with pessimistic assumptions on the addoption of vehicle-to-grid storage, this sensitivity variant could be considered a worst-case scenario,

aimed to explore the additional material demand in dedicated (stationary) storage under less favourable conditions.

Compared to the default assumptions, the regional storage capacity is doubled between 2020 and 2050, while the available storage capacity in electric vehicles is halved towards 2050. Additionally, the installed capacity of Pumped Hydro Storage (PHS) does not grow after 2030 (the end of the predictions by the IHS [45]) and 50% of the remaining regional storage demand (after PHS) is considered to be fulfilled by dedicated storage, which could be due to financial incentives for consumer which produce their own electricity (prosumers, e.g. through rooftop PV) and might benefit from investing in distributued stationary storage applications (after [88,89]).

Implications for global storage capacity can be found in Figure A6.14, and the effects on overall material use are discussed in section A6.5.3. Figure A6.12, below, shows the implictions of the 'high storage' assumptions on regional storage deployment towards 2050. For comparison to the default model setting, please see Figure A6.8.

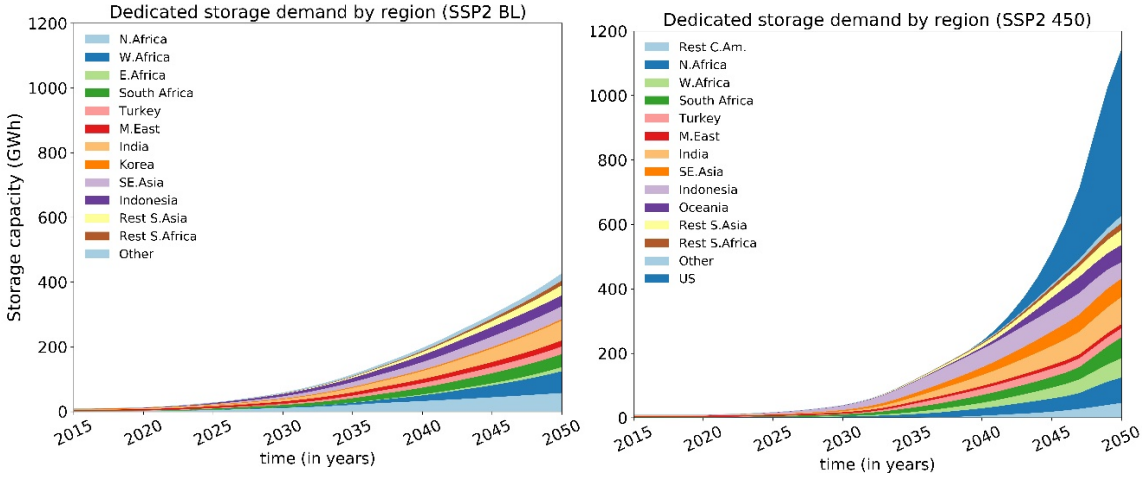

Figure A6.12. *Regional deployment of dedicated storage under the 'high storage' sensitivity variant. Results are given for the 'high storage' sensitivity variant of the SSP2 baseline and the 'high storage' sensitivity variant of the SSP2, 2-degrees climate policy scenario (right).*

A6.5.1.2 Sensitivity variant 2: high transmission expansion

Under the high transmission expansion assumptions we implement a slightly different growth of the high voltage (HV) electricity transmission network, while maintaining the default lengtht of the Medium and Low voltage levels. We choose to do so, because most available studies only elaborate on the expansion of HV (interregional) transmission capacity, see for example [89,92]. Based on these two studies with quanititative indications on

the additional transmission line length in renewable energy scenarios for Europe (Figure A6.13), we conclude that our default assumptions on the expansion of HV transmission line lengths might be on the high side in the SSP2 Baseline scenario, while in the SSP2 2-degree scenario it might be on the low side.

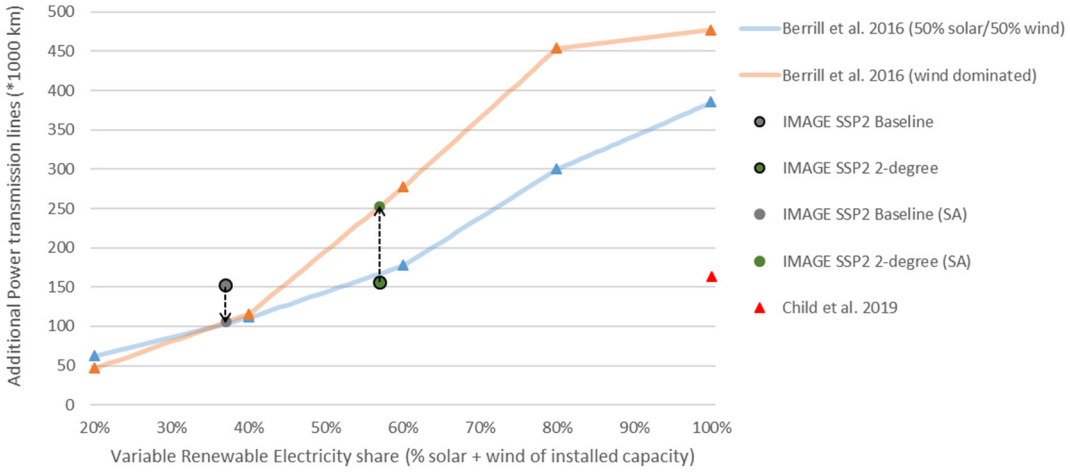

Figure A6.13. *European High Voltage transmission line expansion (in 1000 km) under different renewable energy shares. Shown are results from two studies compared to our own assumptions using the SSP2 scenario based on the IMAGE model baseline and the 2-degree climate policy assumptions. The arrows indicate the consequences of the sensitivity variant 2, which make the model more sensitive to the adopted levels of variable renewable electricity generation.*

To explore the effects of a model with a HV line length that is a little more sensitive to the penetration levels of variable renewable energy, we adjust our growth assumptions so that variable renewable electricity generation (PV Solar & Wind) will lead to a 100% larger demand for grid expansion, while other baseload technologies require 70% less grid expansion towards 2050. As such a 100% growth of a fully fossil-based generation capacity would lead to a 30% increase in the HV line length, but a 100% growth in a fully renewable-based generation capacity would lead to a 200% increase in HV transmission line length in the end of the scenario. Though these assumptions should be verified with data on other regions, it can be seen in Figure A6.13 that for Europe this would lead to an additional HV line length that seems comparable to the range found in [92].

Together, the two sensitivity variants describe an alternative development of the drivers of material demand in electricity storage and HV grid lines, as displayed at the global scale in Figure A6.14.

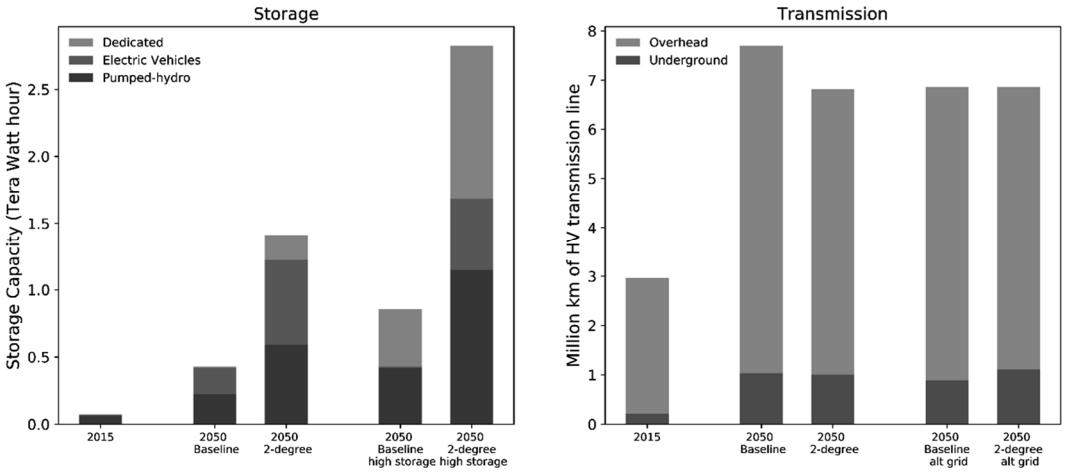

Figure A6.14. *Alternative assumptions on storage capacity and transmission line length under two sensitivity variants (high storage & alt. grid). These panels show the assumptions used in the sensitivity analysis. While the higher storage demand ('high storage') mostly affects the 2-degree scenario, the baseline is most affected by the alternative assumptions on grid expansion ('alt. grid'). Even though the differences between the basline and the 2-degree scenario seem small when implemeniting the alternative grid settings ('alt. grid') the 2-degree scenario now has a larger HV grid, despite much lower generation capacity, which was a consequence of higher efficiency improvements under stricter climate policy assumptions in the IMAGE SSP2 scenario.*

A6.5.2 Alternative assumptions on material intensities

The use of static material intensities in our default model assumptions is not just a convenient modellers choice. There is an inherent uncertainty about technological developments into the future, which simply makes it impossible to model the expected changes in material intensity towards 2050 for all of the 28 generation technologies, the 17 storage technologies, the materials invovled in the infrastructure of 6 different line types as defined in this study. Instead, we explore the impact of three foreseeable changes in the material composition of a few of the technologies used for generation, transmission and storage based on sparesly available literature. The details are discussed below, followed by an elaborate discussion on the outcomes of the sensitivity analysis based on the three different sensitivity variants.

A6.5.2.1 Sensitivity variant 3: dynamic material intensities

First of all, we model the potential impacts of reduced cobalt content in lithium-ion batteries after a recent study by [93]. This sensitivity variant enforces a continually decreasing

cobalt content of NCA & NMA battery types between 2020 and 2050, effectively eradicating cobalt from these battery types in new batteries by 2050. Mind that this battery composition change is enforced simultaneously with the battery density improvements that are part of the default assumptions. Given that we do not assess the demand for nickel, we are unable to fully assess the trade-off in terms of additional demand for substituting materials.

Secondly, we explore the possible impact of an increasing share of transmission lines being High Voltage Direct Current (HVDC lines) between 2020 and 2050. Though the default model does not strictly distinguish between Alternating Current (AC) or Direct Current (DC) transmission and bases the material intensities of underground cables on a mix of both AC & DC lines found in [43], the sensitivity variant addresses the possible increase in the share of new HVDC lines (especially in intercontinental transmission) [90] by increasing the copper content of underground HV lines, which is notably higher in HVDC lines [43], to represent 75% of the additions to be HVDC by 2050 (up from 50% in the default scenario). In terms of material intensity, this represents a 13% increase in the copper content (in kg/km).

Finally, we implement an annual material efficiency improvement of the structural use of steel and aluminium in solar- and wind based generation technolgies between 2020 and 2050. Given that these technolgies are still in development, we address the posibility of ongoing improvements in material efficiency of the newly installed generation capacity, by assuming an annual material efficiency improvement of 1%. Over the 2020-2050 period this would lead to a 26% decrease in the material intensity (kg/MW) for wind and solar technologies. This could for example be achieved through the development of lighter solar panels [94] or through the increased substitution of materials in windmills by composites [95] or even wood [96].

A6.5.3. Results of the sensitivity analysis

Figure A6.15 shows the results from the sensitivity analysis in terms of total stock for the four materials that are affected by each sensitivity variant. Table A6.15 shows more details regarding the deviation from the reference scenarios (the SSP2 Baseline & 2-degree scenario) towards 2050, including the consequences on material inflow, outflow and the resulting ratio. Table A6.16 shows some additional details with regard to the material use in dedicated storage applications.

The alternative assumptions explored in the three sensitivity variants do not have a large effect on the amount of materials contained in the stock. For the period 2045 to 2050, the largest increase compared to the default assumptions is a 9% increase in cobalt stocks under alternative storage assumptions in the 2-degree scenario. The largest decrease in material use found for the same period is 7.7% less steel as a consequence of the dynamic material

intensities (due to a 1% annual material efficiency improvement in solar- and wind-based electricity generation).

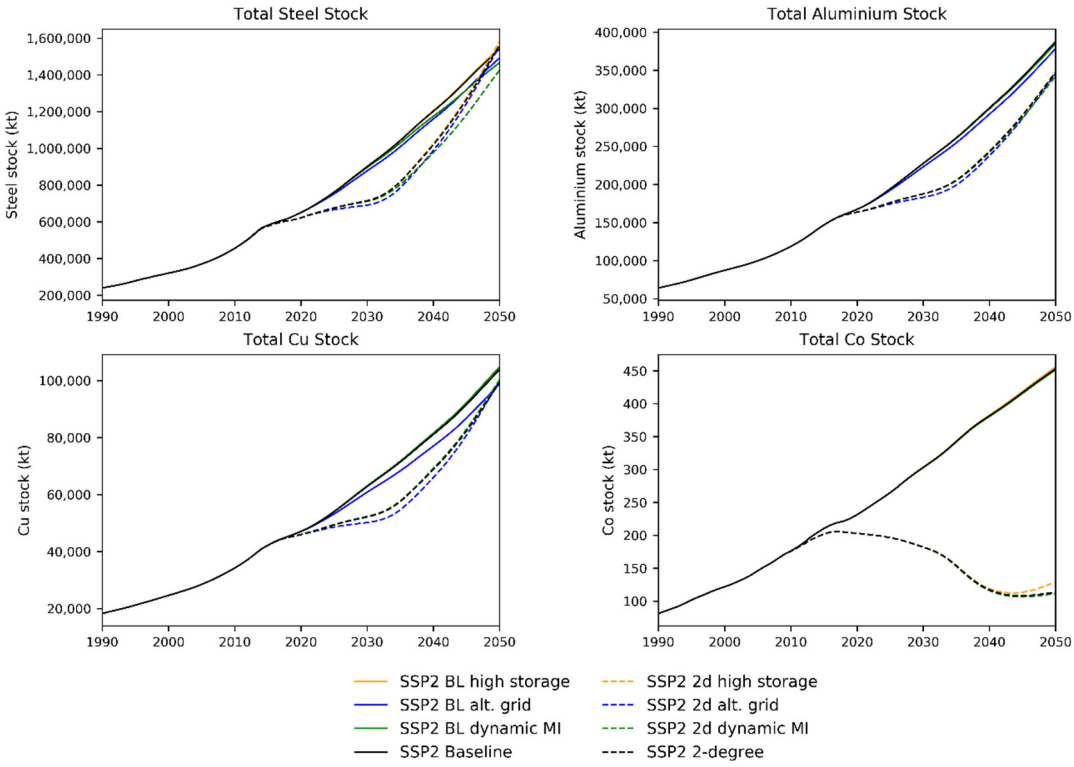

Figure A6.15. *Results of the sensitivity analysis on the stock of steel, aluminium, copper (Cu), and Cobalt (Co). Dashed lines describe the SSP2 2-degree scenario and its sensitivity variants. A solid line refers to the Baseline.*

The effects of the sensitivity analysis on the inflow indicators are larger. For the inflow, the largest increase related to the sensitivity variants is also found for cobalt and steel. However, the roughly 13% decrease of annual steel demand (i.e. inflow) and the roughly 60% increase in annual cobalt demand show a larger effect of the sensitivity analysis on the inflow indicators. The large increase of cobalt demand in the 'high storage' variant of the 2-degree scenario can be explained by the assumed doubling of the storage capacity, and an increase of the share of dedicated electricity storage in a period that other uses of cobalt (such as high-temperature steel in electricity generation) are no longer expanding their stock.

Table A6.15. *Results of the sensitivity analysis: percentage deviation of the three sensitivity variants compared to the default model outcome by the end of the scenario period (average of 2045-2050). Shown are the deviations in terms of total stock and in terms of inflow, for those materials that are affected by the three sensitivity variants, being: 1) alternative growth of the high voltage grid ('alt. grid'), 2) High storage demand combined with pessimistic assumptions on the availability of pumped hydro storage and vehicle-to-grid tehcnolgy ('High storage') and 3) implementing a dynamic material intensity based on foreseeable shifts in technologies of material efficiencies ('dynamic MI'). Readers guide: the 'dynamic material intensity' variant, which implements a 1% annual steel efficiency improvement in solar- and wind-based electricity generation, causes a 4.2% decrease in the steel contained in stocks over the last five years of the SSP2 Baseline, compared to the last five years of the default Baseline explored in Chapter 6 (e.g. Table 6.2).*

		Sensitivity Analysis: Difference in 2045-2050 results					
		SSP2 Baseline			SSP2 2-degree scenario		
		Alt. grid	High storage	Dynamic MI	Alt. grid	High storage	Dynamic MI
Stock	Steel	-3.4%	0.4%	-4.2%	-1.0%	1.1%	-7.7%
	Aluminium	-2.6%	0.1%	-0.6%	-0.9%	0.3%	-1.3%
	Cu	-5.0%	0.1%	0.9%	-0.5%	0.4%	0.9%
	Co		0.6%	-0.3%		9.0%	-1.5%
Inflow	Steel	-1.3%	0.7%	-8.6%	3.3%	2.3%	-12.8%
	Aluminium	-0.8%	0.2%	-1.3%	2.9%	0.9%	-2.1%
	Cu	-2.7%	0.2%	1.3%	7.6%	1.0%	1.4%
	Co		2.8%	-1.5%		60.3%	-6.4%

Based on the sensitivity responses of the 'high storage' and the 'dynamic material intensity' variants, it seems fair to conclude that the uncertainty regarding the analysis of the material use in the electricity sector seems to increase when looking at a climate policy scenario and may be even more pronounced when focusing on inflow indicators. The only case where this doesn't seem to hold is in the variant exploring 'alternative grid' expansion rules under baseline conditions, this has to do with the timing of the deployment of generation capacity and, consequentially, the lower grid size. Here, the inertia of the stock composition causes a lag between changes in the materials inflow and the materials in in the stock.

The 'high storage' sensitivity variant specifically, could have large consequences on the demand for materials in dedicated storage applications, as shown in Table A6.16. Compared to the default model settings, the materials contained in the in-use stocks is more than doubled. Differences between materials occur due to the dynamic deployment of different storage technologies, each with their own material composition. While in-use stocks for

steel and copper grow by a factor 2.1 in the 2-degree scenario, cobalt stocks grow by a factor 5.2. This effect is higher than expected based on the doubling of total storage demand alone. Therefore, the future availability of vehicle-to-grid storage capacity (and to a lesser extent that of pumped hydro), could play an important role in lowering material demand for dedicated storage applications.

Table A6.16. *In-use material stocks for dedicated electricity storage under the 'high storage' sensitivity variant by 2050 (in kt). Similar to Table A6.15, results are shown for the SSP2 baseline and the SSP2 2-degree scenario and values refer to an average of model outcomes (2010-2015 & 2045-2050).*

		Default settings		'high storage' sensitivity variant	
		Baseline	2-Degree	Baseline	2-Degree
	2015	**2050**	**2050**	**2050**	**2050**
Steel	1566	6943	14400	12800	29600
Aluminium	63	302	375	597	1230
Glass	0.4	6.1	7.7	13	30
Cu	35	161	334	300	711
Nd	1.8	8.3	10	17	35
Co	0.1	1.9	2.4	4.4	12
Pb	11.7	98	126	217	537

A6.6 Detailed results & model code

Detailed results with respect to other materials can be found in the supplementary information for the original article. Furthermore, the pyhton code used for the analysis is made available for review and future improvement online, via github.com/SPDeetman/ELMA This repository also contains the raw output data. In case of future improvements or corrections, updates will be posted and managed there.

References to Appendix 6

1. Stehfest, E., Vuuren, D. van, Kram, T. & Bouwma, L. *Integrated Assessment of Global Environmental Change with IMAGE 3.0*. (PBL Netherlands Environmental Assessment Agency, 2014).
2. van Vuuren, D. P. *et al.* Energy, land-use and greenhouse gas emissions trajectories under a green growth paradigm. *Glob. Environ. Chang.* 42, 237–250 (2017).
3. Riahi, K. *et al.* The Shared Socioeconomic Pathways and their energy, land use, and greenhouse gas emissions implications: An overview. *Glob. Environ. Chang.* 42, 153–168 (2017).
4. van Vuuren, D. P. Energy systems and climate policy - Long-term scenarios for an uncertain future. *Dept. of Science, Technology and Society, Faculty of Science* (Utrecht University, 2006).
5. Pauliuk, S. & Heeren, N. ODYM—An open software framework for studying dynamic material

systems: Principles, implementation, and data structures. *J. Ind. Ecol.* jiec.12952 (2019). doi:10.1111/jiec.12952

6. Balzer, G. & Schorn, C. *Asset Management for Infrastructure Systems: Energy and Water*. (Springer International Publishing, 2015).
7. Deetman, S., Pauliuk, S., van Vuuren, D. P., van der Voet, E. & Tukker, A. Scenarios for Demand Growth of Metals in Electricity Generation Technologies, Cars, and Electronic Appliances. *Environ. Sci. Technol.* 0, null (2018).
8. Elshkaki, A. & Graedel, T. E. Dynamic analysis of the global metals flows and stocks in electricity generation technologies. *J. Clean. Prod.* 59, 260–273 (2013).
9. Öhrlund, I. Future Metal Demand from Photovoltaic Cells and Wind Turbines–Investigating the Potential Risk of Disabling a Shift to Renewable Energy Systems. *Science and Technology Options Assessment (STOA)* 72 (2012).
10. BBF Associates; Kundig, K. J. A. Market study: Current and projected wind and solar renewable electric generating capacity and resulting copper demand. (2011).
11. Moss, R. L., Tzimas, E., Kara, H., Willis, P. & Kooroshy, J. *Critical Metals in Strategic Energy Technologies, Assessing Rare Metals as Supply-Chain Bottlenecks in Low-Carbon Energy Technologies*. *JRC Scientific and Technical Reports* (Publications Office of the European Union, 2011). doi:doi:10.2790/35716
12. Sullivan, J. L., Clarck, C. E., Yuan, L., Han, J. & Wang, M. *Life-Cycle Analysis Results for Geothermal Systems in Comparison to Other Power Systems: Part II*. (2011).
13. Ehtiwesh, I. A. S., Coelho, M. C. & Sousa, A. C. M. Exergetic and environmental life cycle assessment analysis of concentrated solar power plants. *Renew. Sustain. Energy Rev.* 56, 145–155 (2016).
14. Crawford, R. H. Life cycle energy and greenhouse emissions analysis of wind turbines and the effect of size on energy yield. *Renew. Sustain. Energy Rev.* 13, 2653–2660 (2009).
15. Dones, R. *et al.* Life Cycle Inventories of Energy Systems: Results for Current Systems in Switzerland and other UCTE Countries. (2007).
16. Haapala, K. R. & Prempreeda, P. Comparative life cycle assessment of 2.0 MW wind turbines. *Int. J. Sustain. Manuf.* 3, 170 (2014).
17. Bonou, A., Laurent, A. & Olsen, S. I. Life cycle assessment of onshore and offshore wind energy-from theory to application. *Appl. Energy* 180, 327–337 (2016).
18. Marimuthu, C. & Kirubakaran, V. Carbon pay back period for solar and wind energy project installed in India: A critical review. *Renew. Sustain. Energy Rev.* 23, 80–90 (2013).
19. Guezuraga, B., Zauner, R. & Pölz, W. Life cycle assessment of two different 2 MW class wind turbines. *Renew. Energy* 37, 37–44 (2012).
20. Habib, K. Critical Ressources in Clean Energy Technologies and Waste Flows. (Syddansk Universitet, 2015).
21. Wilburn, D. R. Wind energy in the United States and materials required for the land-based wind turbine industry from 2010 through 2030. in *Wind Turbine Manufacturing in the U.S.: Developments and Considerations* (2012).
22. Energinet. *Technical Project Description for Offshore Wind Farms (200 MW)*. (2015).
23. van Exter, P., Bosch, S., Schipper, B., Sprecher, B. & Kleijn, R. *Metal Demand for Renewable Electricity Generation in the Netherlands - Navigating a Complex Supply Chain*. (2018).
24. Vici Ventus. Offshore Wind Turbines: Concrete Foundations. (2020).
25. Flury, K. & Frischknecht, R. Life cycle inventories of hydroelectric power generation. *ESU-Services, Fair Consult. Sustain. Comm. by€ Oko-Institute eV* 1–51 (2012).

26. S&T2 consultants. *A Review of GHG emissions from Plant Construction and DEcommissioning*. (Natural Resources Canada, 2006).

27. Dones, R. Teil VII: Kernenergie. in *Sachbilanzen von Energiesystemen: Grundlagen fur den okologischen Vergleich von Energiesystemen und den Einbezug von Energiesystemen in Okobilanzen fur die Schweiz. Ecoinvent report No. 6* (ed. Dones, R. et al.) 208 (Ecoinvent, 2007).

28. Albers, J. P., Bawiec, W. J., Rooney, L. F., Goudarzi, G. H. & Shaffer, G. L. *Demand and Supply of Nonfuel Minerals and Materials for the United States Energy Industry, 1975-1990*. (1977).

29. Weitzel, P. S. *et al. Advanced Ultra-Supercritical Power Plant (700 to 760C) Design for Indian Coal*. *Proceedings of Power-Gen Asia, Thailand* (2012).

30. Dones, R., Bauer, C. & Roder, A. Teil VI: Kohle. in *Sachbilanzen von Energiesystemen: Grundlagen fur den okologischen Vergleich von Energiesystemen und den Einbezug von Energiesystemen in Okobilanzen fur die Schweiz. Ecoinvent report No. 6* (ed. Dones, R. et al.) 208 (Ecoinvent, 2007).

31. Singh, B., Bouman, E. A., Strømman, A. H. & Hertwich, E. G. Material use for electricity generation with carbon dioxide capture and storage: Extending life cycle analysis indices for material accounting. *Resour. Conserv. Recycl.* 100, 49–57 (2015).

32. Jungbluth, N. Teil IV: Erdoel. in *Sachbilanzen von Energiesystemen: Grundlagen fur den okologischen Vergleich von Energiesystemen und den Einbezug von Energiesystemen in Okobilanzen fur die Schweiz. Ecoinvent report No. 6* (ed. Dones, R.) (Swiss Centre for Life Cycle Inventories, 2007).

33. Faist-Emmenegger, M., Heck, T., Jungbluth, N. & Tuchschmid, M. Teil V: Erdgas. in *Sachbilanzen von Energiesystemen: Grundlagen fur den okologischen Vergleich von Energiesystemen und den Einbezug von Energiesystemen in Okobilanzen fur die Schweiz. Ecoinvent report No. 6* (ed. Dones, R. et al.) 208 (Ecoinvent, 2007).

34. Moss, R. L. *et al.* Critical metals in the path towards the decarbonisation of the EU energy sector. *Assessing rare metals as supply-chain bottlenecks in low-carbon energy technologies. JRC Report EUR* 25994, (2013).

35. Bauer, C. Teil IX: Holzenergie. in *Sachbilanzen von Energiesystemen: Grundlagen fur den okologischen Vergleich von Energiesystemen und den Einbezug von Energiesystemen in Okobilanzen fur die Schweiz. Ecoinvent report No. 6* (ed. Dones, R. et al.) 208 (Ecoinvent, 2007).

36. Seneca Group. *Major Infrastructure Projects in Mexico - A Resource Guide for the U.S. Industry*. (2014).

37. Eurelectric. *Power Distribution in Europe - Facts & Figures*. (2013).

38. Arderne, C., Zorn, C., Nicolas, C. & Koks, E. E. Predictive mapping of the global power system using open data. *Sci. Data* 7, 19 (2020).

39. Harrison, G. P., Maclean, E. (Ned). J., Karamanlis, S. & Ochoa, L. F. Life cycle assessment of the transmission network in Great Britain. *Energy Policy* 38, 3622–3631 (2010).

40. Turconi, R., Simonsen, C. G., Byriel, I. P. & Astrup, T. Life cycle assessment of the Danish electricity distribution network. *Int. J. Life Cycle Assess.* 19, 100–108 (2014).

41. Jones, C. I. & McManus, M. C. Life-cycle assessment of 11kV electrical overhead lines and underground cables. *J. Clean. Prod.* 18, 1464–1477 (2010).

42. Jorge, R. S., Hawkins, T. R. & Hertwich, E. G. Life cycle assessment of electricity transmission and distribution—part 2: transformers and substation equipment. *Int. J. Life Cycle Assess.* 17, 184–191 (2012).

43. Jorge, R. S., Hawkins, T. R. & Hertwich, E. G. Life cycle assessment of electricity transmission and distribution—part 1: power lines and cables. *Int. J. Life Cycle Assess.* 17, 9–15 (2012).

44. Ueckerdt, F. *et al.* Decarbonizing global power supply under region-specific consideration of

challenges and options of integrating variable renewables in the REMIND model. *Energy Econ.* 64, 665–684 (2017).

45. Rogner, M. & Troja, N. *The world's water battery: Pumped hydropower storage and the clean energy transition*. (2018).
46. Gernaat, D. E. H. J., Bogaart, P. W., Vuuren, D. P. van, Biemans, H. & Niessink, R. High-resolution assessment of global technical and economic hydropower potential. *Nat. Energy* 2, 821–828 (2017).
47. Girod, B., Vuuren, D. P. van & Deetman, S. Global travel within the 2 degree climate target. *Accept. to Energy Policy* (2011). doi:10.1016/j.enpol.2012.02.008
48. Jian, L., Zechun, H., Banister, D., Yongqiang, Z. & Zhongying, W. The future of energy storage shaped by electric vehicles: A perspective from China. *Energy* 154, 249–257 (2018).
49. Geske, J. & Schumann, D. Willing to participate in vehicle-to-grid (V2G)? Why not! *Energy Policy* 120, 392–401 (2018).
50. IEA. *Tracking Clean Energy Progress 2017*. (2017). doi:https://www.iea.org/reports/tracking-clean-energy-progress-2017
51. IRENA. *Electricity storage and renewables: Costs and markets to 2030*. *Electricity-storage-and-renewables-costs-and-markets* (2017).
52. Majeau-Bettez, G., Hawkins, T. R. & Strømman, A. H. Life Cycle Environmental Assessment of Lithium-Ion and Nickel Metal Hydride Batteries for Plug-In Hybrid and Battery Electric Vehicles. *Environ. Sci. Technol.* 45, 4548–4554 (2011).
53. Wikipedia. Nickel–metal hydride battery. (2019). Available at: https://en.wikipedia.org/wiki/Nickel–metal_hydride_battery. (Accessed: 25th November 2019)
54. Batteryuniversity.com. Types of Lithium-ion. (2019). Available at: https://batteryuniversity.com/learn/article/types_of_lithium_ion. (Accessed: 25th November 2019)
55. Berg, H. & Zackrisson, M. Perspectives on environmental and cost assessment of lithium metal negative electrodes in electric vehicle traction batteries. *J. Power Sources* 415, 83–90 (2019).
56. Xu, G. *et al.* Li 4 Ti 5 O 12 -based energy conversion and storage systems: Status and prospects. *Coord. Chem. Rev.* 343, 139–184 (2017).
57. Yang, Y. *et al.* Lithium Titanate Tailored by Cathodically Induced Graphene for an Ultrafast Lithium Ion Battery. *Adv. Funct. Mater.* 24, 4349–4356 (2014).
58. Gür, T. M. Review of electrical energy storage technologies, materials and systems: challenges and prospects for large-scale grid storage. *Energy Environ. Sci.* 11, 2696–2767 (2018).
59. Van den Bossche, P., Matheys, J. & Van Mierlo, J. Battery Environmental Analysis. in *Electric and Hybrid Vehicles* 347–374 (Elsevier, 2010). doi:10.1016/B978-0-444-53565-8.00014-2
60. Rydh, C. J. Environmental assessment of vanadium redox and lead-acid batteries for stationary energy storage. *J. Power Sources* 80, 21–29 (1999).
61. Batteryuniversity.com. Why does Sodium-sulfur need to be heated. (2019). Available at: https://batteryuniversity.com/learn/article/bu_210a_why_does_sodium_sulfur_need_to_be_heated. (Accessed: 25th November 2019)
62. Li, G. *et al.* Advanced intermediate temperature sodium–nickel chloride batteries with ultra-high energy density. *Nat. Commun.* 7, 10683 (2016).
63. Patel, K. Lithium-Sulfur Battery: Chemistry, Challenges, Cost, and Future. *J. Undergrad. Res. Univ. Illinois Chicago* 9, (2016).
64. Deng, Y., Li, J., Li, T., Gao, X. & Yuan, C. Life cycle assessment of lithium sulfur battery for electric vehicles. *J. Power Sources* 343, 284–295 (2017).

65. Yu, S. *et al.* Insights into a layered hybrid solid electrolyte and its application in long lifespan high-voltage all-solid-state lithium batteries. *J. Mater. Chem. A* 7, 3882–3894 (2019).
66. Albertus, P., Babinec, S., Litzelman, S. & Newman, A. Status and challenges in enabling the lithium metal electrode for high-energy and low-cost rechargeable batteries. *Nat. Energy* 3, 16–21 (2018).
67. Collins, B. & BloombergNEF. Innolith Battery Strikes at 'Flammable' Lithium-Ion: Q&A. (2019).
68. Gerssen-Gondelach, S. J. & Faaij, A. P. C. Performance of batteries for electric vehicles on short and longer term. *J. Power Sources* 212, 111–129 (2012).
69. Zackrisson, M., Fransson, K., Hildenbrand, J., Lampic, G. & O'Dwyer, C. Life cycle assessment of lithium-air battery cells. *J. Clean. Prod.* 135, 299–311 (2016).
70. Tan, P. *et al.* Advances and challenges in lithium-air batteries. *Appl. Energy* 204, 780–806 (2017).
71. Zhu, Z. *et al.* Anion-redox nanolithia cathodes for Li-ion batteries. *Nat. Energy* 1, 16111 (2016).
72. Gallagher, K. G. *et al.* Quantifying the promise of lithium–air batteries for electric vehicles. *Energy Environ. Sci.* 7, 1555 (2014).
73. Luo, X., Wang, J., Dooner, M. & Clarke, J. Overview of current development in electrical energy storage technologies and the application potential in power system operation. *Appl. Energy* 137, 511–536 (2015).
74. Gardiner, M. R. Hydrogen for Energy Storage. *Presentation* (2014). Available at: https://www.h2fc-fair.com/hm14/images/tech-forum-presentations/2014-04-09-1700.pdf.
75. Cusenza, M. A., Bobba, S., Ardente, F., Cellura, M. & Di Persio, F. Energy and environmental assessment of a traction lithium-ion battery pack for plug-in hybrid electric vehicles. *J. Clean. Prod.* 215, 634–649 (2019).
76. Nelson, P. A., Ahmed, S., Gallagher, K. G. & Dees, D. W. *Modeling the Performance and Cost of Lithium-Ion Batteries for Electric-Drive Vehicles*. (2019).
77. Dakota Lithium. Safety Data Sheet Lithium Phosphate (LiFePO4). 6 (2019).
78. Olofsson, Y. & Romare, M. Life Cycle Assessment of Lithium-ion Batteries for Plug-in Hybrid Buses. (Chalmers Univesity of Technology, Sweden, 2013).
79. Chen, C., Agrawal, R. & Wang, C. High Performance Li4Ti5O12/Si Composite Anodes for Li-Ion Batteries. *Nanomaterials* 5, 1469–1480 (2015).
80. Sullivan, J. L. & Gaines, L. *A Review of Battery Life-Cycle Analysis: State of Knowledge and Critical Needs*. (2010).
81. Axpo. *Environmental Product declaration Löntsch high head storage power plant*. (2018).
82. Eller, A., McClanney, I. & Gauntlett, De. *North American Energy Storage Copper Content Analysis*. (2018).
83. Liu, K. & Chen, X.-G. Development of Al–Mn–Mg 3004 alloy for applications at elevated temperature via dispersoid strengthening. *Mater. Des.* 84, 340–350 (2015).
84. Azo Materials. AISI 4340 Alloy Steel (UNS G43400). (2020). Available at: https://www.azom.com/article.aspx?ArticleID=6772. (Accessed: 19th May 2020)
85. Werfel, F. N. *et al.* 250 kW flywheel with HTS magnetic bearing for industrial use. *J. Phys. Conf. Ser.* 97, 012206 (2008).
86. Deetman, S. *et al.* Modelling global material stocks and flows for residential and service sector buildings towards 2050. *J. Clean. Prod.* 245, (2020).
87. Koskinen, O. & Breyer, C. Energy Storage in Global and Transcontinental Energy Scenarios: A Critical Review. *Energy Procedia* 99, 53–63 (2016).
88. Laugs, G. A. H., Benders, R. M. J. & Moll, H. C. Balancing responsibilities: Effects of growth of variable

renewable energy, storage, and undue grid interaction. *Energy Policy* 139, 111203 (2020).

89. Child, M., Kemfert, C., Bogdanov, D. & Breyer, C. Flexible electricity generation, grid exchange and storage for the transition to a 100% renewable energy system in Europe. *Renew. Energy* 139, 80–101 (2019).
90. Chatzivasileiadis, S., Ernst, D. & Andersson, G. The Global Grid. *Renew. Energy* 57, 372–383 (2013).
91. Hof, A. F. *et al.* From global to national scenarios: Bridging different models to explore power generation decarbonisation based on insights from socio-technical transition case studies. *Technol. Forecast. Soc. Change* 151, 119882 (2020).
92. Berrill, P., Arvesen, A., Scholz, Y., Gils, H. C. & Hertwich, E. G. Environmental impacts of high penetration renewable energy scenarios for Europe. *Environ. Res. Lett.* 11, 014012 (2016).
93. Li, W., Lee, S. & Manthiram, A. High-Nickel NMA: A Cobalt-Free Alternative to NMC and NCA Cathodes for Lithium-Ion Batteries. *Adv. Mater.* 32, 2002718 (2020).
94. Reese, M. O. *et al.* Increasing markets and decreasing package weight for high-specific-power photovoltaics. *Nat. Energy* 3, 1002–1012 (2018).
95. Lefeuvre, A., Garnier, S., Jacquemin, L., Pillain, B. & Sonnemann, G. Anticipating in-use stocks of carbon fibre reinforced polymers and related waste generated by the wind power sector until 2050. *Resour. Conserv. Recycl.* 141, 30–39 (2019).
96. Steen, P., Landel, P., Dölerud, E. & Otto Lundman. Structural design methods for tall timber towers with large wind turbine. in *International Conference on Computational Methods in Wood Mechanics* 27 (2019).

Appendix 7

A7.1 Material composition of vehicles

Table A7.1. *Material composition by type of vehicle bodies (including drivetrain & wheels)*

Cat.	Vehicle	Type	Steel	Al	Cu	Plastics	Glass	Ti	Wood	Rubber	Pb	Nd	Sources
Passenger	Car	ICE-HEV	63.2%	9.7%	1.8%	12.5%	2.7%			3.1%	0.8%	0.02%	1–5
		PHEV-BEV	47.8%	13.8%	7.4%	10.2%	2.4%		0.75%	2.4%	0.1%	0.09%	
		FCV	45%	24.9%	1.4%	8.5%	3%			4.3%	0.2%	0.25%	
	Bicycle		34%	46%		12%				7%			6–8
	Bus	Regular	55.3%	19%	0.25%	8.8%	2.2%			2.9%			9
		Midi	31.9%	36.5%	0.25%	14.9%	4.6%			2.6%			
	Train	Regular	60.5%	31%	0.14%	2.1%	0.37%						10,11
		HST	59.6%	25%	1.3%	3.3%	1.9%						
	Airplane	passenger	9%	68%	0.46%	5.3%		6%					12–15
Freight	Truck	LCV	65.6%	6.1%	1%	10.8%	0.6%			3%			9
		MFT	64.2%	0.9%	0.3%	19.6%	0.7%			5.6%			
		HFT	73.9%	3.6%	0.5%	5.6%	0.3%			5.8%			
	Inland ship		91%	1%	1%	2%	0.06%		1%				16–20
	Intern. ship	Small-XL	91%	1%	1%	2%	0.06%		1%				
	Airplane	Cargo	9%	68%		5.3%		6%					12–15
	Rail	Cargo	94.5%	5.4%	0.15%								10,11

A7.2 Dynamic fleet characteristics of international shipping

	Small Vessels		Medium Vessels		Large Vessels		Very Large Vessels	
	DWT	nr	DWT	nr	DWT	nr	DWT	nr
2005	373	23660	7985	29710	53057	5700	138632	2157
2006	378	25122	8078	34794	52920	6974	137670	2682
2007	378	25515	8095	36028	53052	7472	137751	2914
2008	379	26307	8104	37335	53097	7995	138184	3177
2009	379	27084	8077	36285	52912	8183	137611	3399
2010	380	27831	8170	37165	52947	8930	137797	3842
2011	378	28286	8265	36927	53111	9540	138851	4321
2012	374	28843	8196	36144	53324	9867	139949	4617
2013	375	29682	8118	36728	53364	10317	140816	4857
2014	374	31240	8167	37719	53399	10924	142568	5211
2015	374	32136	8170	38351	53285	11309	143482	5437
2016	373	33356	8175	39017	53228	11615	144916	5816
2017	374	33752	8212	39141	53100	11783	145851	6039
2018	375	34495	8215	39452	53051	11997	147805	6307

Table A7.2. *Development of international shipping fleet characteristics. Assumed DWT (Dead weight tonnage) and the total number of ships according to [21,22].*

A7.3 Additional assumptions for trains

Table A7.3. *Additional assumptions on trains in various regions. These sources were used to derive data in Table 7.2. Therefore, Table 7.2 does not compare all global trains, but only the indicated regions. Based on this data, i.c.w. sources stated in Table 7.2, an average of 1.5 locomotives per freight train was assumed.*

Source(s)	Country/ region	year	Regular passenger trains (coaches)	Freight Trains		HST (trains)
[23]	India	2016	55,500	11,500	locomotives	none
				278,000	wagons	
[24]	Canada	2017	512	2,842	Locomotives	none
				55,357	wagons	
[25,26]	China*	2018	52,399	21,482	Locomotives	2600
				839,213	wagons	
[27,28]	US	2018	18,314	29,031	Locomotives	20
				1,690,396	wagons	
[29–33]	Europe	2015/ 2018	88,790	40,000	Locomotives	N.A.
				880,000	Wagons	
[23,34–36]	Japan**	2017	31,319	N.A.		N.A.
[37,38]	Russia	2014	N.A.	20,300	Locomotives	N.A.
				1,229,200	Wagons	

Notes: * In Chinese national statistics the total number of coaches is stated, including high-speed coaches. The World Bank states that Chinese HST usually have 8 coaches per train; therefore, 2600*8 = 20800 is subtracted from the stated 73199 based on the indicated sources. **own estimation based on the stated sources.

References to Appendix 7

1. Deetman, S., Pauliuk, S., Van Vuuren, D. P., Van Der Voet, E. & Tukker, A. Scenarios for Demand Growth of Metals in Electricity Generation Technologies, Cars, and Electronic Appliances. *Environ. Sci. Technol.* 52, null (2018).
2. Wang, D. *et al.* Life cycle analysis of internal combustion engine, electric and fuel cell vehicles for China. *Energy* 59, 402–412 (2013).
3. Klemola, K. *Life-Cycle Impacts of Tesla Model S and Volkswagen Passat*. http://kimmoklemola.fi/data/documents/SF-comparison-USA-20160110.pdf (2016).
4. Hawkins, T. R. *et al.* Comparative Environmental Life Cycle Assessment of Conventional and Electric Vehicles. *J. Ind. Ecol.* 17, 53–64 (2013).
5. Qiao, Q., Zhao, F., Liu, Z., Jiang, S. & Hao, H. Cradle-to-gate greenhouse gas emissions of battery electric and internal combustion engine vehicles in China. *Appl. Energy* 204, 1399–1411 (2017).
6. Leuenberger, M. & Frischknecht, R. *Life Cycle Assessment of Two Wheel Vehicles*. https://treeze.ch/fileadmin/user_upload/downloads/Publications/Case_Studies/Mobility/leuenberger-2010-TwoWheelVehicles.pdf (2010).
7. Chang, Y.-J., Schau, E. & Finkbeiner, M. Application of Life Cycle Sustainability Assessment to the Bamboo and Aluminum Bicycle in Surveying Social Risks of Developing Countries. in *2nd world sustainability forum* (2012). doi:10.3390/wsf2-00953.
8. Bonilla-Alicea, R. J., Watson, B. C., Shen, Z., Tamayo, L. & Telenko, C. Life cycle assessment to quantify the impact of technology improvements in bike-sharing systems. *J. Ind. Ecol.* 24, 138–148 (2020).
9. Hill, N. *et al. Light weighting as a means of improving Heavy Duty Vehicles ' energy efficiency and overall CO2 emissions*. https://ec.europa.eu/clima/sites/clima/files/transport/vehicles/heavy/docs/hdv_lightweighting_en.pdf (2015).
10. Silva, R. F. & Kaewunruen, S. Recycling of Rolling Stocks. *Environments* 4, 39–57 (2017).
11. Rail Network. *Comparing environmental impact of conventional and high speed rail*. https://silo.tips/download/comparing-environmental-impact-of-conventional-and-high-speed-rail (2009).
12. Howe, S., Kolios, A. J. & Brennan, F. P. Environmental life cycle assessment of commercial passenger jet airliners. *Transp. Res. Part D Transp. Environ.* 19, 34–41 (2013).
13. Timmis, A. *et al.* Lifecycle Asessment of CFRP Aircraft Fuselage. *Int. J. Life Cycle Assess.* 20, 233–243 (2015).
14. Asmatulu, E., Overcash, M. & Twomey, J. Recycling of Aircraft: State of the Art in 2011. *J. Ind. Eng.* 2013, 1–8 (2013).
15. Bao, W. *et al.* Comparative study on life cycle environmental impact assessment of copper and aluminium cables. *IOP Conf. Ser. Earth Environ. Sci.* 94, (2017).
16. Jain, K. P., Pruyn, J. F. J. & Hopman, J. J. Quantitative assessment of material composition of end-of-life ships using onboard documentation. *Resour. Conserv. Recycl.* 107, 1–9 (2016).
17. Andersen, A. B. *et al. Technological and economic feasibility study of ship scrapping in Europe*. https://ec.europa.eu/growth/content/study-technological-and-economic-feasibility-ship-scrapping-europe-0_en (2001).
18. Jeong, B., Wang, H., Oguz, E. & Zhou, P. An effective framework for life cycle and cost assessment for marine

vessels aiming to select optimal propulsion systems The International Council on Clean Transportation. *J. Clean. Prod.* 187, 111–130 (2018).

19. Oguchi, M., Murakami, S., Sakanakura, H., Kida, A. & Kameya, T. A preliminary categorization of end-of-life electrical and electronic equipment as secondary metal resources. *Waste Manag.* 31, 2150–2160 (2011).
20. Hess, R., Rushworth, D., Hynes, V. M. & Peters, J. E. *Estimating the amount of recyclable materials and wastes in domestic ship recycling*. https://www.rand.org/content/dam/rand/pubs/monograph_reports/MR1377/MR1377.appa.pdf (2001).
21. Equasis. *The world merchant fleet in 2005-2018*. http://www.equasis.org/EquasisWeb/public/PublicStatistic?fs=HomePage.
22. UNCTAD. *Review of maritime transport 2005-2019*. https://unctad.org/system/files/official-document/rmt2005_en.pdf (2005).
23. IEA. *The Future of Rail: Opportunities for energy and the environment*. https://www.iea.org/reports/the-future-of-rail (2019).
24. Railway Association of Canada. *Rail trends | 2018*. https://www.railcan.ca/wp-content/uploads/2018/12/2018-Rail-Trends.pdf (2018).
25. National Bureau of Statistics of China. Basic conditions of transport. *National Data* (2021).
26. Lawrence, M., Bullock, R. & Liu, Z. *China's High-Speed Rail Development*. https://doi.org/10.1596/978-1-4648-1425-9 (2019) doi:10.1596/978-1-4648-1425-9.
27. Bureau of Transportation Statistics. Rail Profile. *United States Department of Transportation* (2019).
28. National Transit Database. *2018 Vehicles*. https://www.transit.dot.gov/ntd/data-product/2018-vehicles (2019).
29. Rail Freight Forward. *30 by 2030: Rail Freight strategy to boost modal shift*. https://www.railfreightforward.eu/sites/default/files/usercontent/white_paper-30by2030-150dpi6.pdf (2020).
30. Eurostat. Passenger railway vehicles, by type of vehicle. (2020).
31. Deutsche Bahn. *Deutsche Bahn Facts & Figures 2018*. https://www.deutschebahn.com/resource/blob/4045134/f9331633c8a19470629f9e3aa6d5fe8c/19-03_facts_and_figures-data.pdf (2019).
32. Trenitalia. *TRENITALIA S.p.A RELAZIONE FINANZIARIA ANNUALE AL 31 DICEMBRE 2018*. https://www.fsitaliane.it/content/dam/fsitaliane/Documents/il-gruppo/Bilancio_esercizio_Trenitalia_31_12_2018.pdf (2018).
33. Department for Transport. *Rail Factsheet*. https://assets.publishing.service.gov.uk/government/uploads/system/uploads/attachment_data/file/761352/rail-factsheet-2018.pdf (2018).
34. JR East. *Annual report 2017*. https://www.jreast.co.jp/e/investor/ar/2017/pdf/ar_2017-all.pdf (2017).
35. UIC. *High speed rail: Fast track to sustainable mobility*. https://uic.org/IMG/pdf/uic_high_speed_2018_ph08_web.pdf (2018).
36. MLIT. Statistics. (2020).
37. Murray, B. *Russian Railway Reform Programme*. http://www.ebrd.com/documents/evaluation/special-study-russian-railway-sector-evaluation-working-paper-1.pdf (2014).
38. EBRD. *The EBRD 's projects in the Russian railway sector*. http://www.oecd.org/derec/ebrd/EBRD-EVD-Russian-rail-sector.pdf (2016).